

Solitary-Wave Amplification along a Vertical Wall: Theory and Experiment

Harry Yeh
Oregon State University

Joint work with
Wenwen Li (Oregon State U.) and Yuji Kodama (Ohio State U.)

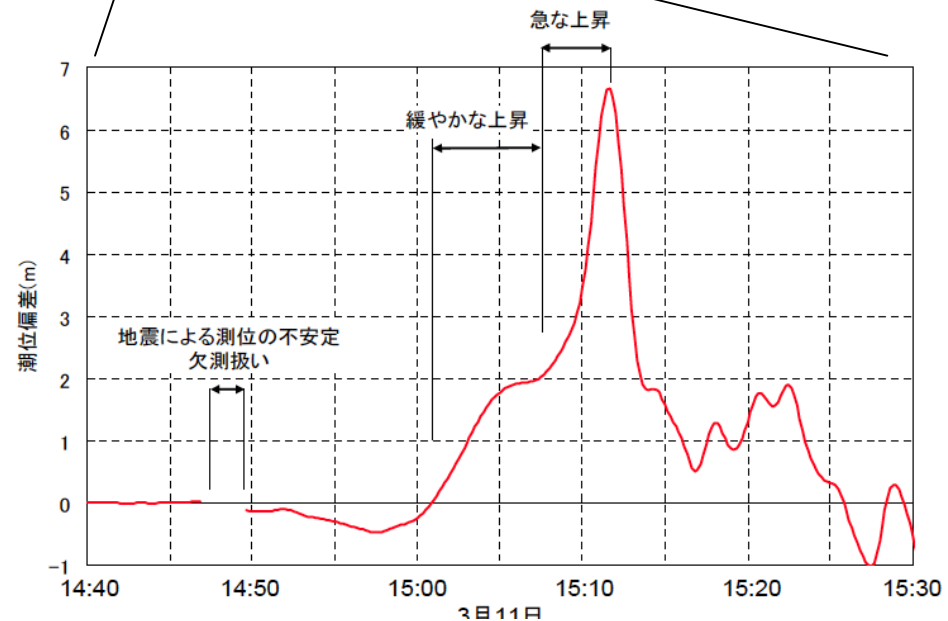
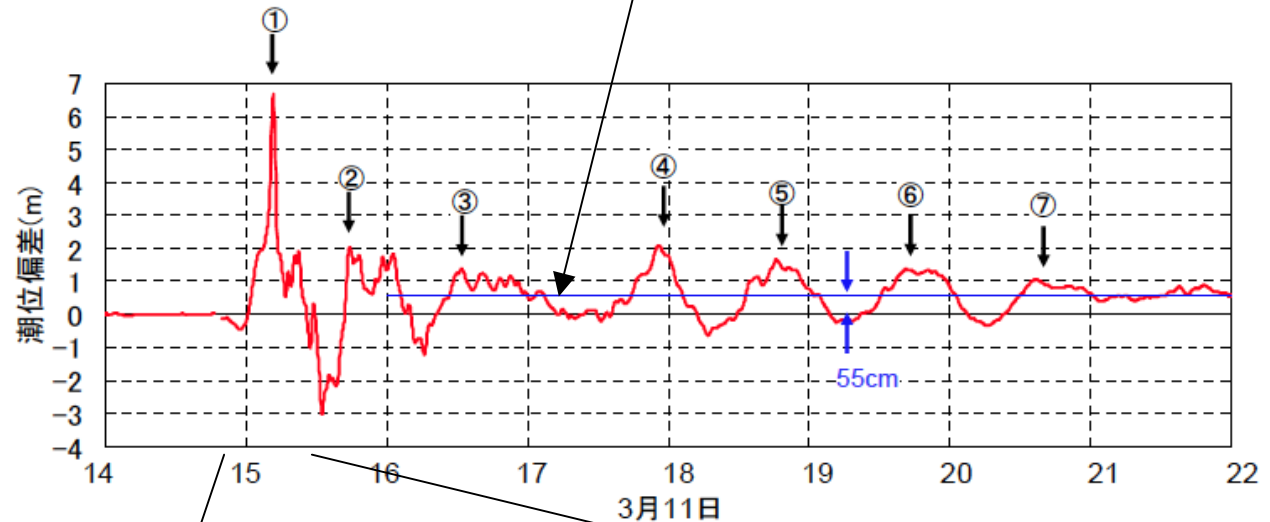
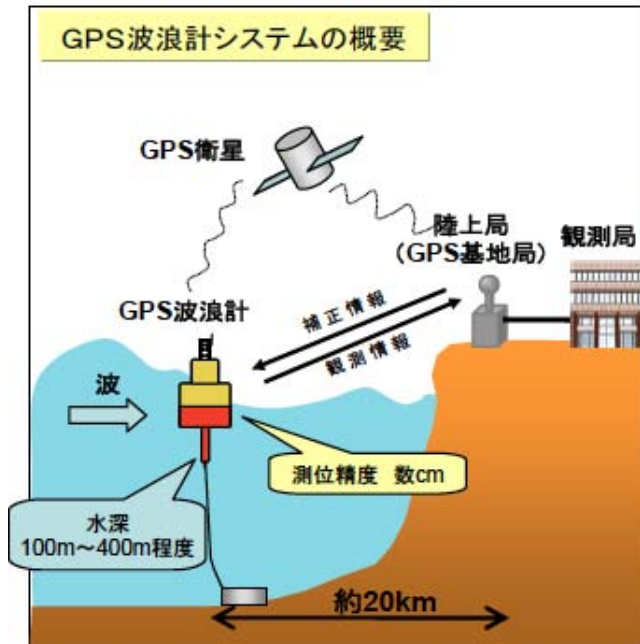
1. Can a real tsunami take a soliton form?

The Very Recent Japan Tsunami: GPS Wave Gage

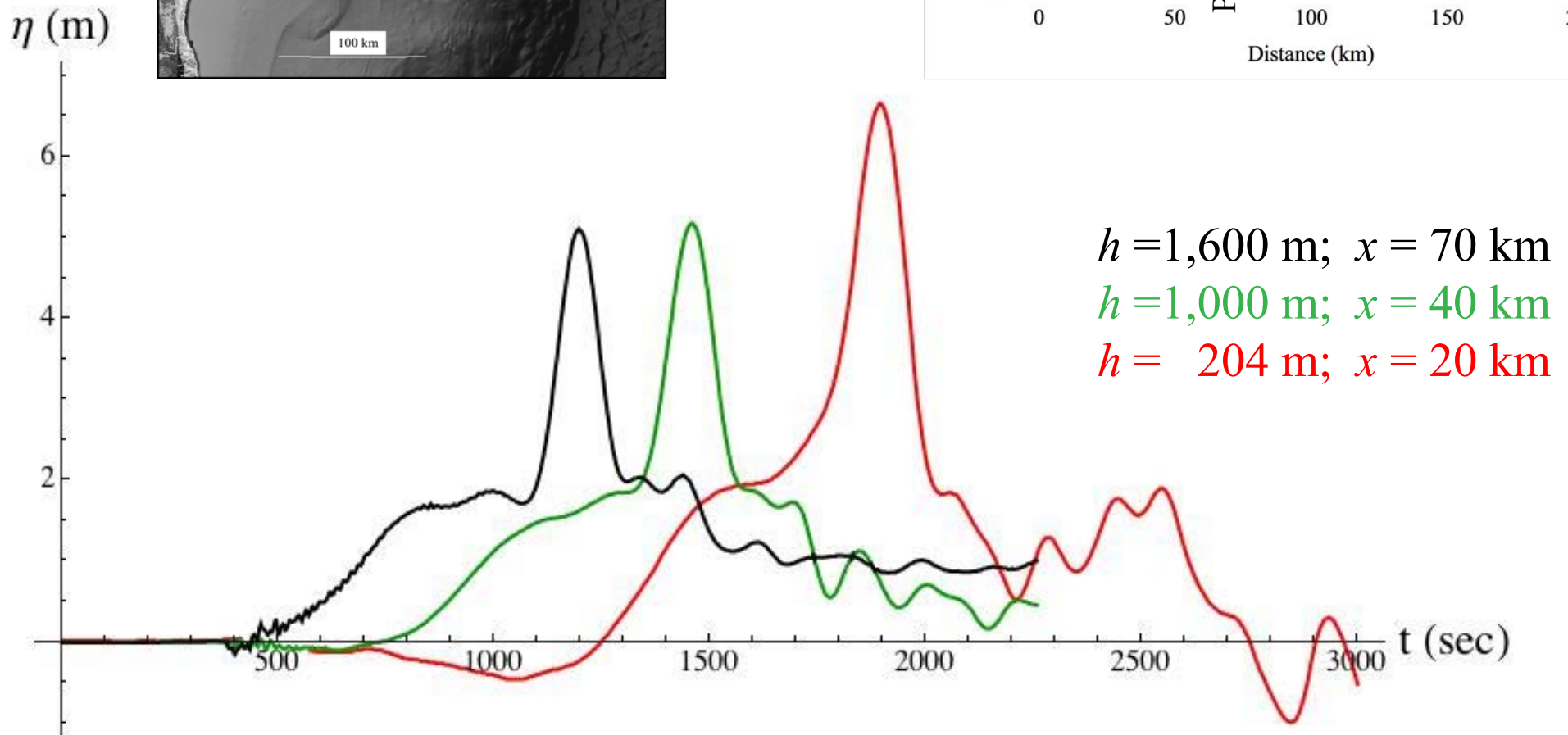
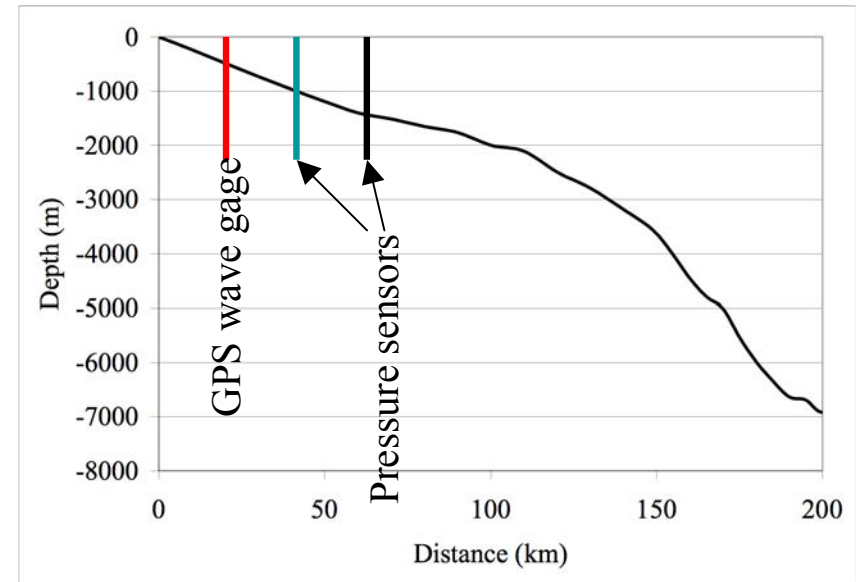
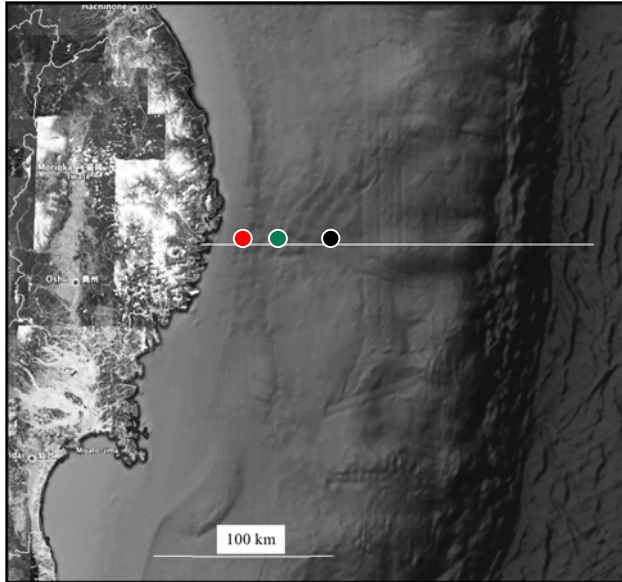
Water depth 204 m

Wave period
40 ~ 50 minutes

55 cm land subsidence



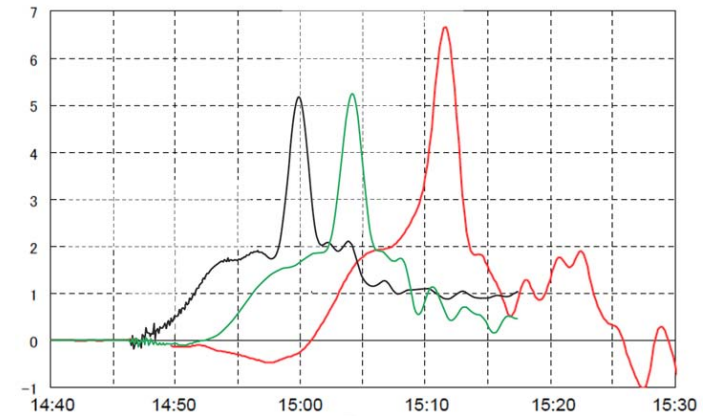
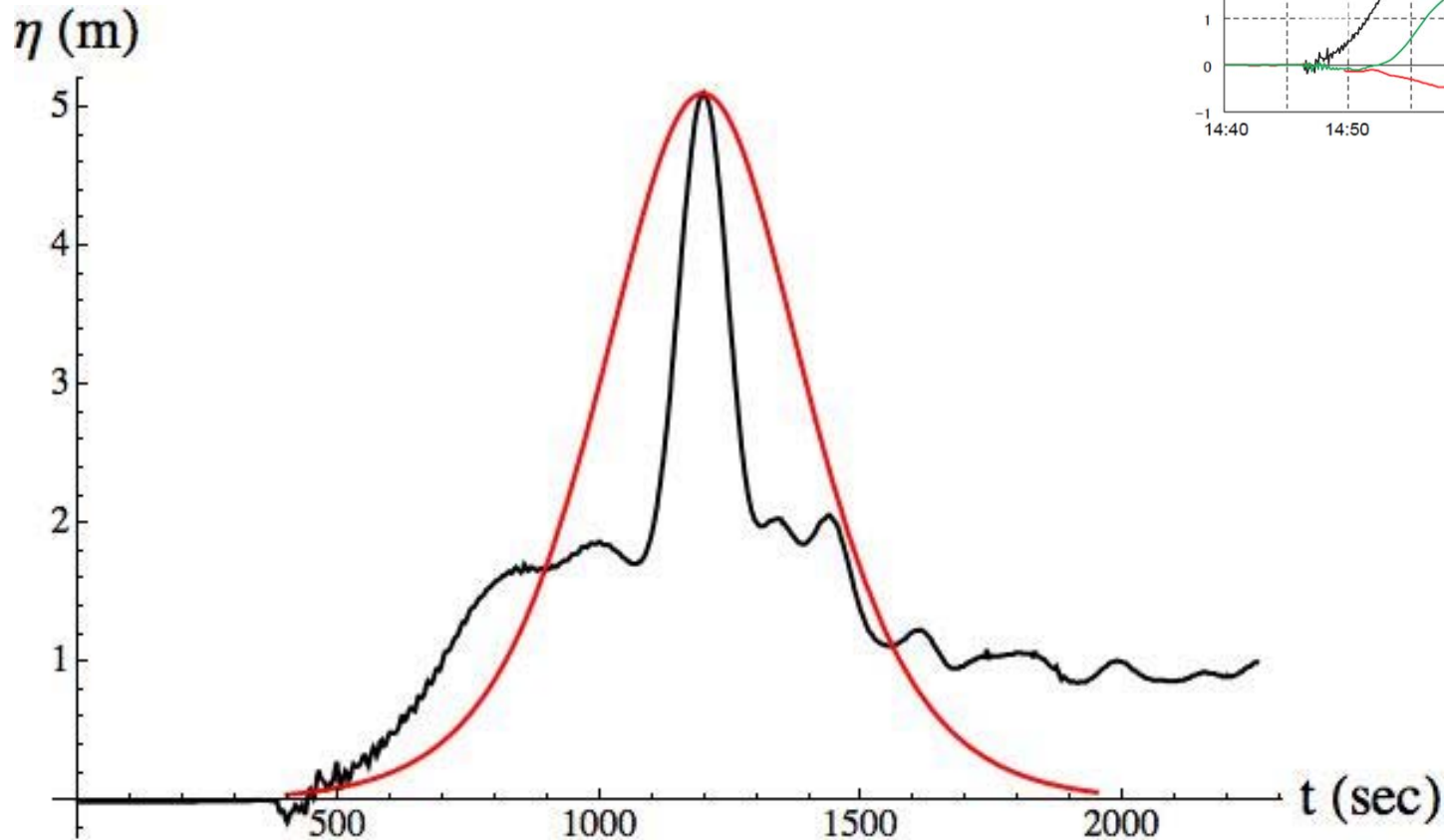
Seabed Pressure Data and GPS Wave Gage Off Kamaishi



Seabed Pressure Transducers (ERI, University of Tokyo)

$h = 1,600$ m; $x = 70$ km. Soliton or not soliton?

$$\eta = a \operatorname{sech}^2 \left[\sqrt{\frac{3a}{4h^3}} \left(x - c_0 \left(1 + \frac{a}{2h} \right) t \right) \right]$$

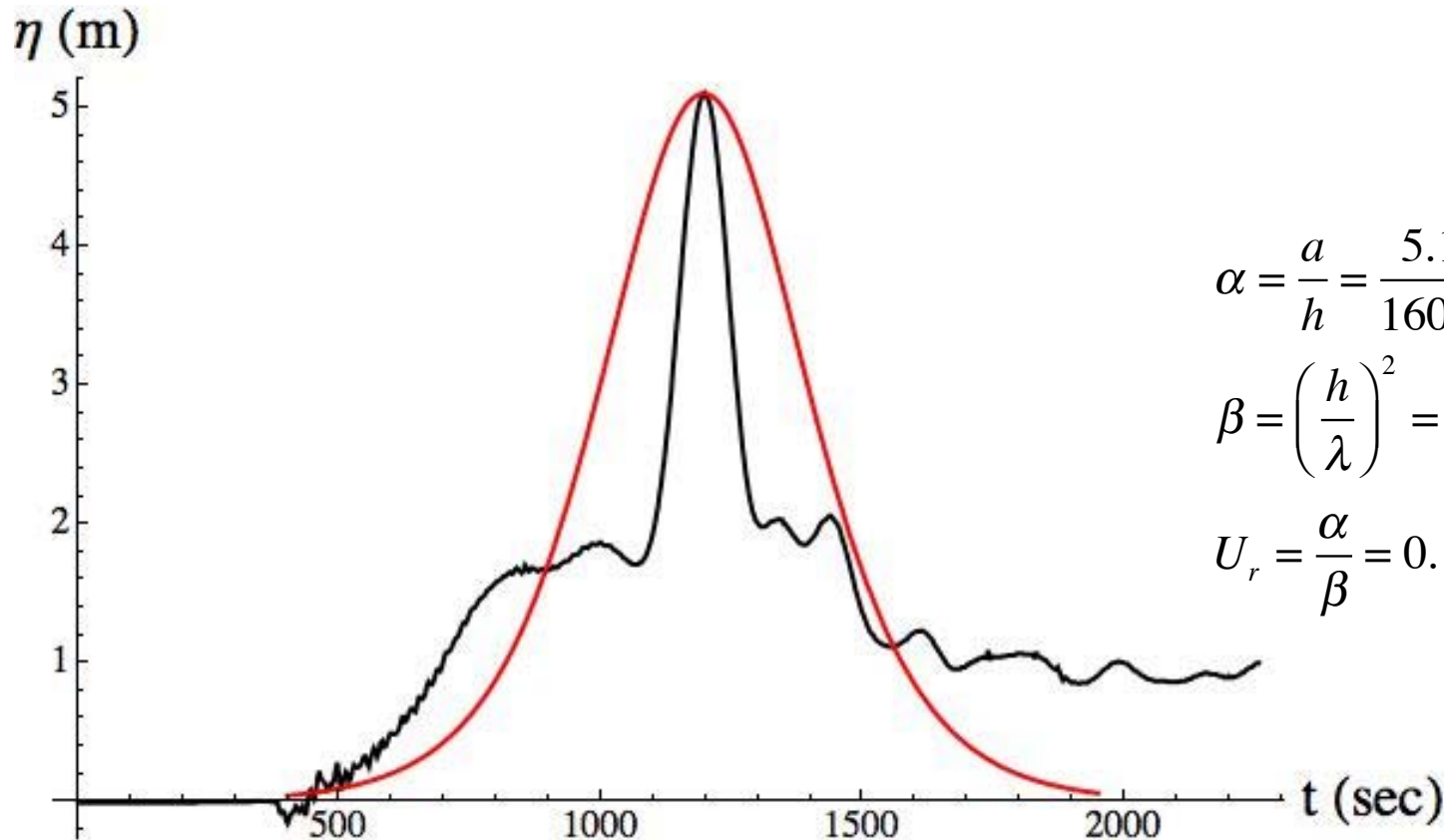


Seabed Pressure Transducers (ERI, University of Tokyo)

$h = 1,600 \text{ m}; \quad x = 70 \text{ km.} \quad \eta = a \operatorname{sech}^2 \left[\sqrt{\frac{3a}{4h^3}} \left(x - c_0 \left(1 + \frac{a}{2h} \right) t \right) \right]$

The breadth of the wave profile 2λ is taken at $\eta = 0.42 a$.

With this choice of length scale, the Ursell number of a solitary wave is $U_r = \alpha/\beta = 1.33$, where $\alpha = a/h$; $\beta = (h/\lambda)^2$



$$\alpha = \frac{a}{h} = \frac{5.1}{1600} \approx 0.0032$$

$$\beta = \left(\frac{h}{\lambda} \right)^2 = \left(\frac{1600}{11000} \right)^2 \approx 0.021$$

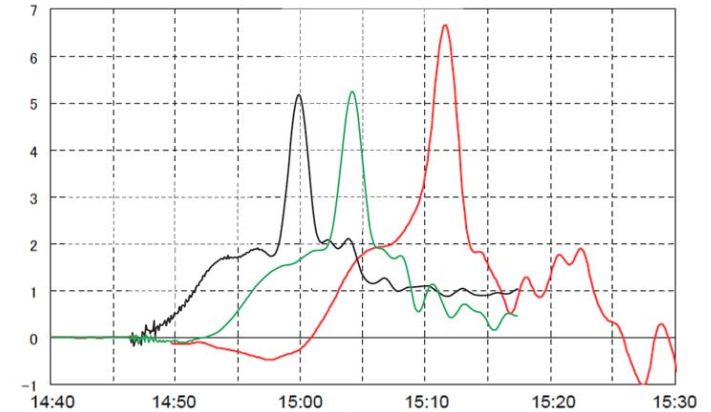
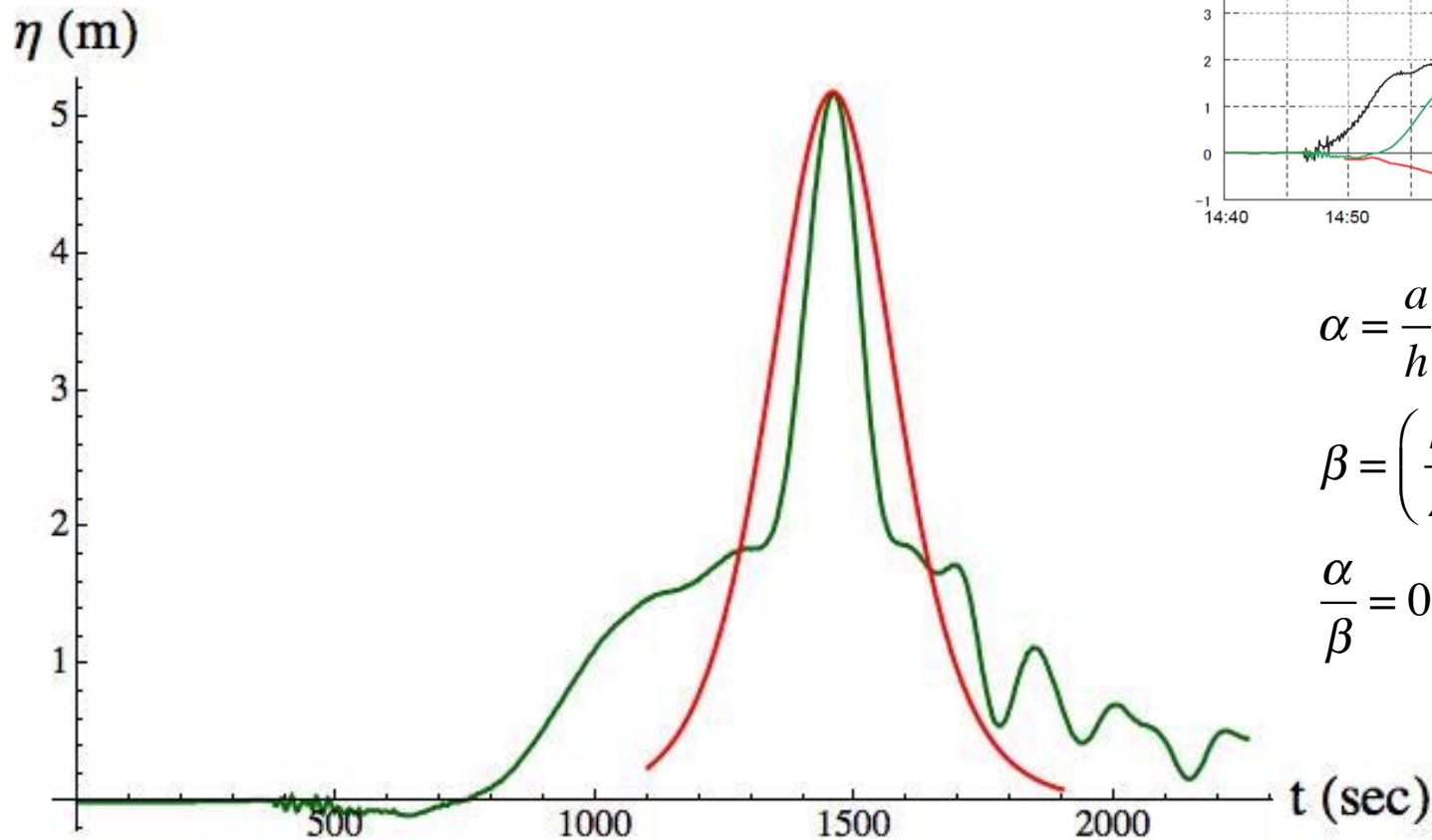
$$U_r = \frac{\alpha}{\beta} = 0.15 \quad (\text{The Ursell Number})$$

Seabed Pressure Transducers (ERI, University of Tokyo)

$h = 1,000$ m; $x = 40$ km.

The wave form becomes closer to that of soliton.

$$\eta = a \operatorname{sech}^2 \left[\sqrt{\frac{3a}{4h^3}} \left(x - c_0 \left(1 + \frac{a}{2h} \right) t \right) \right]$$



$$\alpha = \frac{a}{h} = \frac{5.2}{1000} \approx 0.0052$$

$$\beta = \left(\frac{h}{\lambda} \right)^2 = \left(\frac{1000}{9600} \right)^2 \approx 0.011$$

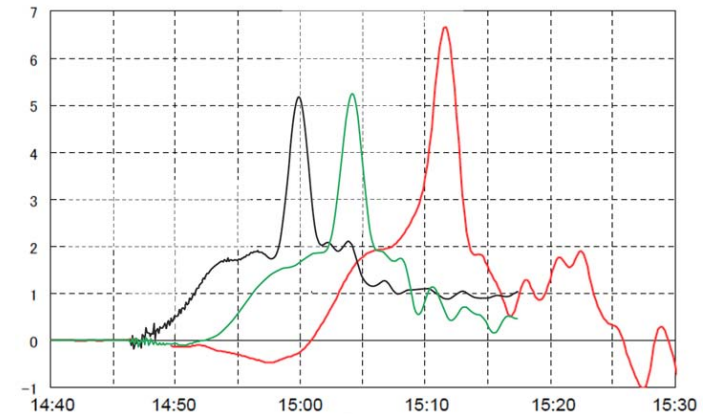
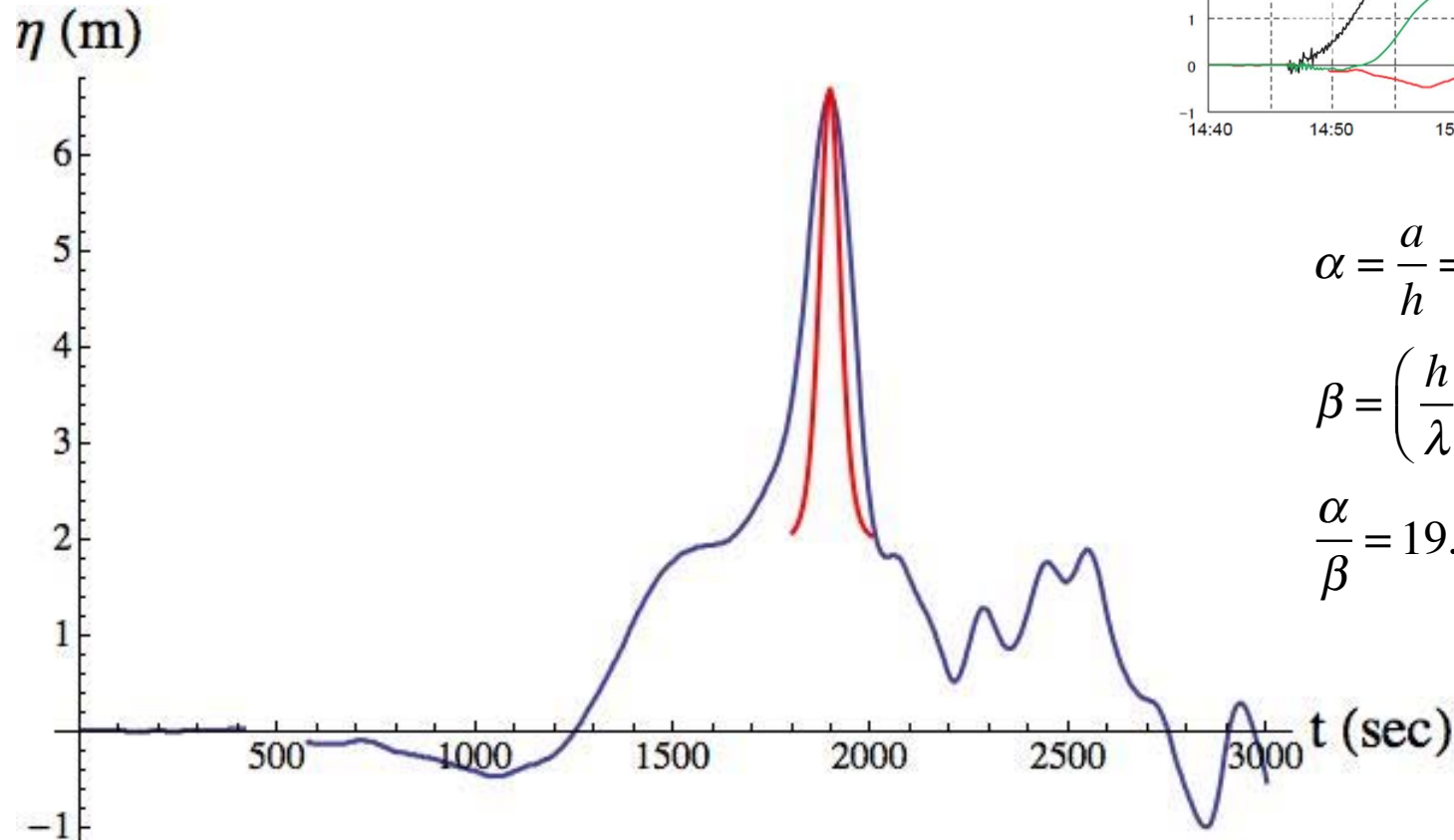
$$\frac{\alpha}{\beta} = 0.47$$

GPS Wave Gage: 20 km off Kamaishi

The Spike Riding on the Broad Tsunami resembles a soliton profile?

$$\eta = a \operatorname{sech}^2 \left[\sqrt{\frac{3a}{4h^3}} \left(x - c_0 \left(1 + \frac{a}{2h} \right) t \right) \right]$$

$$h = 204 \text{ m}; \quad x = 20 \text{ km}$$



$$\alpha = \frac{a}{h} = \frac{6.7}{204} \approx 0.033$$

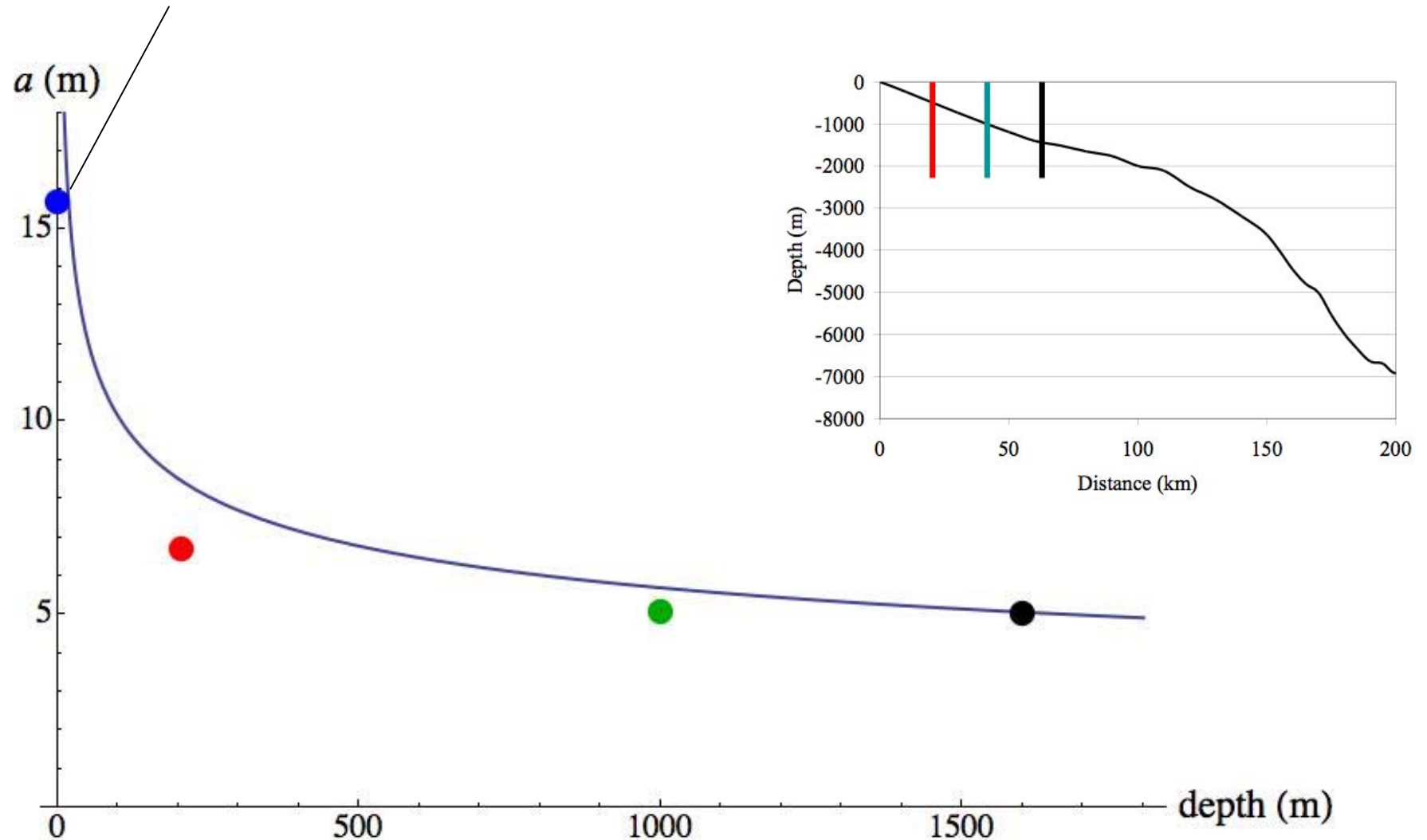
$$\beta = \left(\frac{h}{\lambda} \right)^2 = \left(\frac{204}{5000} \right)^2 \approx 0.0017$$

$$\frac{\alpha}{\beta} = 19.4$$

Tsunami amplification (Shoaling)

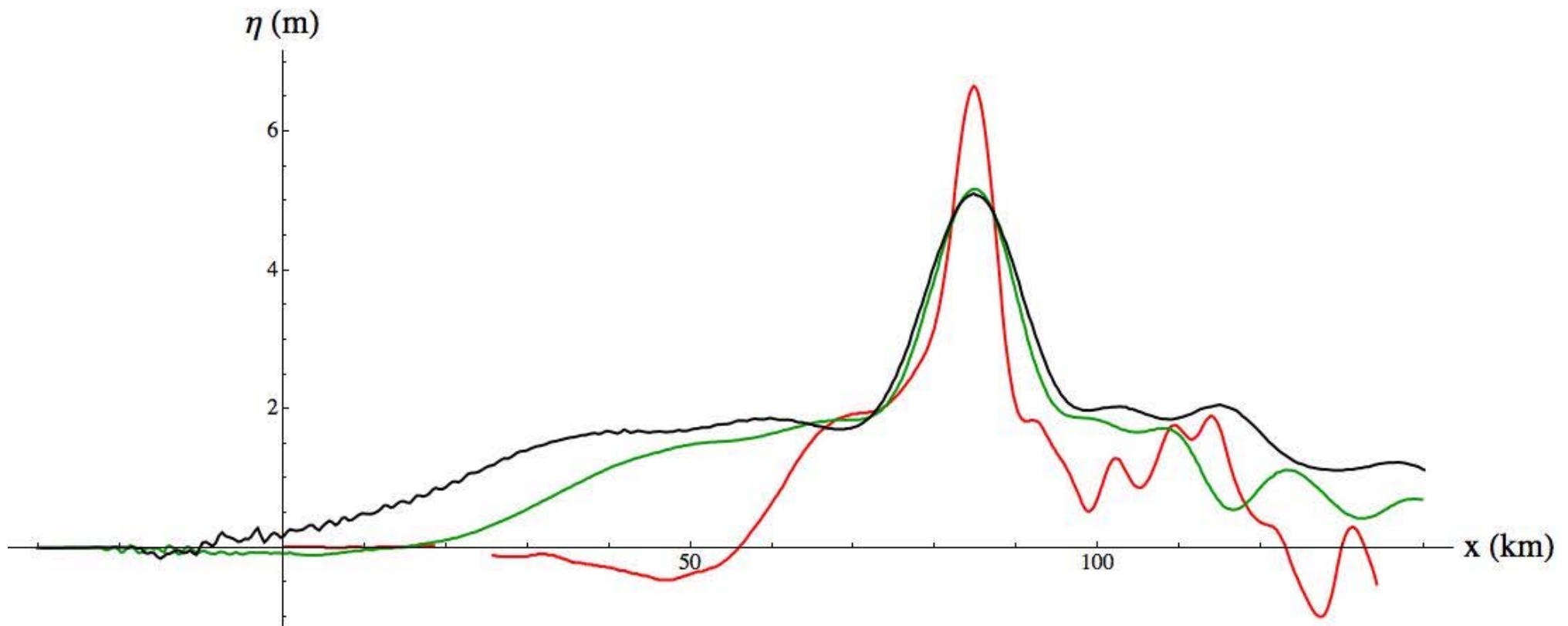
$$\text{Green's Law: } a \propto h^{-1/4}$$

Measured runup heights onshore near Kamaishi: $15.7 \text{ m} \pm 6.7 \text{ m}$.



Spatial Profiles

The sharply peaked wave riding on the broad tsunami base appears to maintain its “symmetrical” waveform with increase in amplitude and narrow in wave breadth.



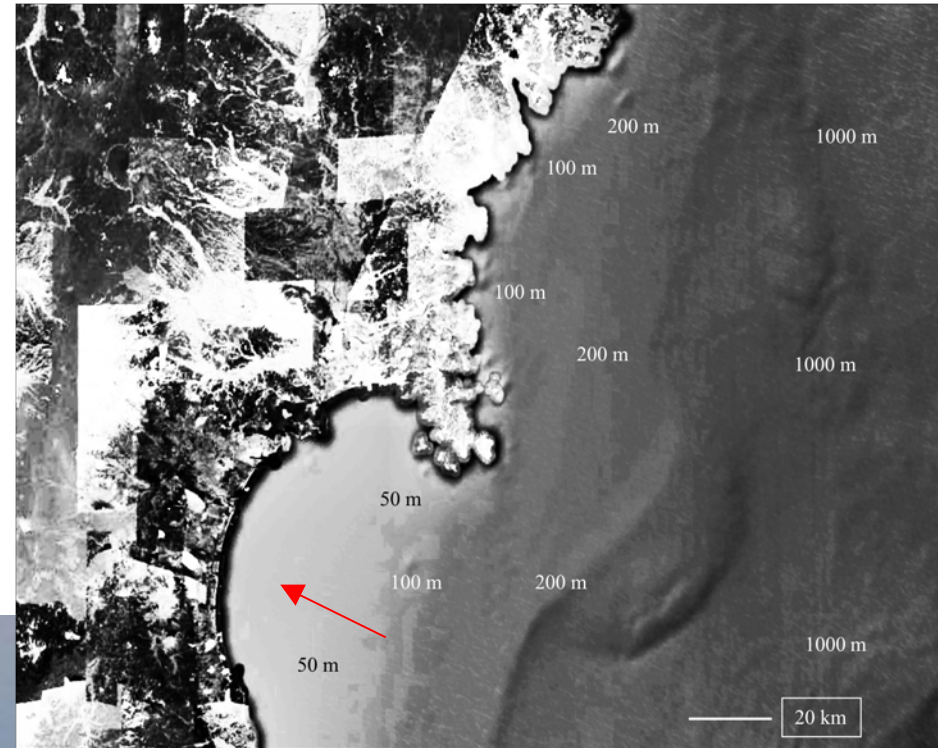
2. Can Miles's four-fold amplification of the Mach reflection be realized in the real fluid environment ?

The 1946 Aleutian Tsunami



Wiegel (1964)

The 2011 East Japan Tsunamis approaching the Sendai Plain



The March 11 2011 East Japan Tsunami

The City of Otsuchi, Japan



The March 11 2011 East Japan Tsunami

The City of Otsuchi, Japan



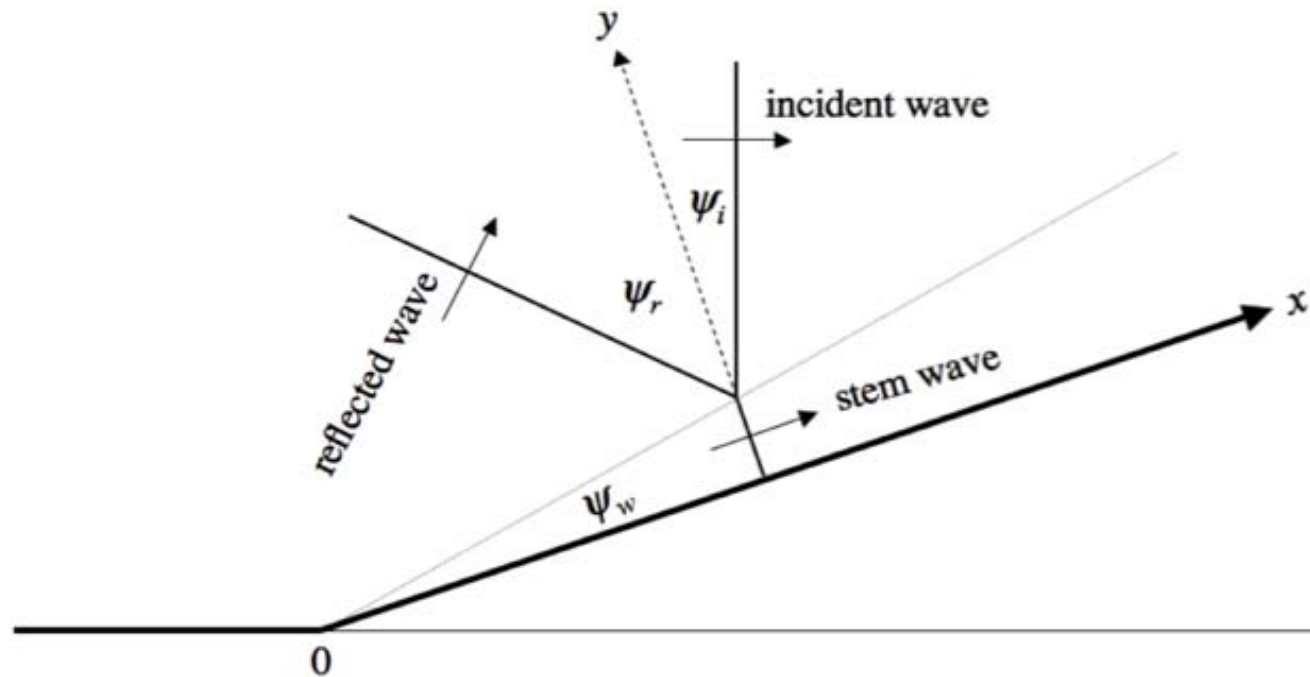
Wave amplification at the reflection must be important



Mach Reflection of Solitary Wave



Definition Sketch: Mach Reflection



- quiescent water depth, h_o
- **incident wave amplitude**, $a_i = a_i^* / h_o$
- **stem-wave amplification**, $\alpha_w = a_w / a_i$
- propagation distance, $x = x^* / h_o$
- propagation time, $t = t^*(g / h_o)^{1/2}$

Shallow-Water-Wave Approximation

For 3D irrotational flows:

$$\tilde{\phi}_{\tilde{x}\tilde{x}} + \tilde{\phi}_{\tilde{y}\tilde{y}} + \tilde{\phi}_{\tilde{z}\tilde{z}} = 0 \quad \text{for } 0 \leq \tilde{z} \leq \tilde{h}_0 + \tilde{\eta}(\tilde{x}, \tilde{y}, \tilde{t})$$

$$\tilde{\phi}_{\tilde{z}} = 0 \quad \text{on } \tilde{z} = 0$$

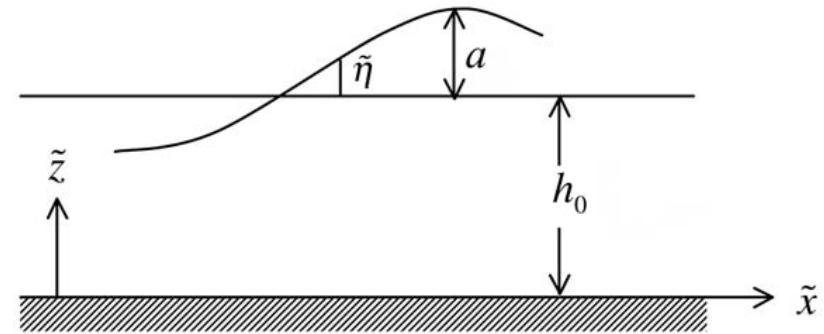
$$\left. \begin{aligned} \tilde{\phi}_{\tilde{t}} + \frac{1}{2}(\tilde{\phi}_{\tilde{x}}^2 + \tilde{\phi}_{\tilde{y}}^2 + \tilde{\phi}_{\tilde{z}}^2) + g\tilde{\eta} &= 0 \\ \tilde{\eta}_{\tilde{t}} + \tilde{\phi}_{\tilde{x}}\tilde{\eta}_{\tilde{x}} + \tilde{\phi}_{\tilde{y}}\tilde{\eta}_{\tilde{y}} - \tilde{\phi}_{\tilde{z}} &= 0 \end{aligned} \right\} \quad \text{on } \tilde{z} = \tilde{\eta} + h_0$$

Scaling:

$\lambda_0 \sim$ dominant horizontal length scale

$h_0 \sim$ vertical length scale

$a_0 \sim$ dominant amplitude scale



Set $h_0/\lambda_0 \ll 1$ for long waves, and:

$$\tilde{x} = x \lambda_0, \quad \tilde{y} = y \lambda_0, \quad \tilde{z} = z h_0, \quad \tilde{t} = \frac{\lambda_0}{C_0} t, \quad \tilde{\eta} = a_0 \eta, \quad \tilde{\phi} = \frac{a_0}{h_0} \lambda_0 C_0 \phi,$$

John Miles 1977

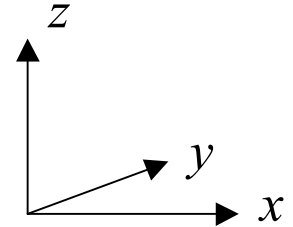
$$\beta \Delta \phi + \phi_{zz} = 0 \quad \text{in } 0 < z < 1 + \alpha \eta$$

$$\phi_z = 0 \quad \text{on } z = 0$$

$$\eta_t + \alpha \nabla \phi \cdot \nabla \eta - \beta^{-1} \phi_z = 0$$

$$\eta + \phi_t + \frac{1}{2} \alpha (\nabla \phi)^2 + \frac{1}{2} \alpha \beta^{-1} \phi_z^2 = 0$$

$$\left. \begin{array}{l} \eta_t + \alpha \nabla \phi \cdot \nabla \eta - \beta^{-1} \phi_z = 0 \\ \eta + \phi_t + \frac{1}{2} \alpha (\nabla \phi)^2 + \frac{1}{2} \alpha \beta^{-1} \phi_z^2 = 0 \end{array} \right\} \quad \text{on } z = 1 + \alpha \eta$$



$$\text{where } \Delta = \partial_{xx} + \partial_{yy}; \quad \nabla = (\partial_x, \partial_y); \quad \alpha = a / h_0; \quad \beta = (h_0 / \lambda_0)^2$$

Expand in z to satisfy the field equation and the bottom boundary condition:

$$\phi(x, y, z, t) = f - \beta \Delta f \frac{z^2}{2} + \beta^2 \Delta^2 f \frac{z^4}{4!} + O(\beta^3) \quad f = f(x, y, t)$$

Substituting this form into the free surface boundary conditions on $z = 1 + \alpha \eta$:

$$f_{tt} - \Delta f = -\alpha \left[\frac{1}{2} f_t^2 + (\nabla f)^2 \right]_t + \frac{1}{3} \beta f_{ttt} + O(\alpha^2, \beta^2, \alpha \beta) = 0$$

John Miles 1977

Weak Interactions:

$$\xi_i = x \cos \psi_i + y \sin \psi_i - t, \quad i = 1, 2$$

$$\tau = \varepsilon t$$

$$\psi = \frac{1}{2} |\psi_1 - \psi_2|$$



$$(\partial_1 + \partial_2) \left[2\alpha \partial_\tau f + \frac{1}{3} \beta (\partial_1 + \partial_2)^3 f + \alpha \left\{ \frac{3}{2} ((\partial_1 f)^2 + (\partial_2 f)^2) + (3 - 4K) (\partial_1 f) (\partial_2 f) \right\} \right] - 4K \partial_1 \partial_2 f = O(\alpha^2)$$

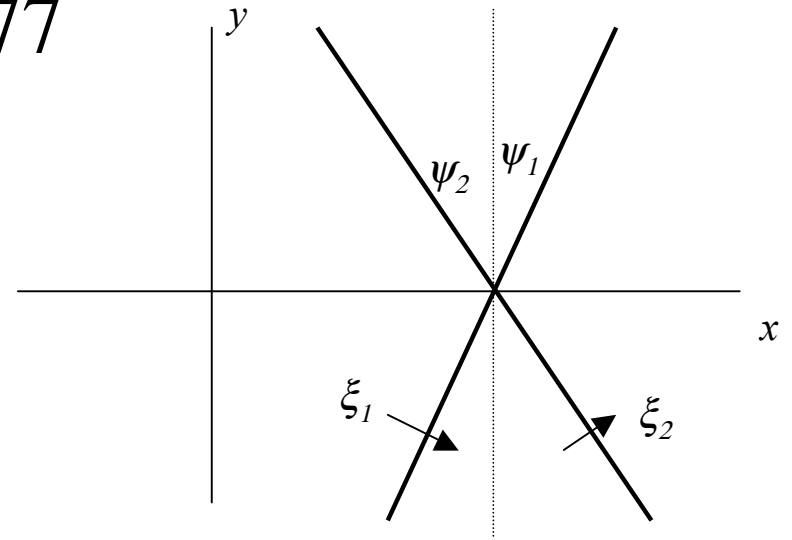
where $K = \sin^2 \psi = \sin^2 \frac{1}{2} (\psi_1 - \psi_2)$ and $\partial_i = \partial / \partial \xi_i$

Take the interaction of the form: $f(\xi_1, \xi_2, \tau) = F_1(\xi_1, \tau) + F_2(\xi_2, \tau) + \alpha F_{12}(\xi_1, \xi_2, \tau)$

When $\sin^2 \psi \gg O(\alpha)$, the interaction amplitude:

$$\frac{a_w}{a_i} = \alpha_w = 2 + \alpha_i \left(\frac{3}{2 \sin^2 \psi_i} - 3 + 2 \sin^2 \psi_i \right).$$

“Non-Grazing” Interaction



John Miles 1977

Strong Interaction: $K = \sin^2 \psi \sim O(\alpha_i)$

Extend the recipe for unidirectional interaction of two KdV solitons by Whitham (1974), the transformation: $f = (\partial_1 + \partial_2) \log E(\theta_1, \theta_2)$; $\theta_i = x \cos \psi + (-1)^i z \sin \psi - c t$

$$(\partial_1 + \partial_2) \left[2\alpha \partial_\tau f + \frac{1}{3} \beta (\partial_1 + \partial_2)^3 f + \alpha \left\{ \frac{3}{2} \left((\partial_1 f)^2 + (\partial_2 f)^2 \right) + (3 - 4K)(\partial_1 f)(\partial_2 f) \right\} \right] - 4K \partial_1 \partial_2 f = O(\alpha^2)$$

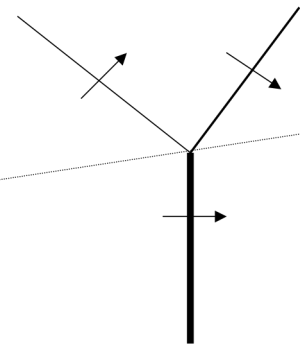
Amplification: $\frac{a_w}{a_i} = \alpha_w = \frac{4}{1 + \sqrt{1 - k^{-2}}}$ where $k = \frac{\sin \psi_i}{\sqrt{3\alpha_i}} > 1$

For $k < 1$, consider resonant triad interaction among three solitons:

$$\sin \psi_i \approx \tan \psi_i \approx \psi_i \quad \text{and} \quad \cos \psi_i \approx 1$$

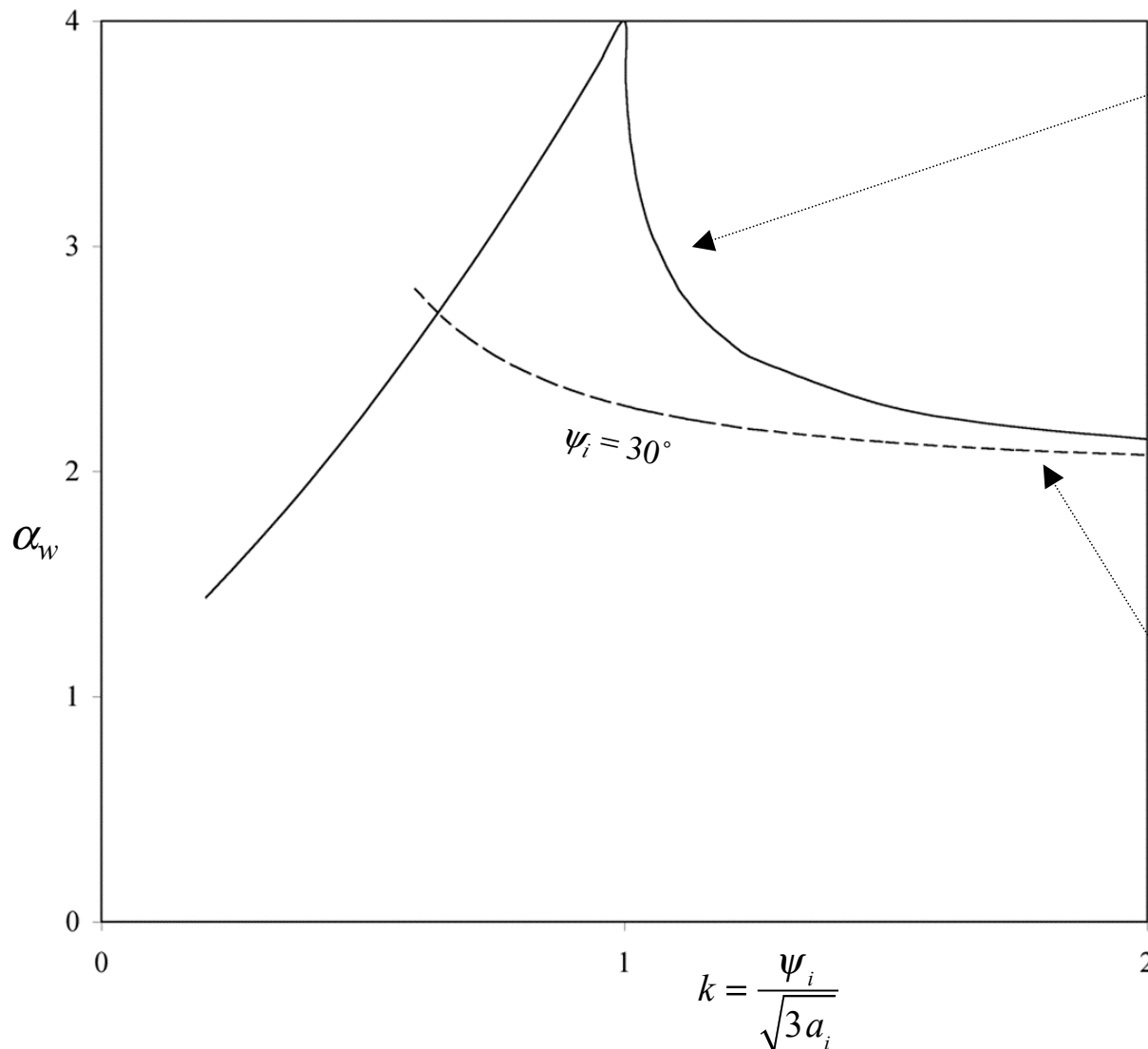
Resonant triad: $k_3 = k_2 \pm k_1$; $k_3 \psi_3 = k_2 \psi_2 \pm k_1 \psi_1$

Amplification: $\frac{a_w}{a_i} = \alpha_w = (1 + k)^2$ where $k = \frac{\psi_i}{\sqrt{3\alpha_i}} < 1$



John Miles, 1977

Summary of stem-wave amplification at the wall



Solid line - strong interaction:
For $\psi \approx O(a)$

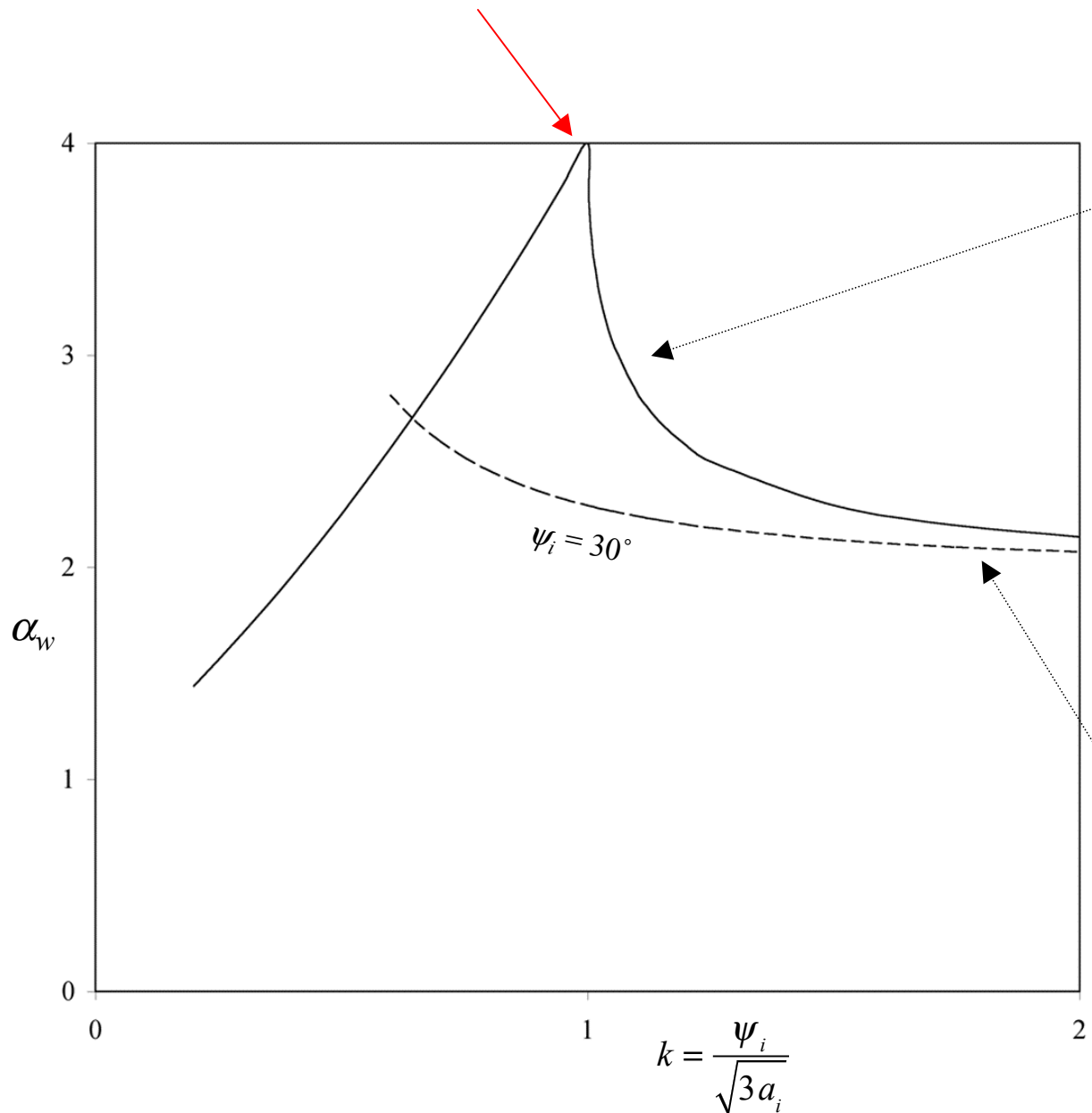
$$\alpha_w = \begin{cases} \frac{4}{1 + \sqrt{1 - k^{-2}}} & \text{for } k^2 > 1 \\ (1 + k)^2 & \text{for } k^2 \leq 1 \end{cases}$$

Broken line
Non-grazing (weak) interaction
= regular reflection.
For $\sin^2 \psi \gg a$

$$\alpha_w = 2 + a_i \left(\frac{3}{2 \sin^2 \psi_i} - 3 + 2 \sin^2 \psi_i \right).$$

John Miles, 1977

Four-fold amplification! but not 2 – crucial for engineering design



Solid line - resonant interaction:
For $\psi \approx O(a)$:

$$\alpha_w = \begin{cases} \frac{4}{1 + \sqrt{1 - k^{-2}}} & \text{for } k^2 > 1 \\ (1 + k)^2 & \text{for } k^2 \leq 1 \end{cases}$$

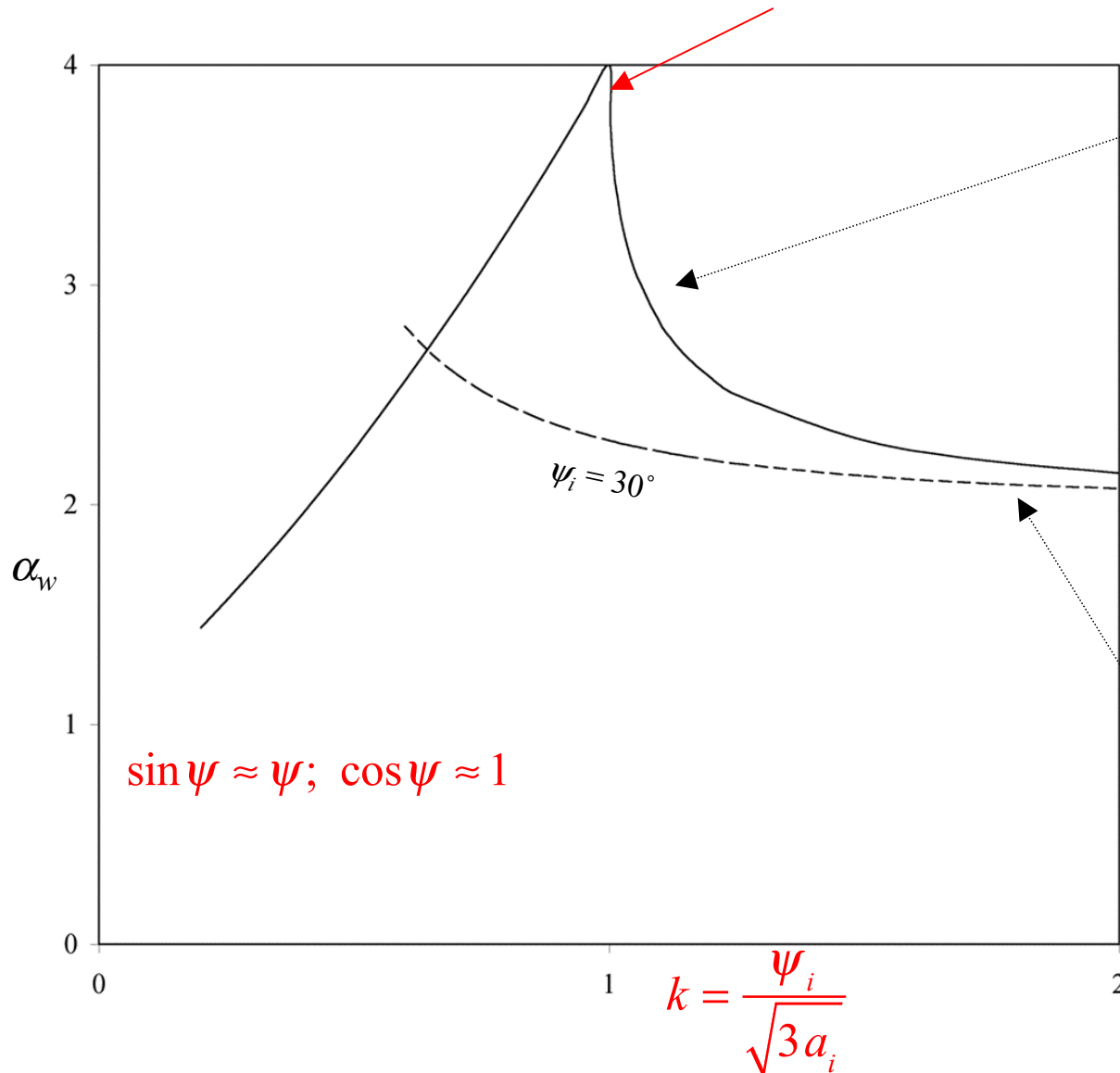
Broken line
Non-grazing (weak) interaction
= regular reflection.
For $\sin^2 \psi \gg a$

$$\alpha_w = 2 + a_i \left(\frac{3}{2 \sin^2 \psi_i} - 3 + 2 \sin^2 \psi_i \right).$$

John Miles, 1977

Four-fold amplification

But, difficult to realize the critical condition in the real-fluid environment



Solid line - resonant interaction:
For $\psi \approx O(a)$:

$$\alpha_w = \begin{cases} \frac{4}{1 + \sqrt{1 - k^{-2}}} & \text{for } k^2 > 1 \\ (1 + k)^2 & \text{for } k^2 \leq 1 \end{cases}$$

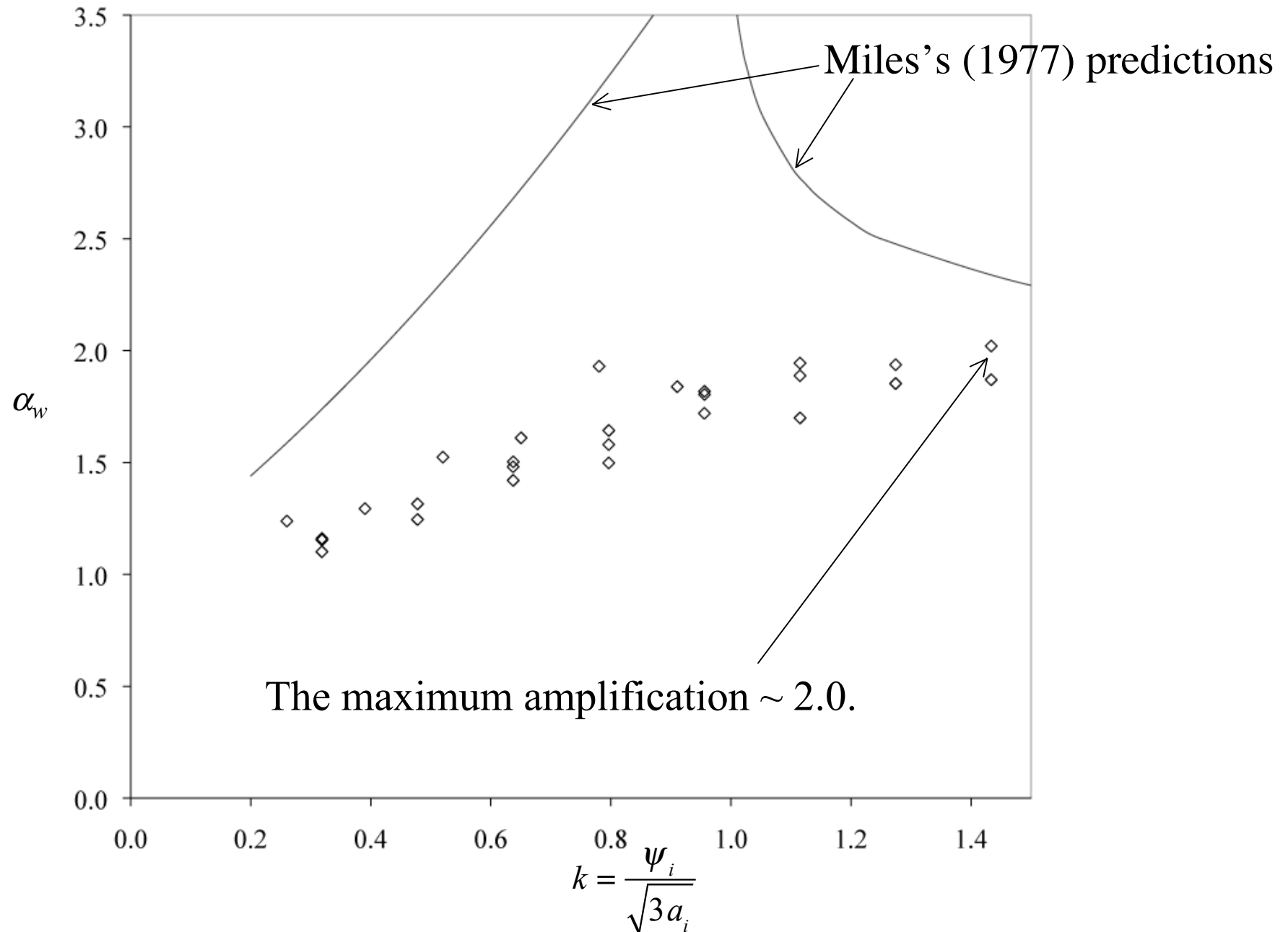
Broken line
Non-grazing (weak) interaction
= regular reflection.
For $\sin^2 \psi \gg a$ (or $k \gg 1$)

$$\alpha_w = 2 + a_i \left(\frac{3}{2 \sin^2 \psi_i} - 3 + 2 \sin^2 \psi_i \right).$$

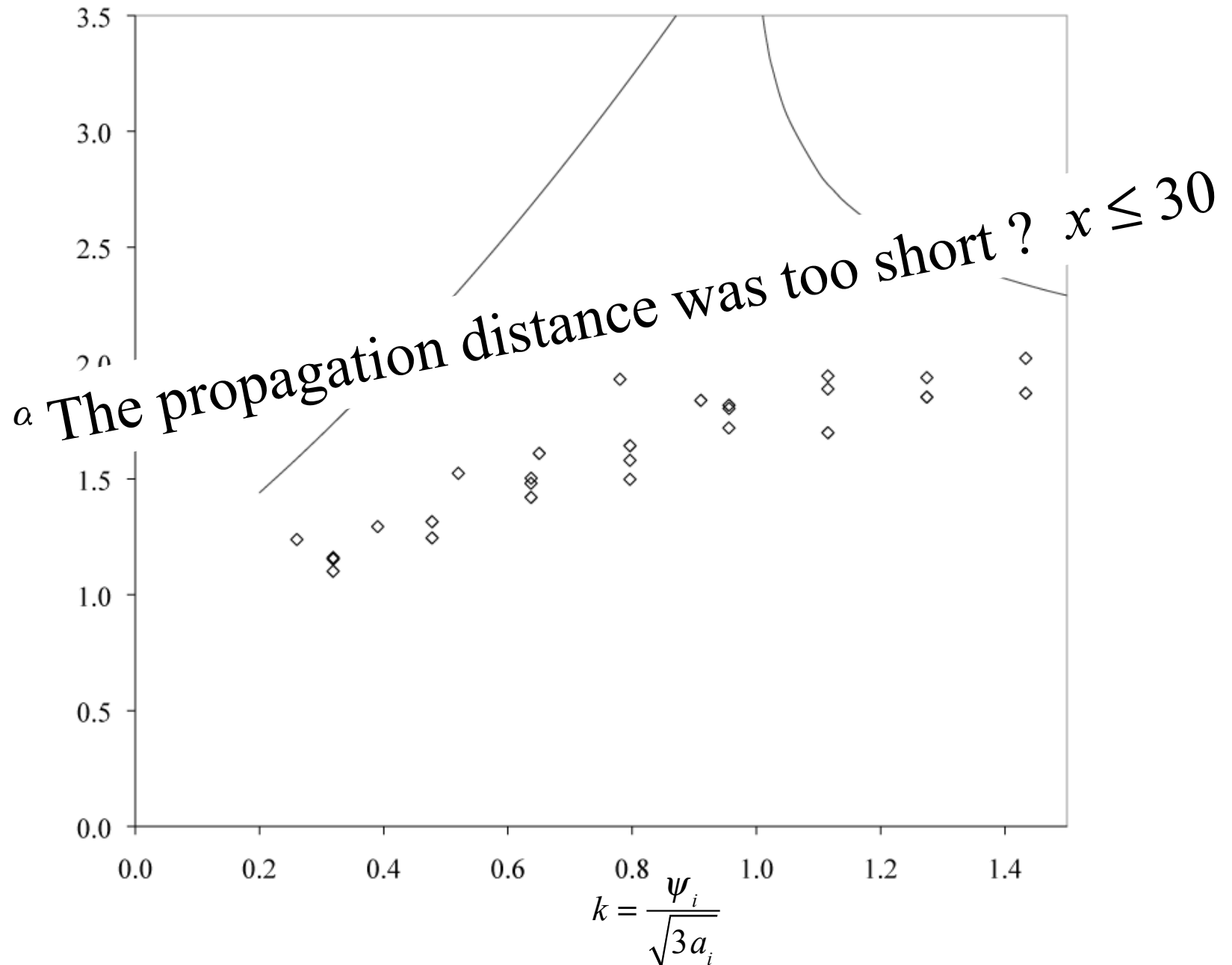
Laboratory Experiments by Melville (1980)

- Wave basin: 18.3 m long and 6.2 m wide with water of 0.2 and 0.3 m depth.
- Used small wave amplitudes $a_i = 0.10$ & 0.15 , $10^\circ \leq \psi_i \leq 45^\circ$
- The propagation distance was rather short: $24 \leq x \leq 30$, $h_0 = 20$ and 30 cm.

Laboratory Experiments by Melville (1980)

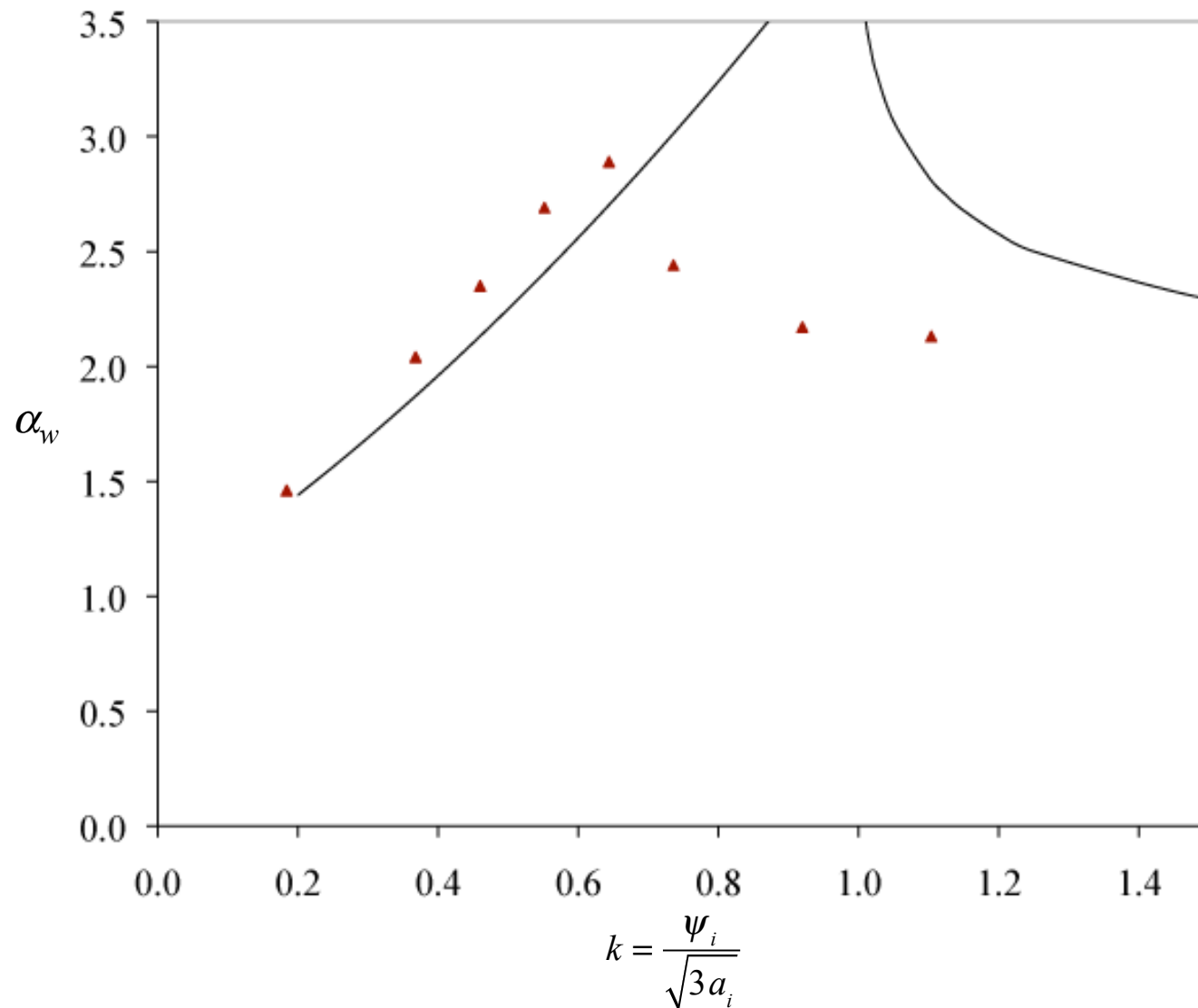


Laboratory Experiments by Melville (1980)



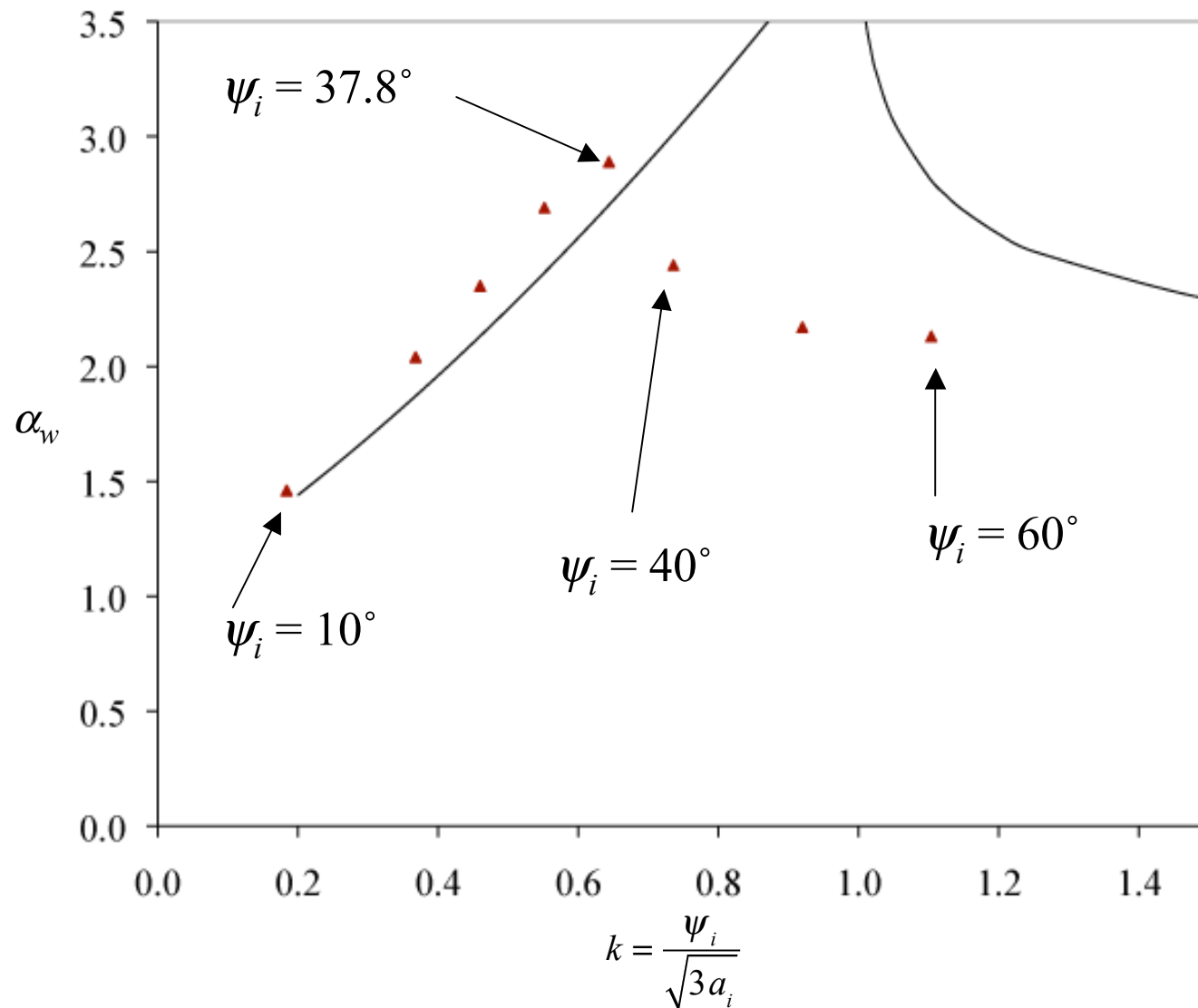
Numerical Experiments by Tanaka (1993)

Numerical simulations of the Euler model with $a_i = 0.3$ using the high-order spectral method.



Numerical Experiments by Tanaka (1993)

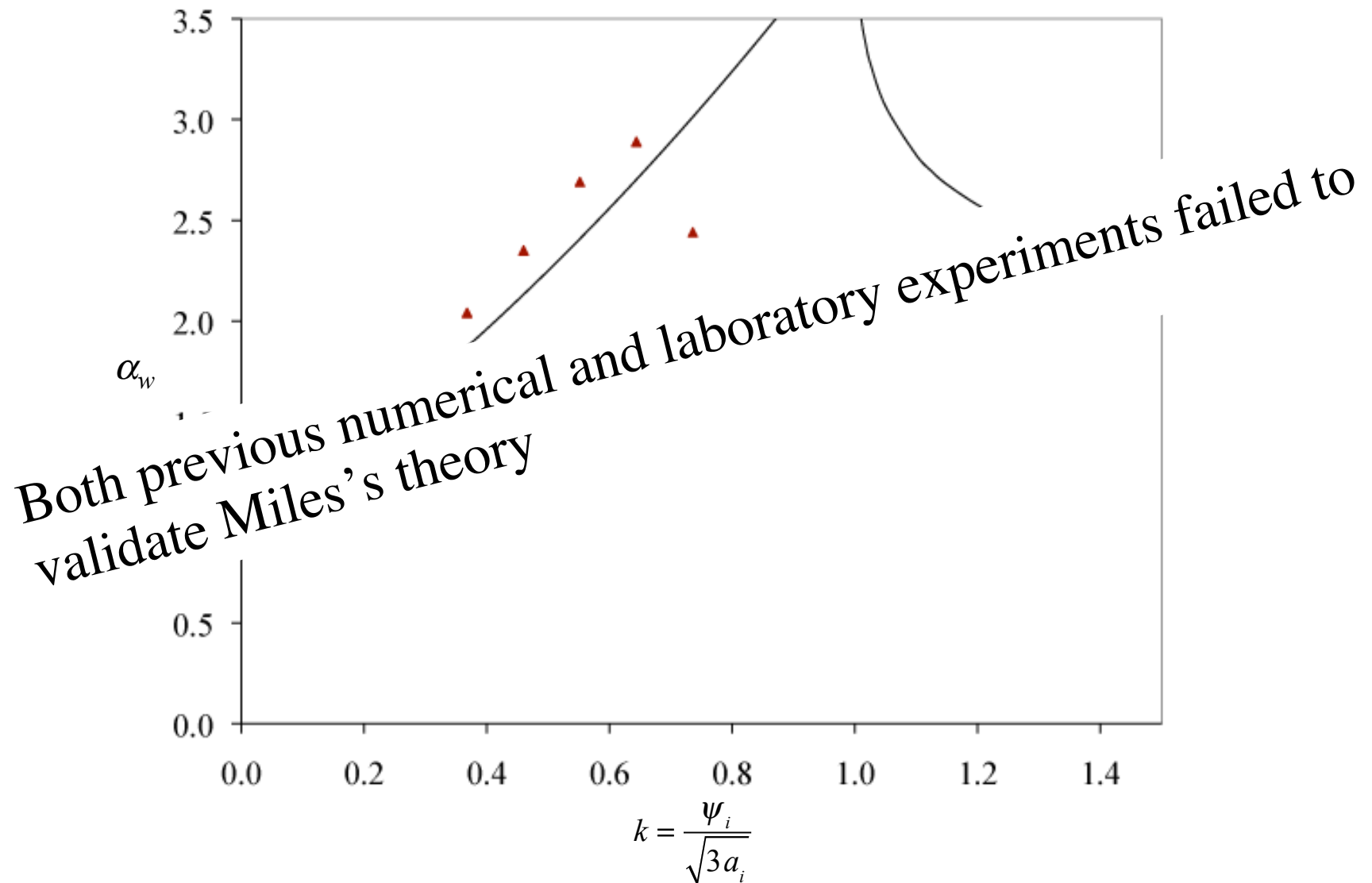
Numerical simulations of the Euler model with $a_i = 0.3$ (fixed) using the high-order spectral method.



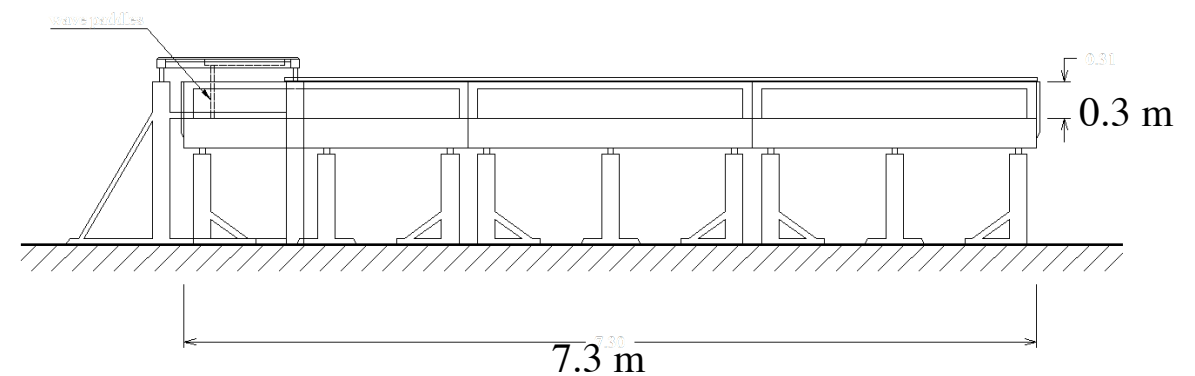
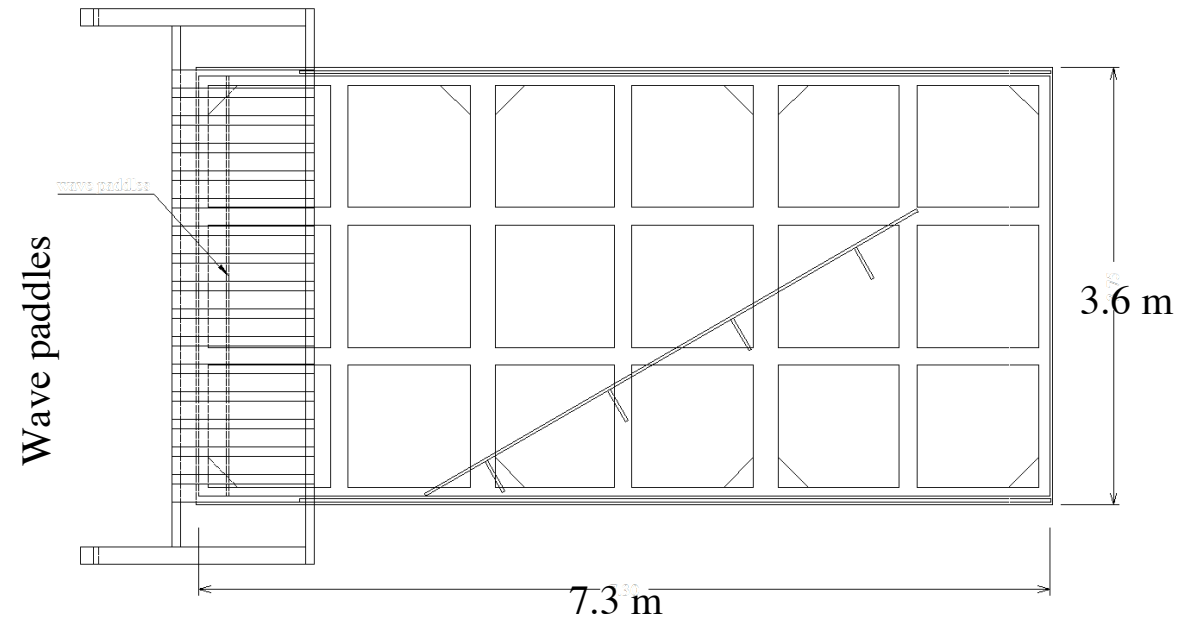
$\psi_i = O(\varepsilon) ??$

Numerical Experiments by Tanaka (1993)

Numerical simulations of the Euler model with $a_i = 0.3$ using the high-order spectral method.

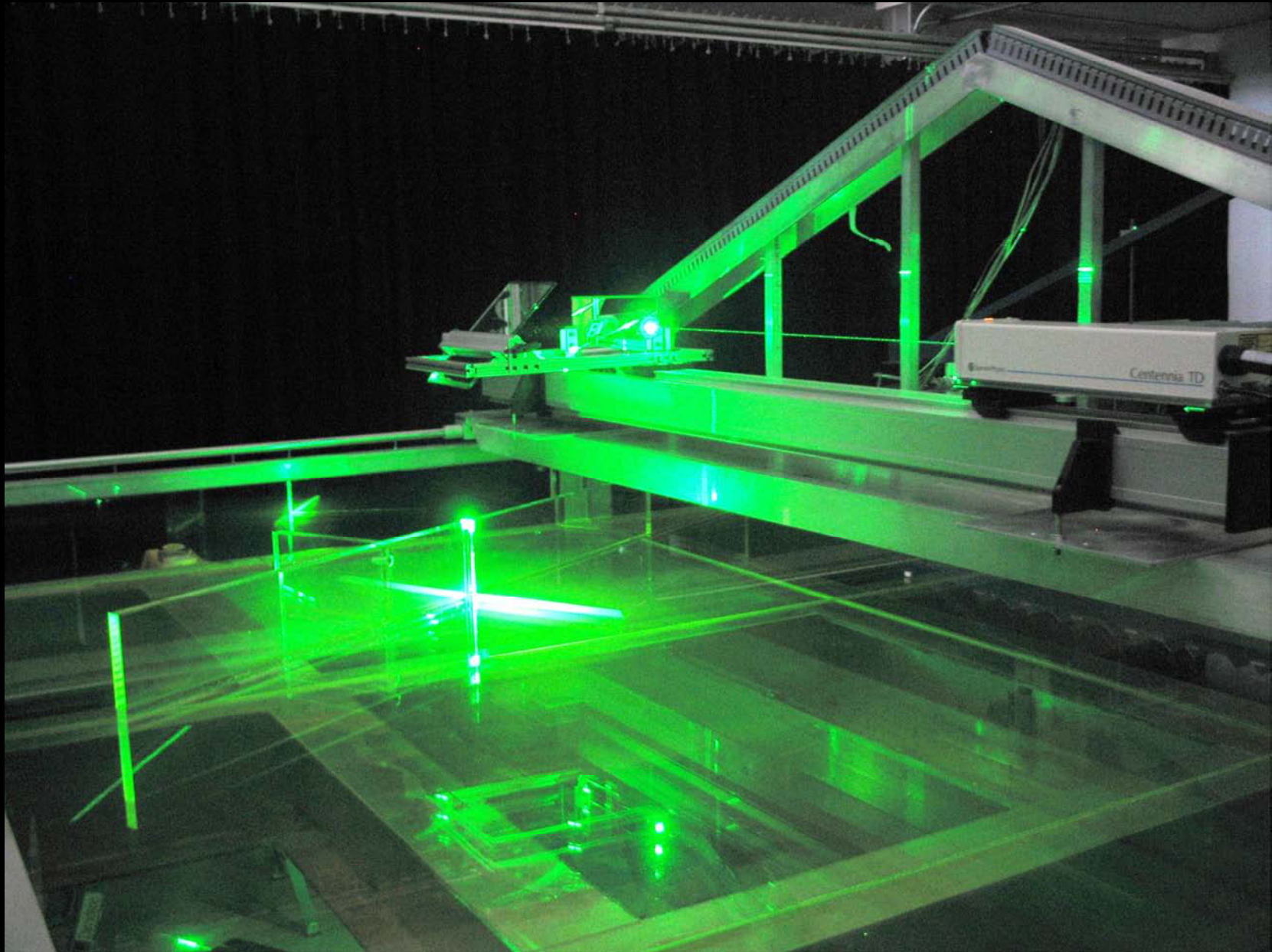


Wave Tank in Graf Hall, Oregon State U.

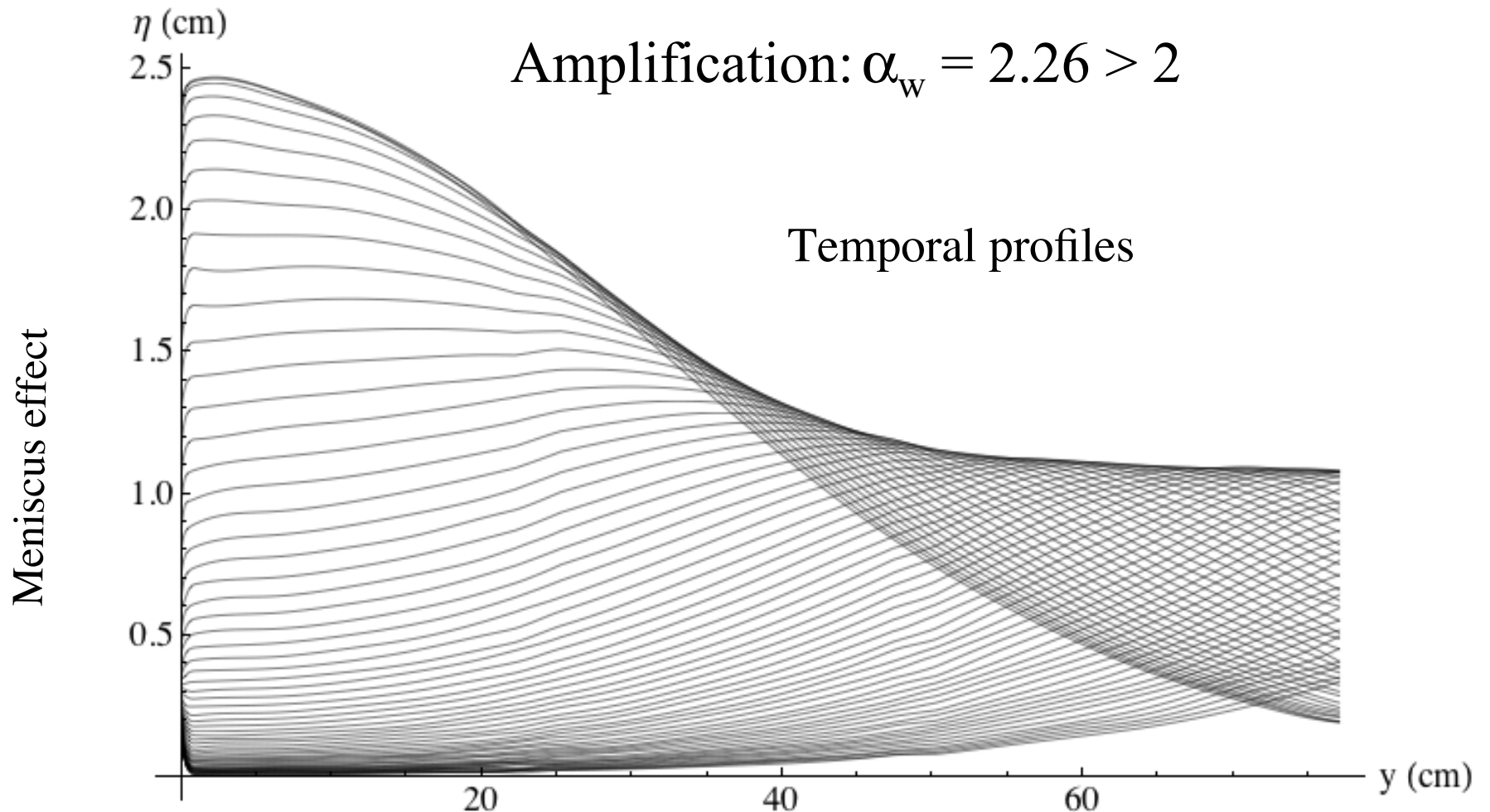


Wave paddles driven by 16 linear motors

Laser Induced Fluorescent Technique to Capture Water-Surface Profiles



Wave Profiles along the Direction Normal to the Wall

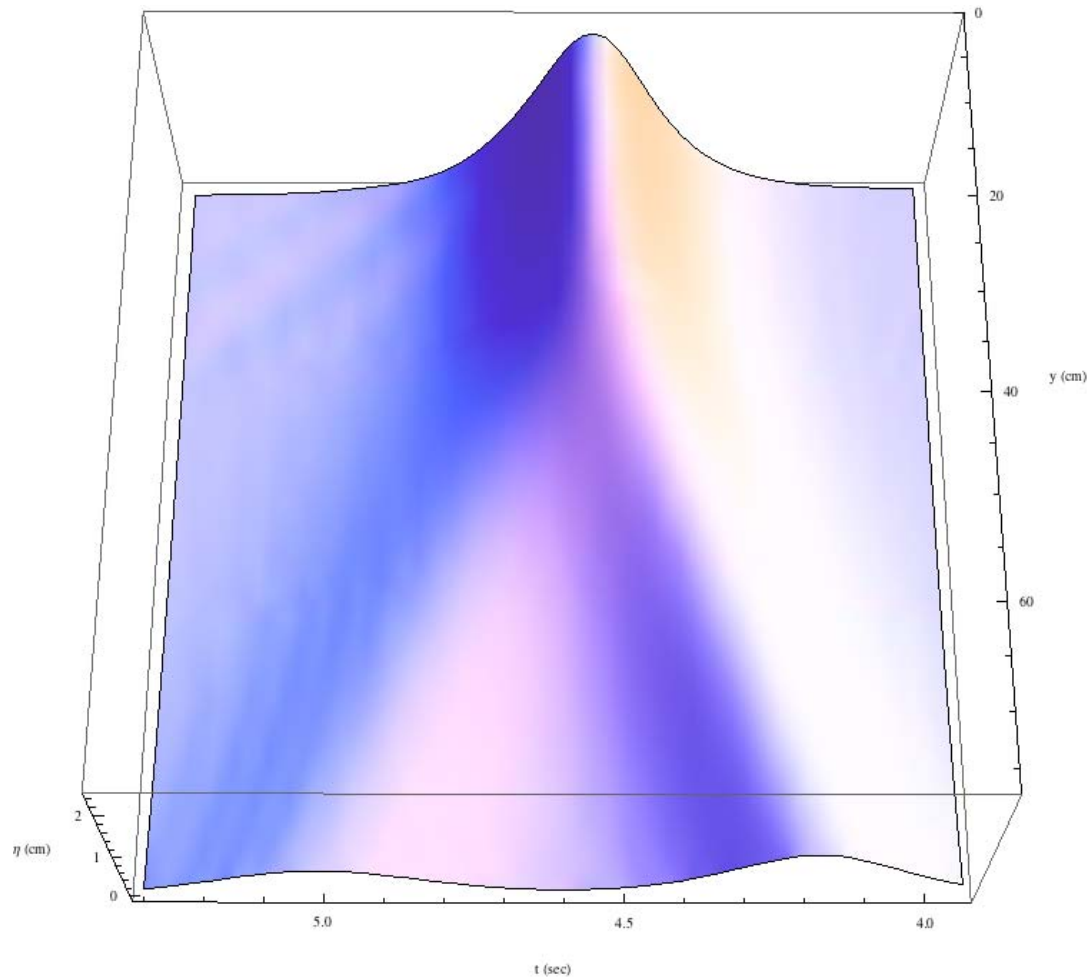


$$h_0 = 6.0 \text{ cm}; \quad \psi_i = 30^\circ; \quad a_i = 0.182 \text{ (1.09 cm)}; \quad x = 71.1 \text{ (427 cm)}$$

Recall that Melville's experiment: $x < 30$

Temporal Variation of Measured Water-Surface

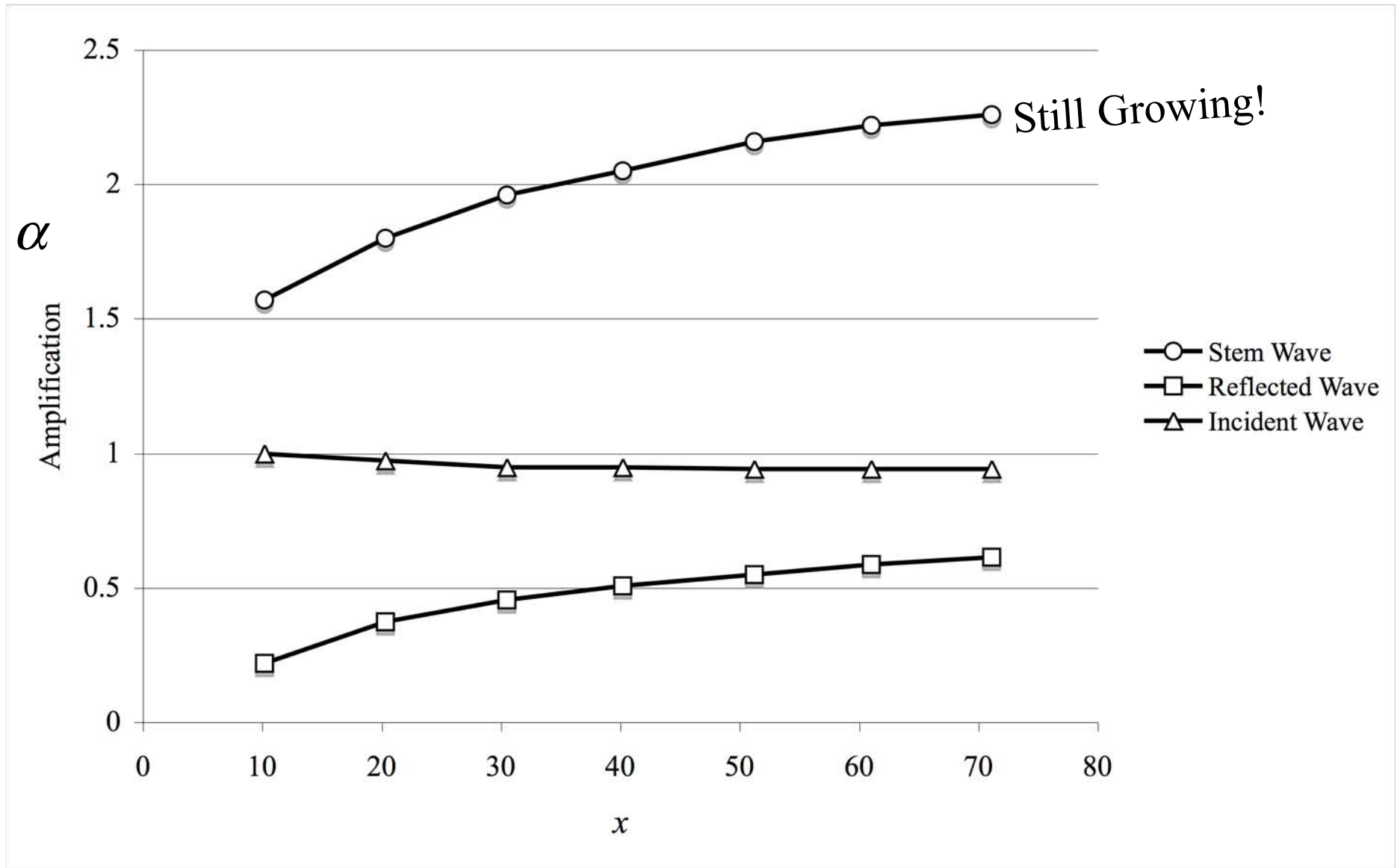
($t - y$ plane; the wall at $y = 0$)



$$\alpha_w = 2.26 > 2$$

$$h_0 = 6.0 \text{ cm}; \quad \psi_i = 30^\circ; \quad a_i = 0.182; \quad x = 71.1$$

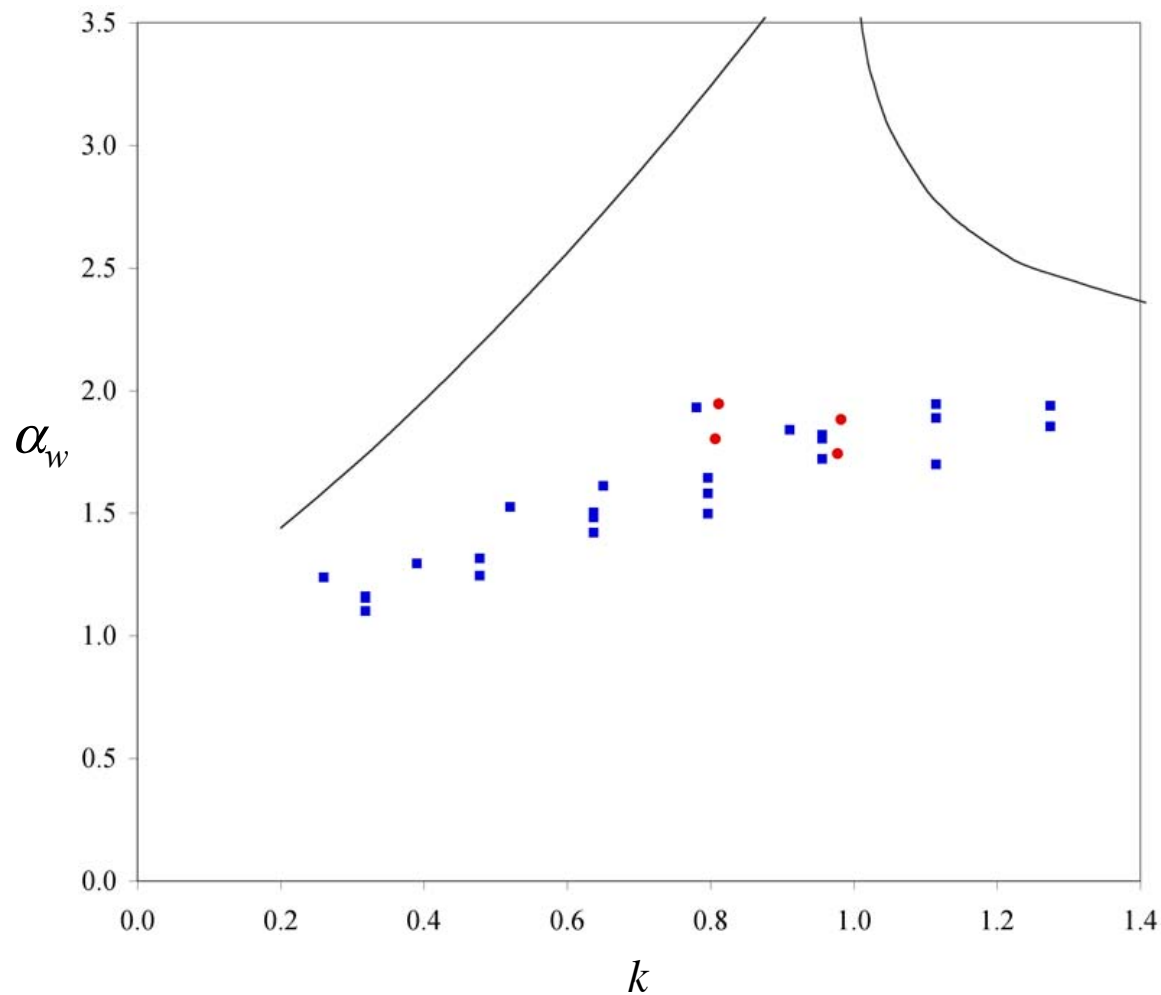
Growth of the stem-wave amplification



$h_0 = 6.0$ cm; $\psi_i = 30^\circ$; $a_i = 0.193$ (1.16 cm) at $x = 10.2$ (61 cm)

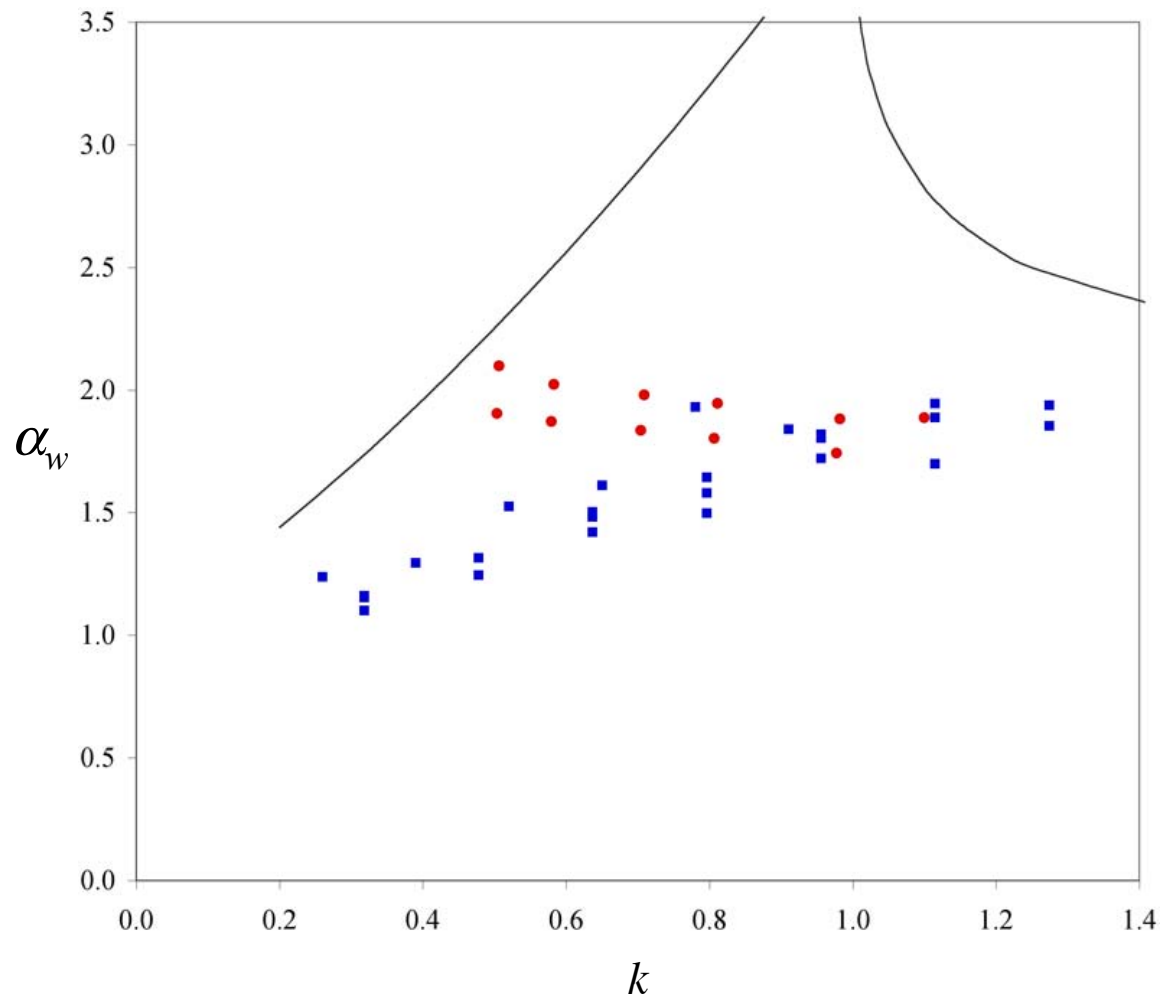
Comparison with Melville's Data (1980)

- Melville: $a_i = 0.10$ & 0.15 , $10^\circ \leq \psi_i \leq 45^\circ$, $24 \leq x \leq 30$, $h_0 = 20$ and 30 cm
- Our data: $0.099 < a_i < 0.147$, $\psi_i = 30^\circ$, $x = 20.32$ and 30.48 , $h_0 = 6.0$ cm



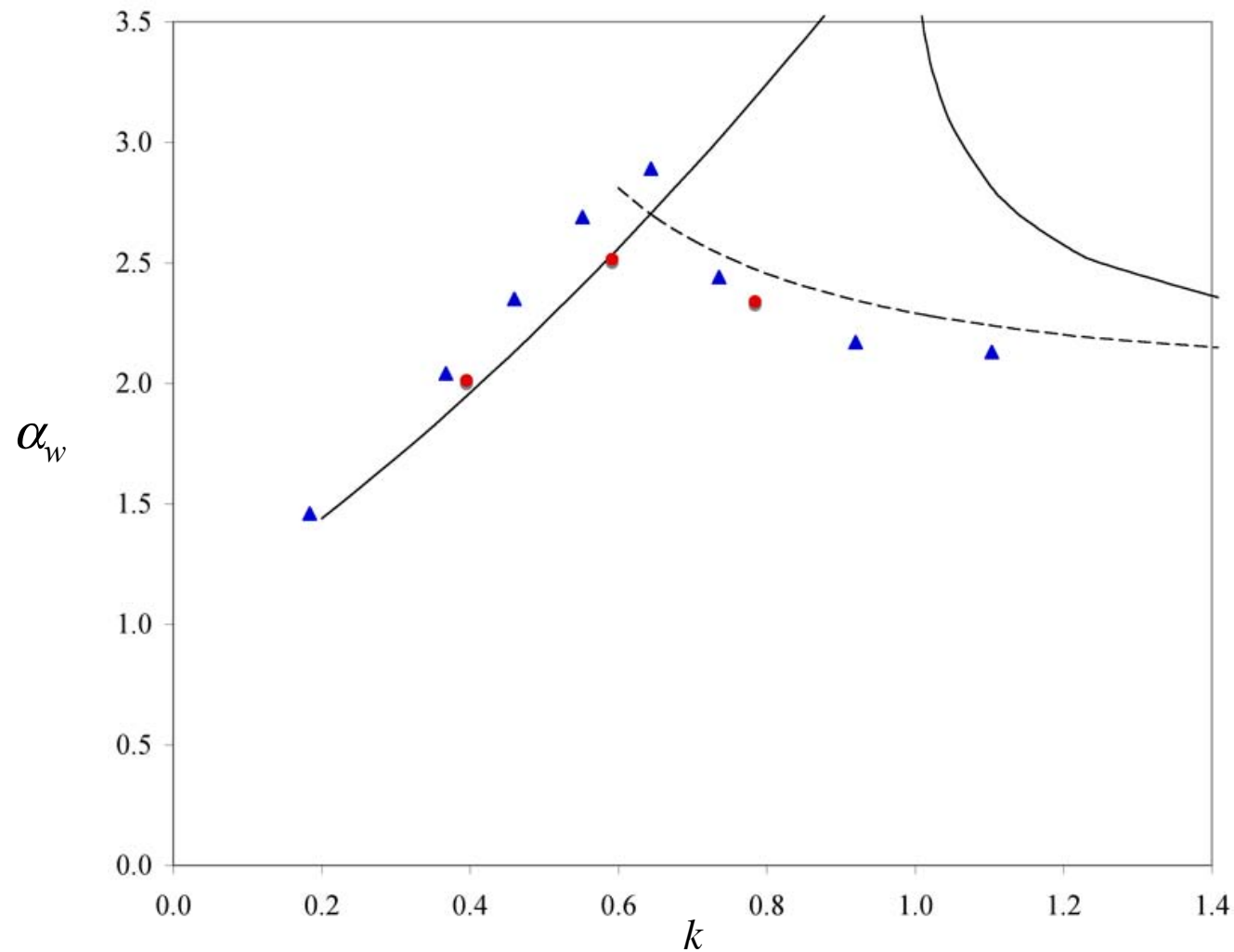
Comparison with Melville's Data (1980)

- Melville: $a_i = 0.10$ & 0.15 , $10^\circ \leq \psi_i \leq 45^\circ$, $24 \leq x \leq 30$, $h_0 = 20$ and 30 cm
- Our data: **$0.076 < a_i < 0.360$** , $\psi_i = 30^\circ$, $x = 20.32$ and 30.48 , $h_0 = 6.0$ cm



Comparison with Tanaka's Data (1993)

- Tanaka (blue): $a_i = 0.30$, $10^\circ \leq \psi_i \leq 60^\circ$, $x = 150$
- Our data (red): $a_i = 0.28$, $20^\circ \leq \psi_i \leq 40^\circ$, $x = 71.1$

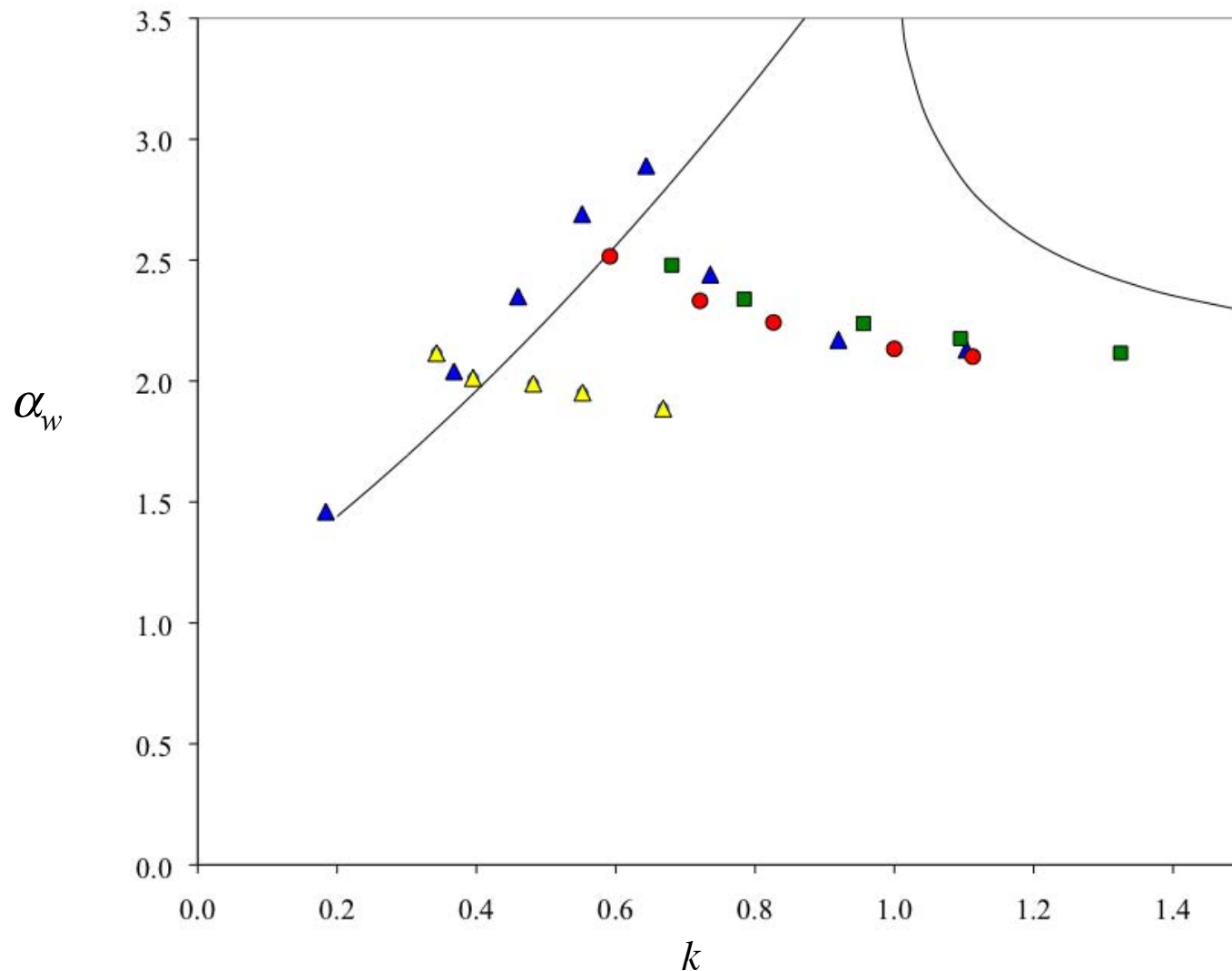


Stem Wave Amplification

Tanaka **(blue)**: $x = 150$, $10^\circ \leq \psi_i \leq 60^\circ$, $a_i = 0.30$.

Our data $x = 71.1$: **(Green)** $\psi_i = 40^\circ$, $0.093 < a_i < 0.35$; **(Red)** $\psi_i = 30^\circ$, $0.074 < a_i < 0.26$;

(Yellow) $\psi_i = 20^\circ$, $0.091 < a_i < 0.35$

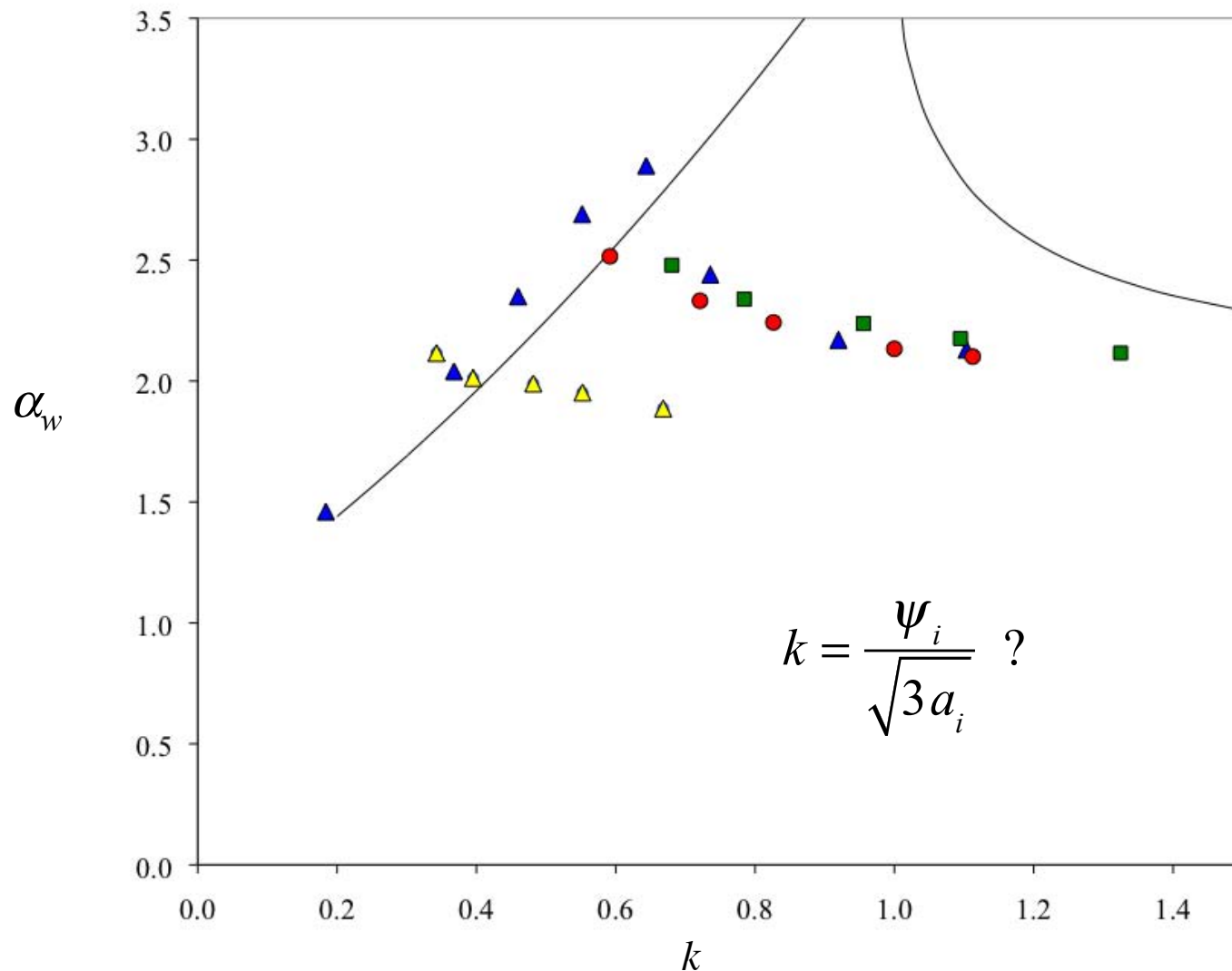


Stem Wave Amplification

Tanaka **(blue)**: $x = 150$, $10^\circ \leq \psi_i \leq 60^\circ$, $a_i = 0.30$.

Our data $x = 71.1$: **(Green)** $\psi_i = 40^\circ$, $0.093 < a_i < 0.35$; **(Red)** $\psi_i = 30^\circ$, $0.074 < a_i < 0.26$;

(Yellow) $\psi_i = 20^\circ$, $0.091 < a_i < 0.35$



Remarks

- Our laboratory results are consistent with the previous laboratory and numerical experiments (Melville, 1980; Tanaka, 1993): previous laboratory experiments were made with the limited propagation distance x and the numerical experiments were with single amplitude $a_i = 0.3$.
- Once again, Miles's theory failed to characterize the Mach stem phenomenon observed in the laboratory.
- Note that Miles's theory is for the asymptotic state and $\psi = O(\varepsilon)$ and $a = O(\varepsilon)$ for the strong interaction case.

Issues

- Interaction parameter $k = \psi_i / (3 a_i)^{1/2}$ must be inadequate for the comparison of laboratory data with theory partly because the incident angle ψ_i is finite in the experiments.
 - Melville (1980): $\psi_i = 0.17 \sim 0.79$ radians ($10 \sim 45^\circ$)
 - Tanaka (1993): $\psi_i = 0.17 \sim 1.05$ radians ($10 \sim 60^\circ$)
 - Present study: $\psi_i = 0.35 \sim 0.70$ radians ($20 \sim 40^\circ$)
- The limited physical dimension of the laboratory apparatus prevents the stem formation from reaching its fully developed asymptotic state.
- The Mach reflection is a transient phenomenon in the laboratory environment; the Kadomtsev-Petviashvili (K-P) theory can be used for modeling such.

Kadomtsev-Petviashvili (K-P) equation

For 3D irrotational flows:

$$\tilde{\phi}_{\tilde{x}\tilde{x}} + \tilde{\phi}_{\tilde{y}\tilde{y}} + \tilde{\phi}_{\tilde{z}\tilde{z}} = 0 \quad \text{for } 0 \leq \tilde{z} \leq \tilde{h}_0 + \tilde{\eta}(\tilde{x}, \tilde{y}, \tilde{t})$$

$$\tilde{\phi}_{\tilde{z}} = 0 \quad \text{on } \tilde{z} = 0$$

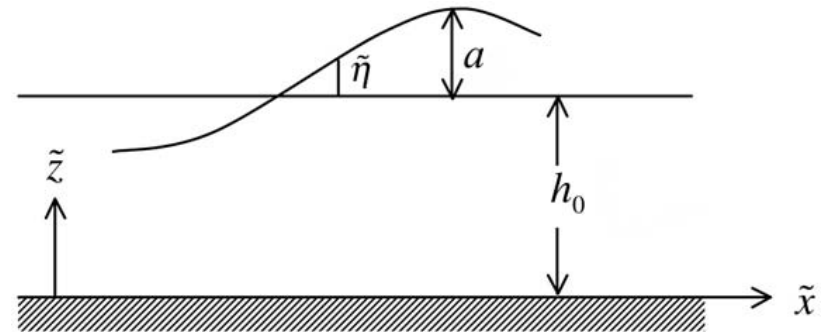
$$\left. \begin{aligned} \tilde{\phi}_{\tilde{t}} + \frac{1}{2}(\tilde{\phi}_{\tilde{x}}^2 + \tilde{\phi}_{\tilde{y}}^2 + \tilde{\phi}_{\tilde{z}}^2) + g\tilde{\eta} &= 0 \\ \tilde{\eta}_{\tilde{t}} + \tilde{\phi}_{\tilde{x}}\tilde{\eta}_{\tilde{x}} + \tilde{\phi}_{\tilde{y}}\tilde{\eta}_{\tilde{y}} - \tilde{\phi}_{\tilde{z}} &= 0 \end{aligned} \right\} \quad \text{on } \tilde{z} = \tilde{\eta} + h_0$$

Scaling:

$\lambda_0 \sim$ dominant horizontal length scale

$h_0 \sim$ vertical length scale

$a_0 \sim$ dominant amplitude scale



Set $h_0/\lambda_0 \ll 1$ for long waves, and:

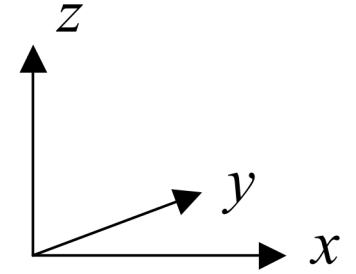
$$\tilde{x} = x\lambda_0, \quad \tilde{y} = y \frac{\lambda_0}{\tan \psi}, \quad \tilde{z} = zh_0, \quad \tilde{t} = \frac{\lambda_0}{C_0} t, \quad \tilde{\eta} = a_0 \eta, \quad \tilde{\phi} = \frac{a_0}{h_0} \lambda_0 C_0 \phi,$$

Normalized formulation:

$$\beta \phi_{xx} + \gamma \beta \phi_{yy} + \phi_{zz} = 0 \quad \text{for } 0 \leq z \leq 1 + \alpha \eta$$

$$\phi_z = 0 \quad \text{on } z = 0$$

$$\left. \begin{aligned} \phi_t + \frac{1}{2} \alpha \phi_x^2 + \frac{1}{2} \alpha \gamma \phi_y^2 + \frac{1}{2} \alpha \beta^{-1} \phi_z^2 + \eta &= 0 \\ \eta_t + \alpha \phi_x \eta_x + \alpha \gamma \phi_y \eta_y - \beta^{-1} \phi_z &= 0 \end{aligned} \right\} \quad \text{on } z = 1 + \alpha \eta$$



where $\alpha = \frac{a_0}{h_0}$; $\beta = \left(\frac{h_0}{\lambda_0} \right)^2$; $\gamma = \tan^2 \psi$

For a weakly nonlinear, weakly dispersive, and weakly unidirectional wave, we take: $O(\alpha) = O(\beta) = O(\gamma) = \varepsilon \ll O(1)$ and $\phi = \phi_0 + \varepsilon \phi_1 + \varepsilon^2 \phi_2 + \dots$

Solving this problem up to $O(\varepsilon)$ and introducing the wave coordinates:

$\xi = x - t$; $\tau = \varepsilon t$, yield the KP equation:

$$\left(6 \eta_\tau + 9 \eta \eta_\xi + \eta_{\xi\xi\xi} \right)_\xi + 3 \eta_{yy} = 0$$

rescaling with $T = \frac{2}{3} \tau$ and $\eta = \frac{2}{3} u$, we found the KP equation of the form:

$$\left(4 u_T + 6 u u_\xi + u_{\xi\xi\xi} \right)_\xi + 3 u_{yy} = 0$$

Solution to the K-P equation (Hirota and his colleagues)

$$\left(4u_T + 6uu_\xi + u_{\xi\xi\xi}\right)_\xi + 3u_{yy} = 0$$

The solution of KP equation can be expressed by the τ -function form:

$$u(\xi, y, T) = 2\partial_\xi^2 \left(\ln \tau(\xi, y, T) \right)$$

Then, the τ -function is the Wronskian determinant of f_i .

For a **two-soliton case**, $\tau = \text{Wronskian}(f_1, f_2) = \begin{vmatrix} f_1 & \partial_\xi f_1 \\ f_2 & \partial_\xi f_2 \end{vmatrix}$

The functions f_1 and f_2 satisfy the linear equations: $\partial_y f_i = \partial_\xi^2 f_i$ and $\partial_T f_i = -\partial_\xi^3 f_i$

A solution can be expressed with exponential functions of the form:

$$\exp(k_j \xi + k_j^2 y - k_j^3 T)$$

Classification of Soliton Solutions: (Kodama and his colleagues)

$$\begin{pmatrix} f_1 \\ f_2 \end{pmatrix} = \begin{pmatrix} a_{11} & a_{12} & a_{13} & a_{14} \\ a_{21} & a_{22} & a_{23} & a_{24} \end{pmatrix} \begin{pmatrix} E_1 \\ E_2 \\ E_3 \\ E_4 \end{pmatrix} = A \begin{pmatrix} E_1 \\ E_2 \\ E_3 \\ E_4 \end{pmatrix} \quad E_j = \exp(k_j \xi + k_j^2 y - k_j^3 T)$$

So, $\tau = \sum_{1 \leq i < j \leq 4} \zeta(i, j) \text{Wr}(E_i E_j)$ where $\zeta(i, j)$ is the $N \times N$ minor of the A -matrix.

- The τ -function leads to the notion of the Grassmannian variety: $\text{Gr}(N, M)$ – in the present case, $N = 2$ and $M = 4$ for the A -matrix.
- Some constraints are applied for the regular soliton solutions – the τ -function can be identified as a point of the totally nonnegative Grassmannian cell.
- The asymptotic soliton solutions for $y \gg 0$ and $y \ll 0$ can be parameterized by the permutations, which lead to the introduction of the chord diagram to express the classification for the soliton solutions as a chord joining a pair of k_i 's following its permutation representation.

One line soliton ($N = 1, M = 2$)

$$\begin{aligned}\tau &= E_1 + a E_2 \\ &= 2\sqrt{a} \exp\left(\frac{1}{2}(\theta_1 + \theta_2)\right) \cosh \frac{1}{2}(\theta_1 - \theta_2 - \ln a)\end{aligned}$$

$$E_j = \exp(k_j \xi + k_j^2 y - k_j^3 T)$$

$$\theta_j = k_j \xi + k_j^2 y - k_j^3 T$$

This leads to the solution of a line-soliton with the propagation direction $\Psi_{[i,j]}$

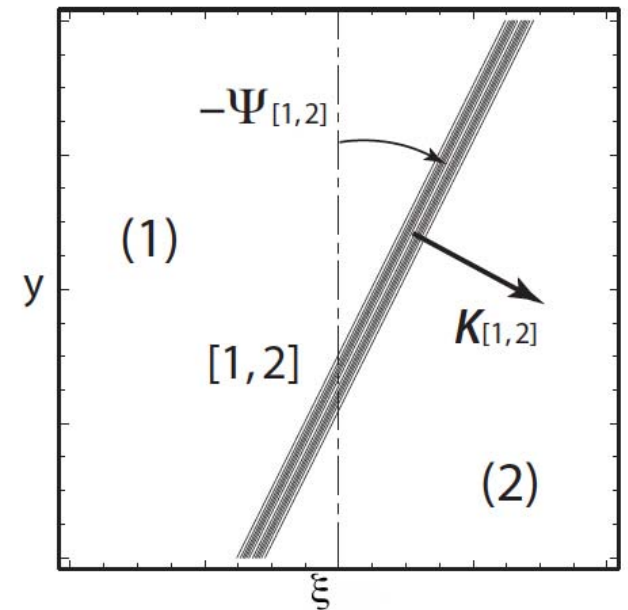
$$u = 2 \partial_\xi^2 (\ln \tau) = \frac{1}{2} (k_1 - k_2)^2 \operatorname{sech}^2 \frac{1}{2}(\theta_1 - \theta_2 - \ln a)$$

$$u = A_{[i,j]} \operatorname{sech}^2 \sqrt{\frac{A_{[i,j]}}{2}} \left(\xi + y \tan \Psi_{[i,j]} - C_{[i,j]} T - x_{[i,j]}^0 \right)$$

$$A_{[i,j]} = \frac{1}{2} (k_j - k_i)^2$$

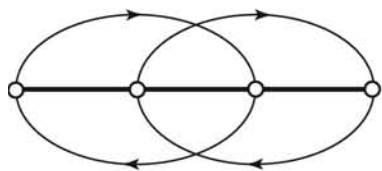
$$\tan \Psi_{[i,j]} = k_i + k_j$$

$$C_{[i,j]} = k_i^2 + k_i k_j + k_j^2 = \frac{1}{2} A_{[i,j]} + \frac{3}{4} \tan^2 \Psi_{[i,j]}$$

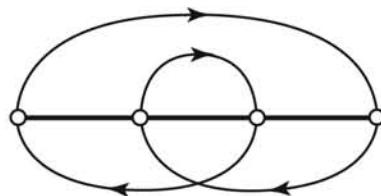


Chord Diagrams

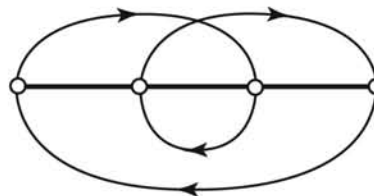
Each diagram corresponds to a totally non-negative Grassmannian cell in $\text{Gr}(2,4)$



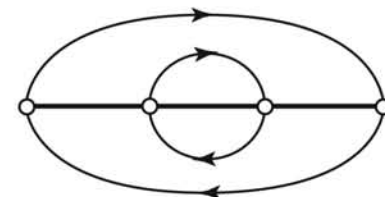
(3412)



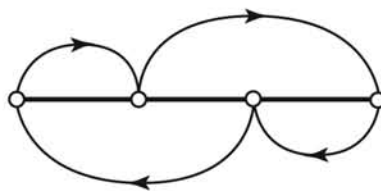
(4312)



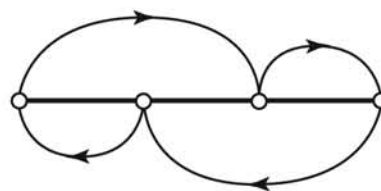
(3421)



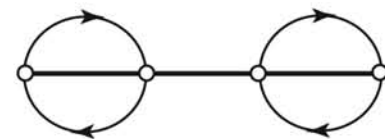
(4321)



(2413)



(3142)



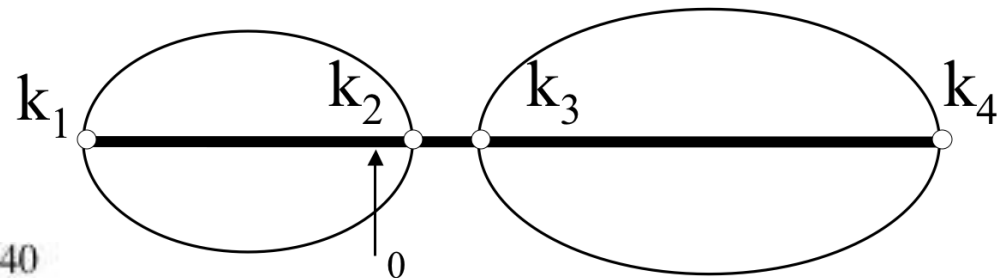
(2143)

O-type

Permutation

$$\pi = \begin{pmatrix} 1 & 2 & 3 & 4 \\ 2 & 1 & 4 & 3 \end{pmatrix}$$

Chord Diagram



$$a_{[1,2]} = 0.35 \text{ cm}; \quad a_{[3,4]} = 0.70 \text{ cm}$$

$$\psi_{[1,2]} = 20^\circ; \quad \psi_{[3,4]} = -30^\circ; \quad h_0 = 6 \text{ cm}$$

$$k_1 = -0.3785; \quad k_2 = 0.01457$$

$$k_3 = 0.03250; \quad k_4 = 0.5448$$

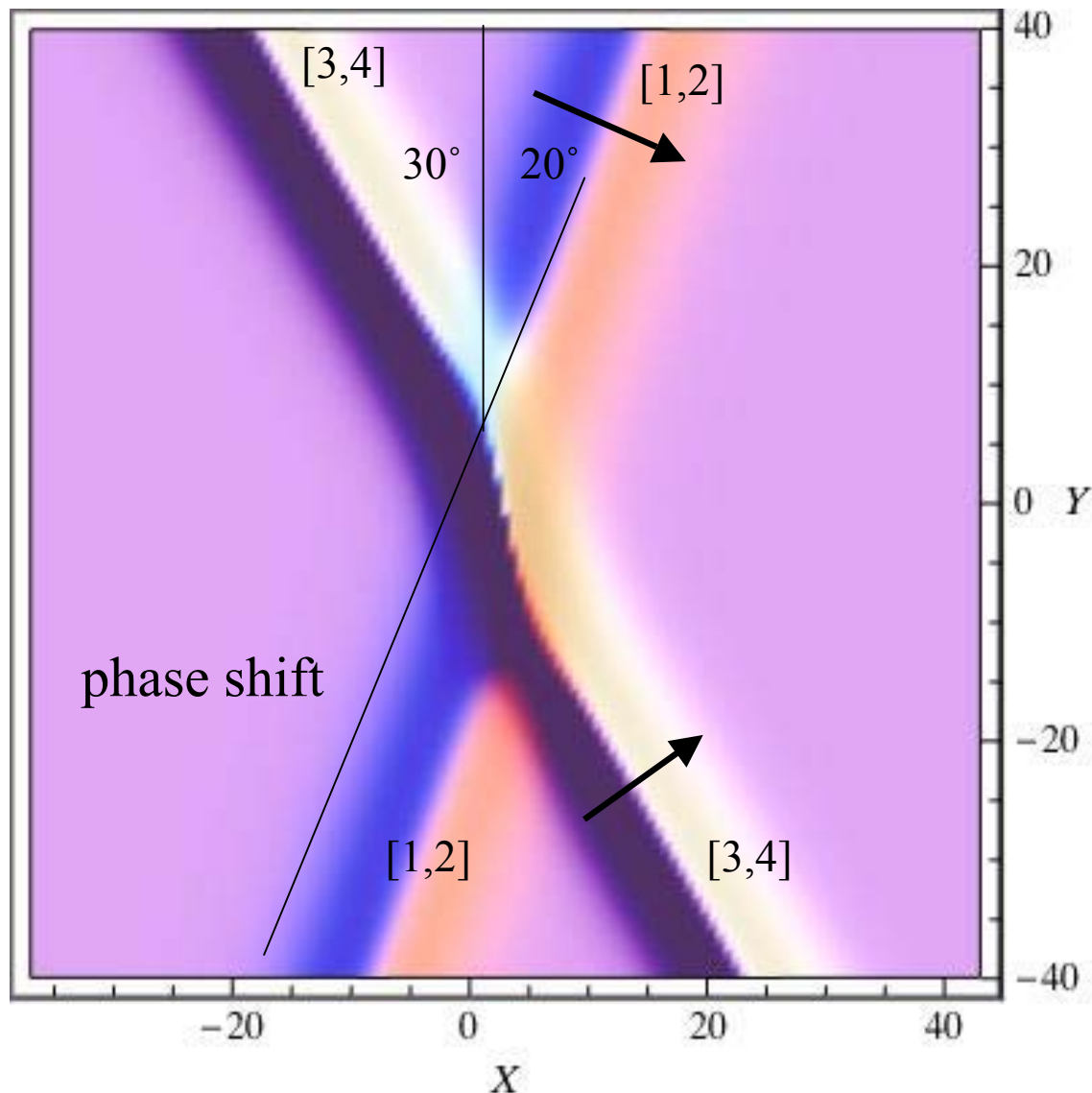
$$A_{[i,j]} = \frac{1}{2} (k_j - k_i)^2$$

$$A_{[1,2]} = 0.07726; \quad A_{[3,4]} = 0.1312$$

$$\tan \Psi_{[i,j]} = k_i + k_j$$

$$\tan \Psi_{[1,2]} = -0.3639; \quad \Psi_{[1,2]} = -20^\circ$$

$$\tan \Psi_{[3,4]} = 0.5773; \quad \Psi_{[3,4]} = 30^\circ$$

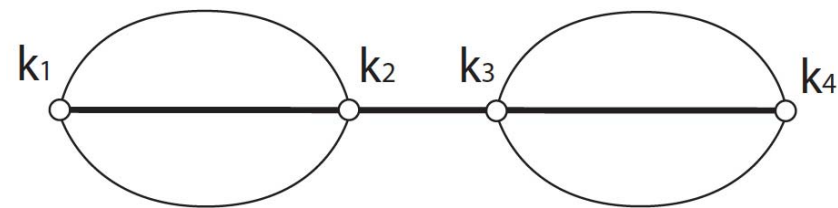


O-type

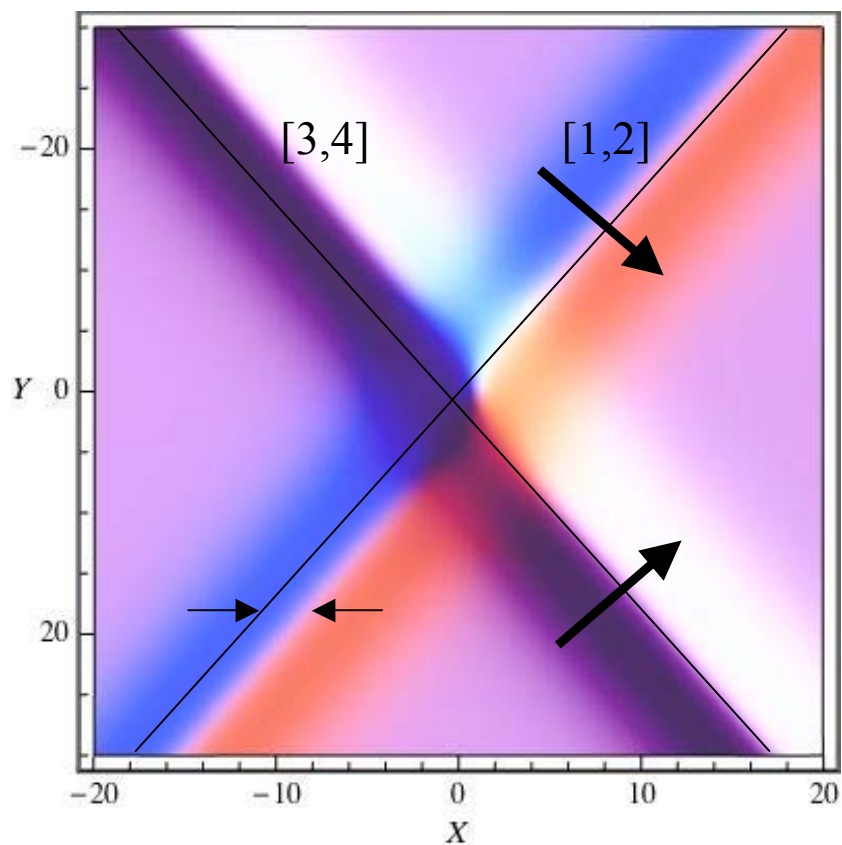
Permutation

$$\pi = \begin{pmatrix} 1 & 2 & 3 & 4 \\ 2 & 1 & 4 & 3 \end{pmatrix}$$

Chord Diagram

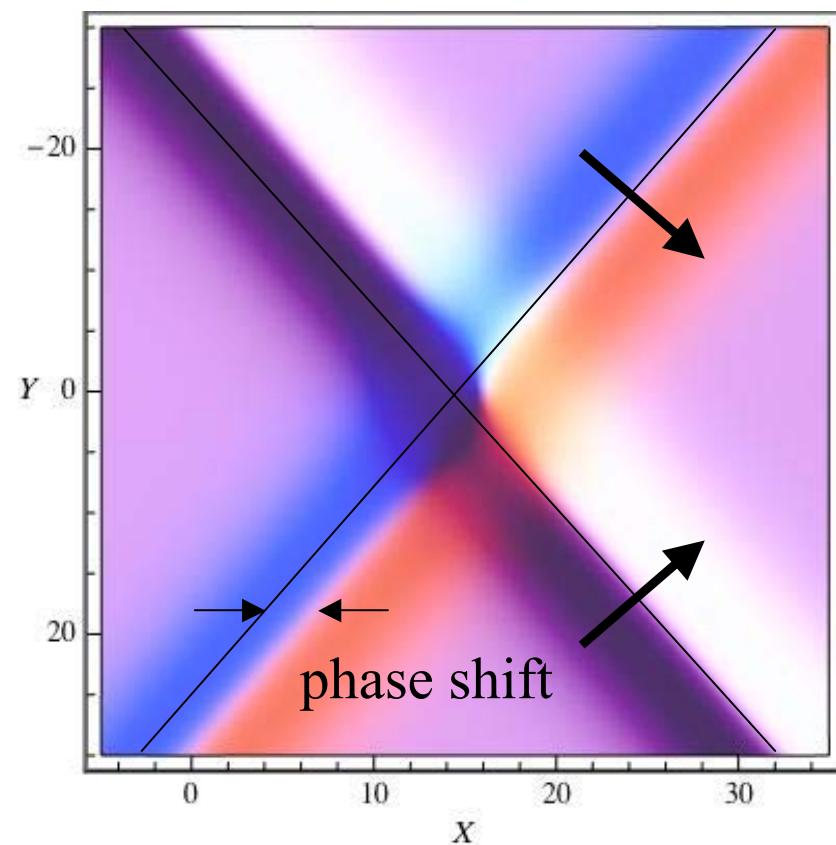


$$A_{[i,j]} = \frac{1}{2} (k_j - k_i)^2; \quad \tan \Psi_{[i,j]} = k_i + k_j$$



$t = 0$

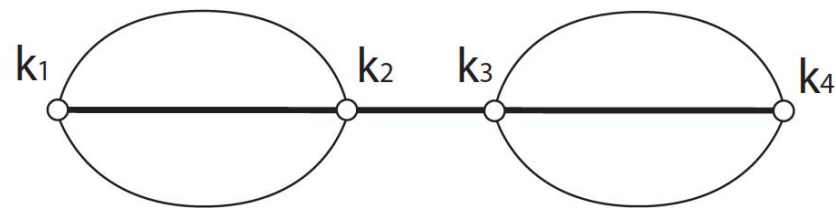
$A_0 = 0.1; \psi = 30^\circ$



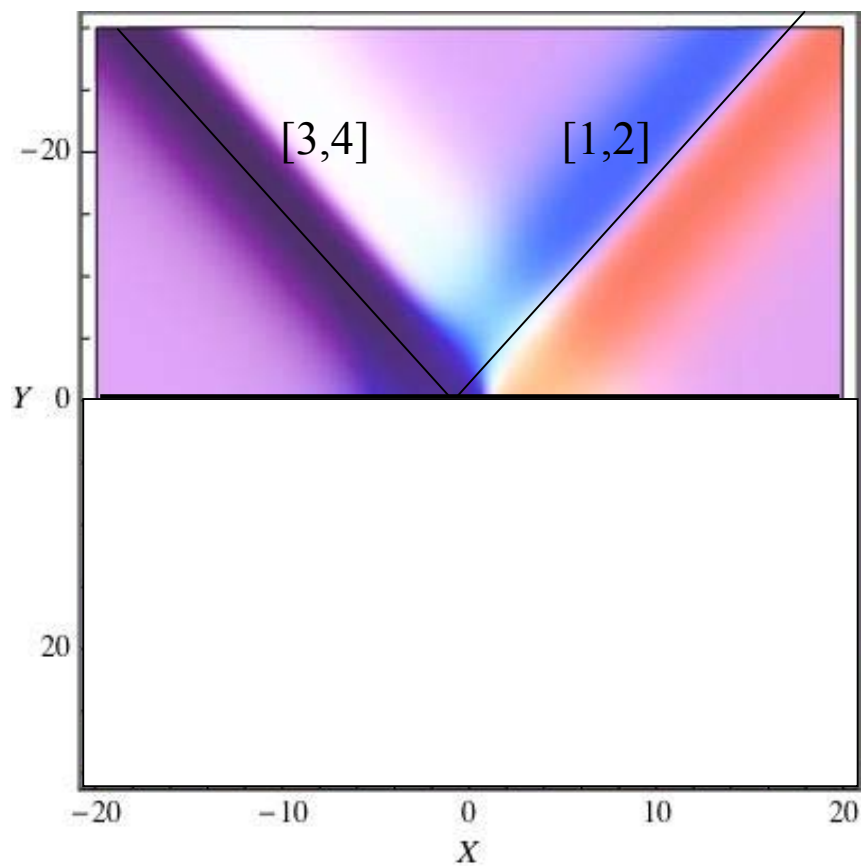
$t = 50$

O-type

$$\pi = \begin{pmatrix} 1 & 2 & 3 & 4 \\ 2 & 1 & 4 & 3 \end{pmatrix}$$

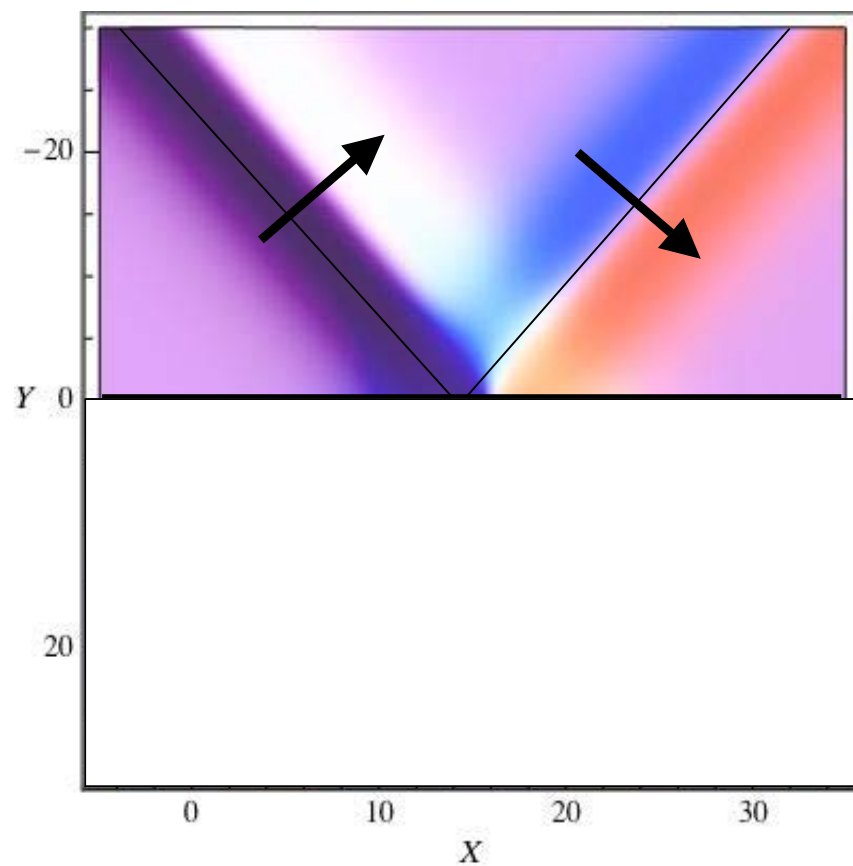


$$A_{[i,j]} = \frac{1}{2} (k_j - k_i)^2; \quad \tan \Psi_{[i,j]} = k_i + k_j$$



$t = 0$

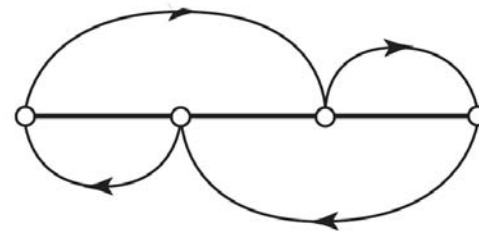
$$A_0 = 0.1; \quad \psi = 30^\circ$$



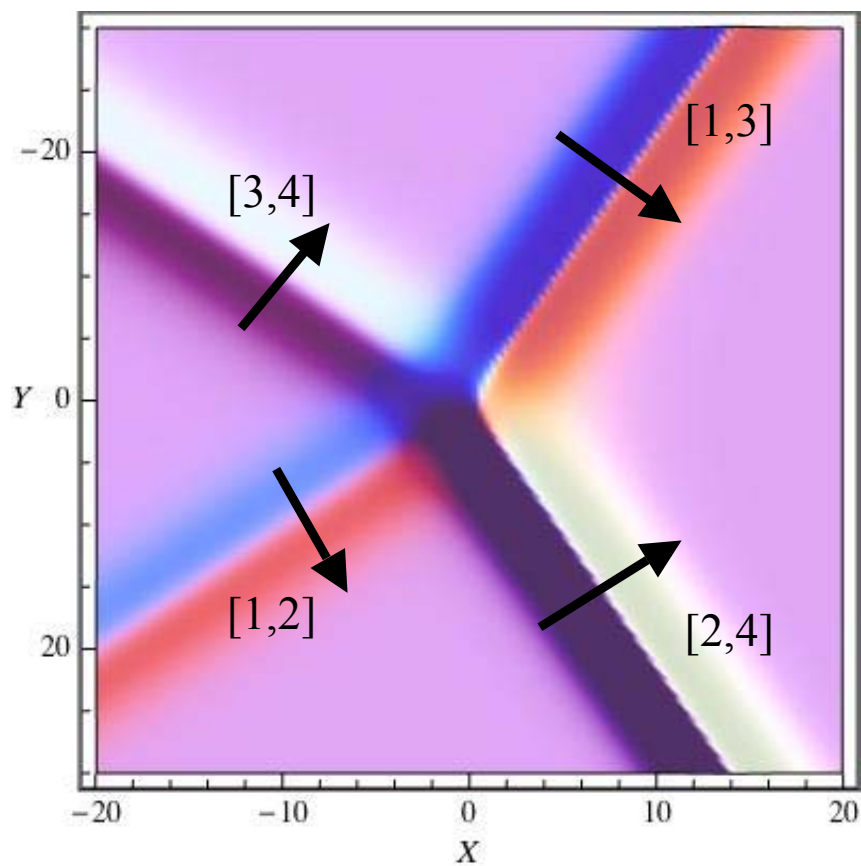
$t = 50$

3142-type

$$\pi = \begin{pmatrix} 1 & 2 & 3 & 4 \\ 3 & 1 & 4 & 2 \end{pmatrix}$$

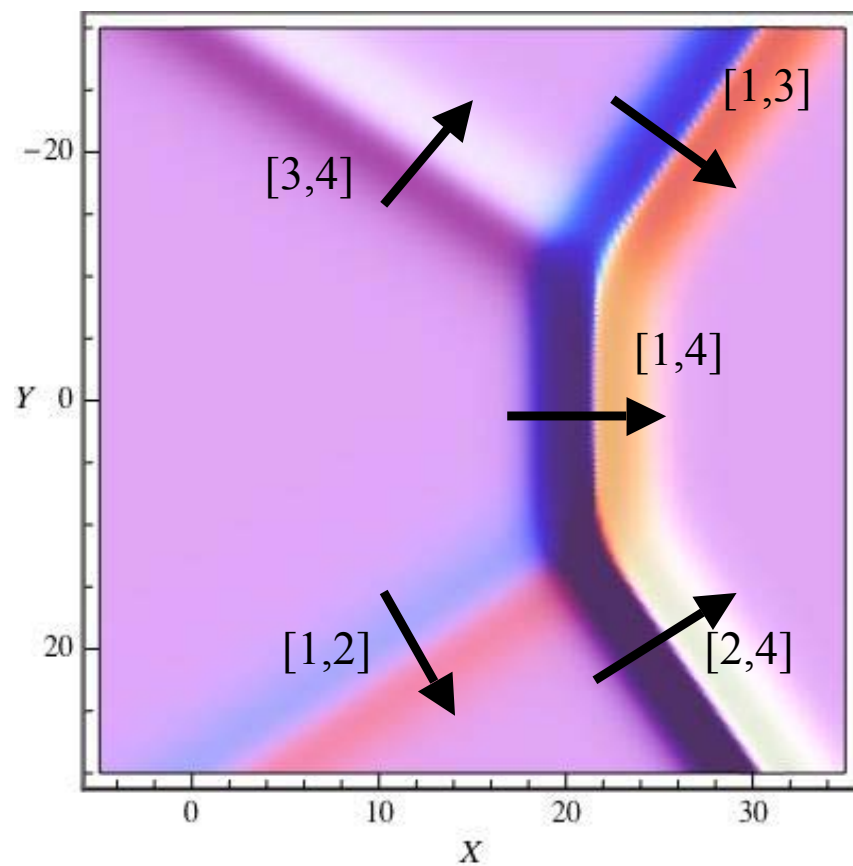


$$A_{[i,j]} = \frac{1}{2} (k_j - k_i)^2; \quad \tan \Psi_{[i,j]} = k_i + k_j$$



$t = 0$

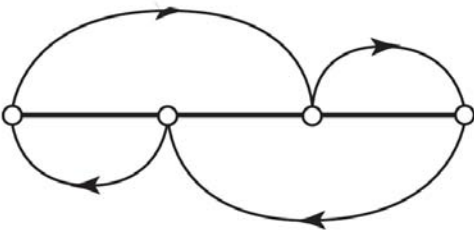
$A_0 = 0.5; \psi = 25^\circ$



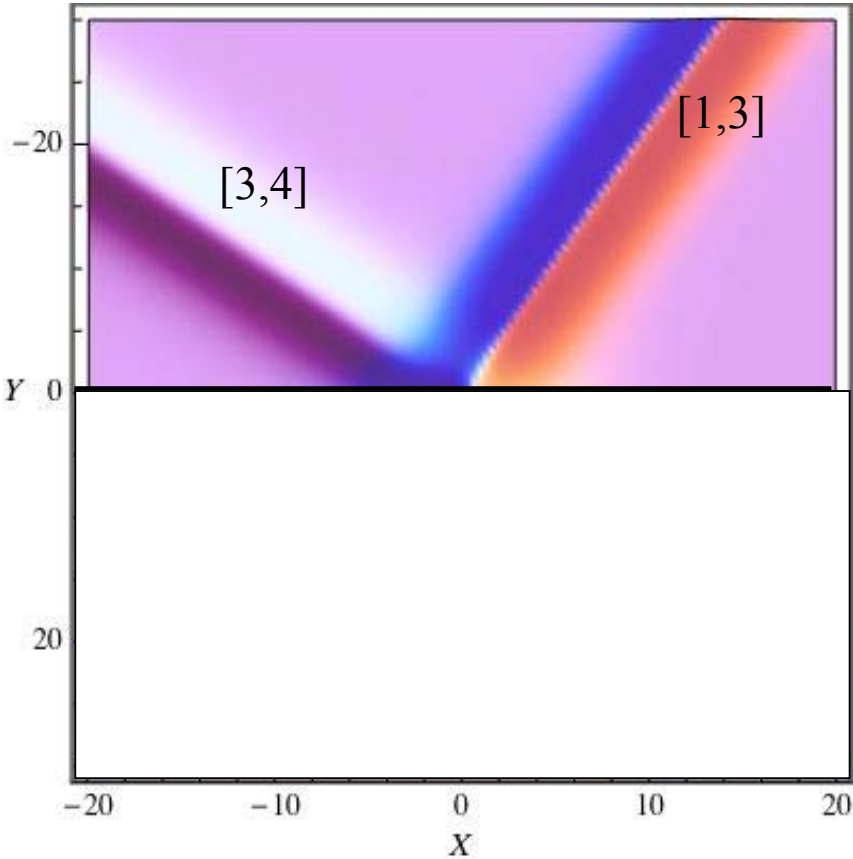
$t = 40$

3142-type

$$\pi = \left(\begin{array}{cccc} 1 & 2 & 3 & 4 \\ 3 & 1 & 4 & 2 \end{array} \right)$$

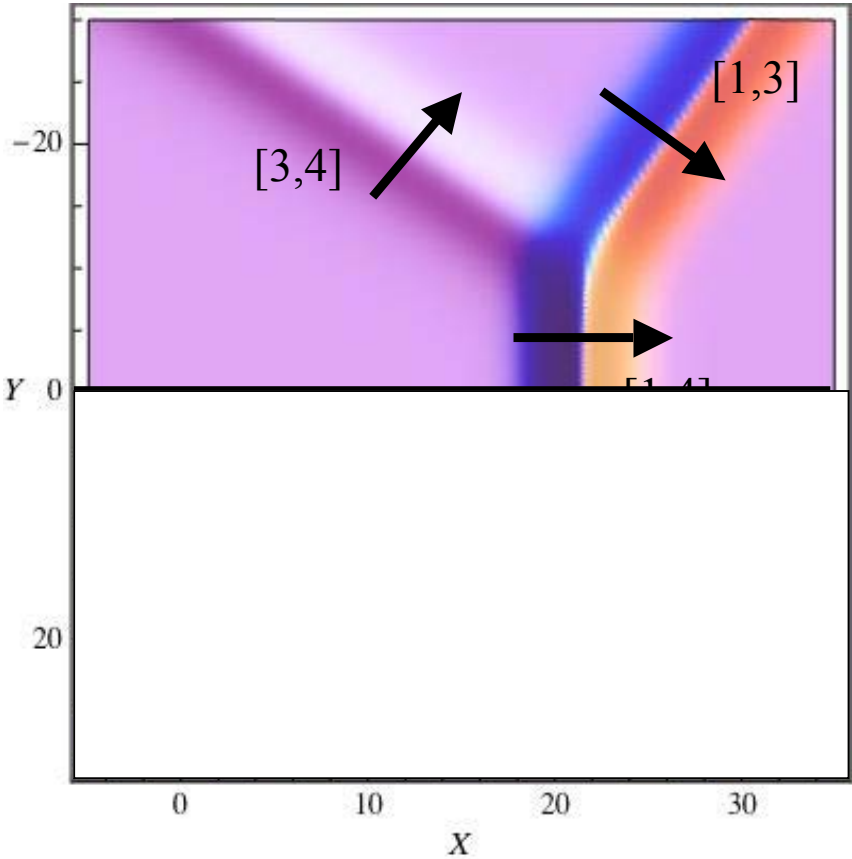


$$A_{[i,j]} = \frac{1}{2} (k_j - k_i)^2; \quad \tan \Psi_{[i,j]} = k_i + k_j$$



$t = 0$

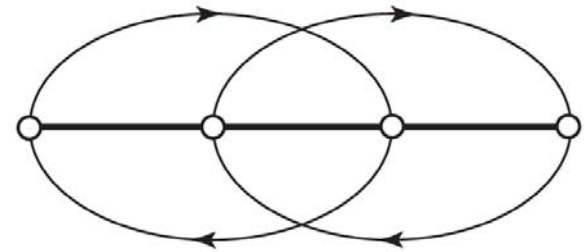
$$A_0 = 0.5; \; \psi = 25^\circ$$



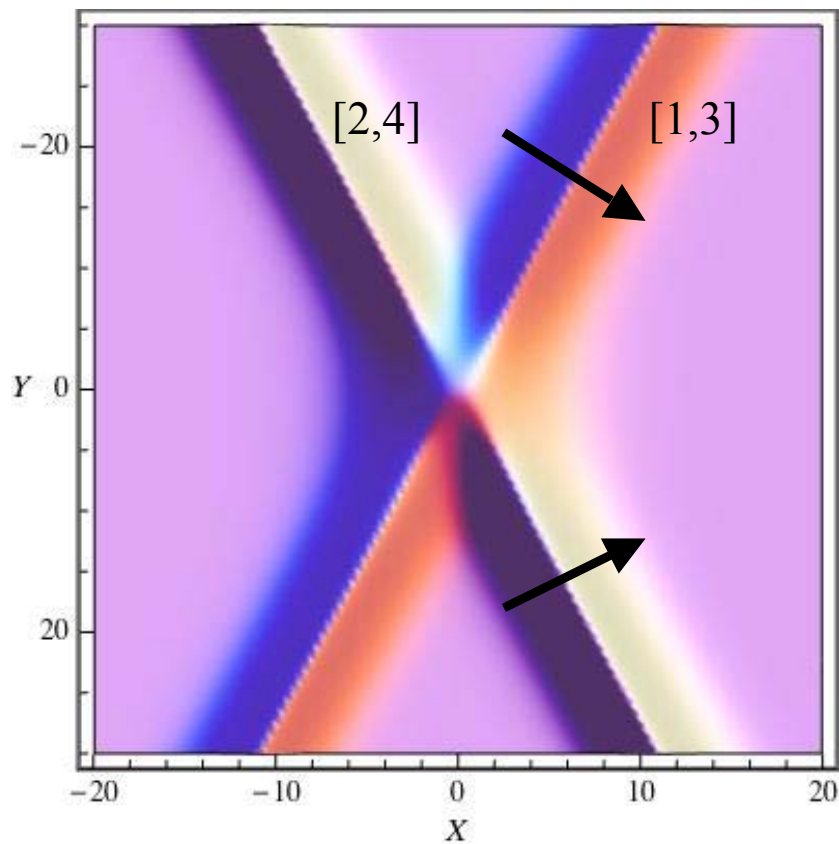
$t = 40$

T-type

$$\pi = \begin{pmatrix} 1 & 2 & 3 & 4 \\ 3 & 4 & 1 & 2 \end{pmatrix}$$

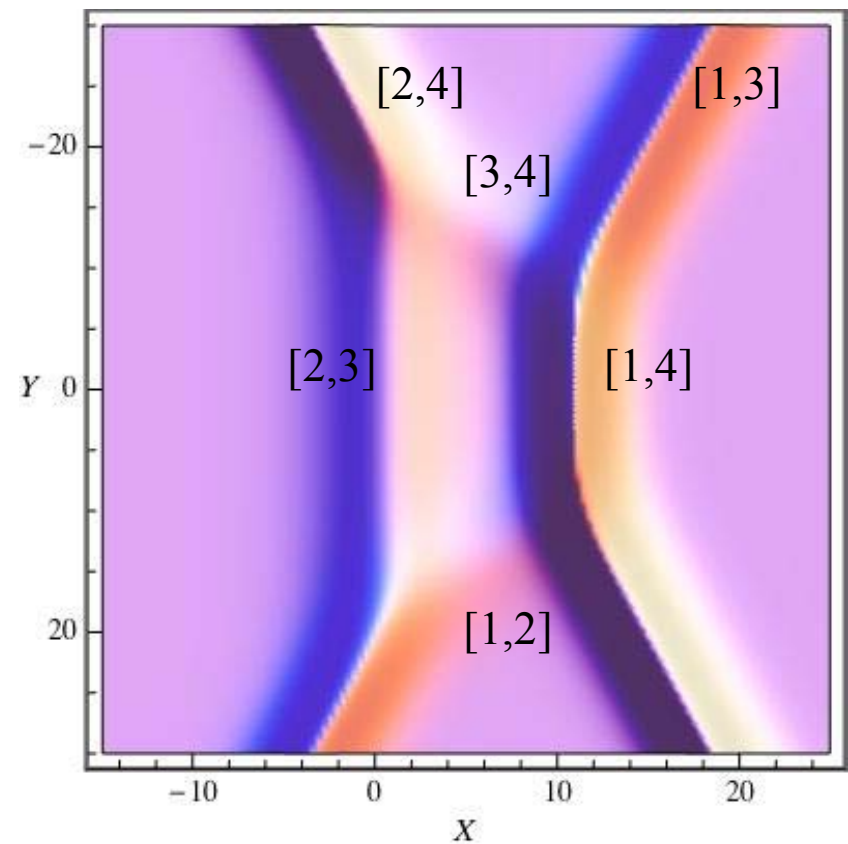


$$A_{[i,j]} = \frac{1}{2} (k_j - k_i)^2; \quad \tan \Psi_{[i,j]} = k_i + k_j$$



$t = 0$

$$A_0 = 0.55; \quad \psi = 20^\circ$$



$t = 20$

The K-P equation in the Laboratory Coordinates

In dimensional form:

$$\partial_x \left(\partial_t \eta + c_0 \partial_x \eta + \frac{3c_0}{2h_0} \eta \partial_x \eta + \frac{c_0 h_0^2}{6} \partial_{xxx} \eta \right) + \frac{c_0}{2} \partial_{yy} \eta = 0$$

$$\frac{a_0}{h_0} = O(\varepsilon); \quad \left(\frac{h_0}{\lambda_0} \right)^2 = O(\varepsilon); \quad \boxed{\gamma = \tan^2 \psi = O(\varepsilon)}, \quad \text{and} \quad \varepsilon \ll O(1)$$

“Exact” solution of the K-P equation for a line soliton is:

$$\eta = a_0 \operatorname{sech}^2 \sqrt{\frac{3a_0}{4h_0^3}} \left[x + y \tan \psi - c_0 \left(1 + \frac{a_0}{2h_0} + \frac{1}{2} \tan^2 \psi \right) t \right]$$

The analysis (Kodama, Oikawa & Tsuji, 2009) leads to the solution similar to Miles's with critical angle at $\gamma_c = 3 a_i$

So, the difference is

$$k = \frac{\psi_i}{\sqrt{3a_i}} \rightarrow \boxed{k = \frac{\tan \psi_i}{\sqrt{3a_i}}}$$

Miles
KP

The K-P equation in the Laboratory Coordinates

$$\eta = a_0 \operatorname{sech}^2 \sqrt{\frac{3 a_0}{4 h_0^3}} \left[x + y \tan \psi - c_0 \left(1 + \frac{a_0}{2 h_0} + \frac{1}{2} \tan^2 \psi \right) t \right]$$

This solution is exact but is coordinate dependent.

Note that in the experiments, we impose a KdV soliton as the incident wave with the oblique angle ψ . This condition must match with the theoretical expression.

Let us make the solution to be invariant under rotation by wave coordinate.

For the first step:

$$\xi \equiv x \cos \psi + y \sin \psi$$

$$\eta = a_0 \operatorname{sech}^2 \sqrt{\frac{3 a_0}{4 h_0^3}} \frac{1}{\cos \psi} \left[\xi - c_0 \cos \psi \left(1 + \frac{a_0}{2 h_0} + \frac{1}{2} \tan^2 \psi \right) t \right]$$

The K-P equation in the Laboratory Coordinates

$$\eta = \hat{a}_0 \cos^2 \psi \operatorname{sech}^2 \sqrt{\frac{3 \hat{a}_0}{4 h_0^3}} \left[\xi - c_0 \cos \psi \left(1 + \frac{\hat{a}_0 \cos^2 \psi}{2 h_0} + \frac{1}{2} \tan^2 \psi \right) t \right]$$

$$\hat{a}_0 = a_0 / \cos^2 \psi$$

$$\xi \equiv x \cos \psi + y \sin \psi$$

Noting

$$\tan^2 \psi = O(\varepsilon), \quad \frac{a_0}{h_0} = O(\varepsilon), \quad \text{and} \quad \cos \psi = 1 - \frac{1}{2} \tan^2 \psi + \dots = 1 + O(\varepsilon)$$

yields

$$\eta = \hat{a}_0 \operatorname{sech}^2 \sqrt{\frac{3 \hat{a}_0}{4 h_0^3}} \left[\xi - c_0 \left(1 + \frac{a_0}{2 h_0} + O(\varepsilon^2) \right) t \right] + O(\varepsilon^2) \quad \text{which is a KdV Soliton}$$

Therefore, the KP wave amplitude a_0 is equivalent to the laboratory (KdV) amplitude \hat{a}_0 : $a_0 = \hat{a}_0 \cos^2 \psi$

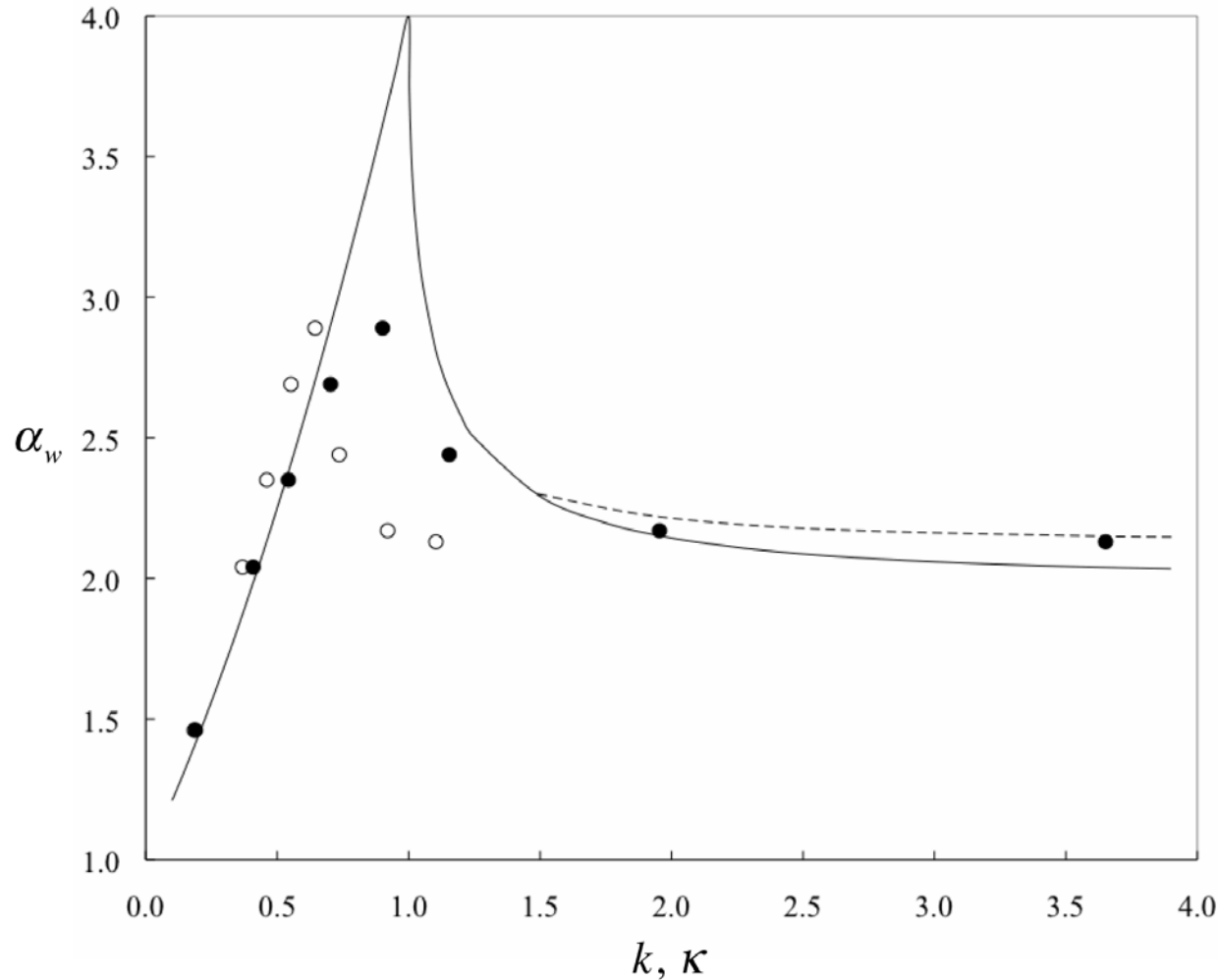
$$\Rightarrow \quad \kappa = \frac{\tan \psi_i}{\sqrt{3 \hat{a}_i} \cos \psi_i}$$

Kadomtsev-Petviashvili (K-P) equation

Jia and Kodama (2011) derived the higher-order correction :

$$\kappa = \frac{\tan \psi_i}{\sqrt{\frac{6a_i}{1 + \sqrt{1 + 5a_i}}} \cos \psi_i}$$

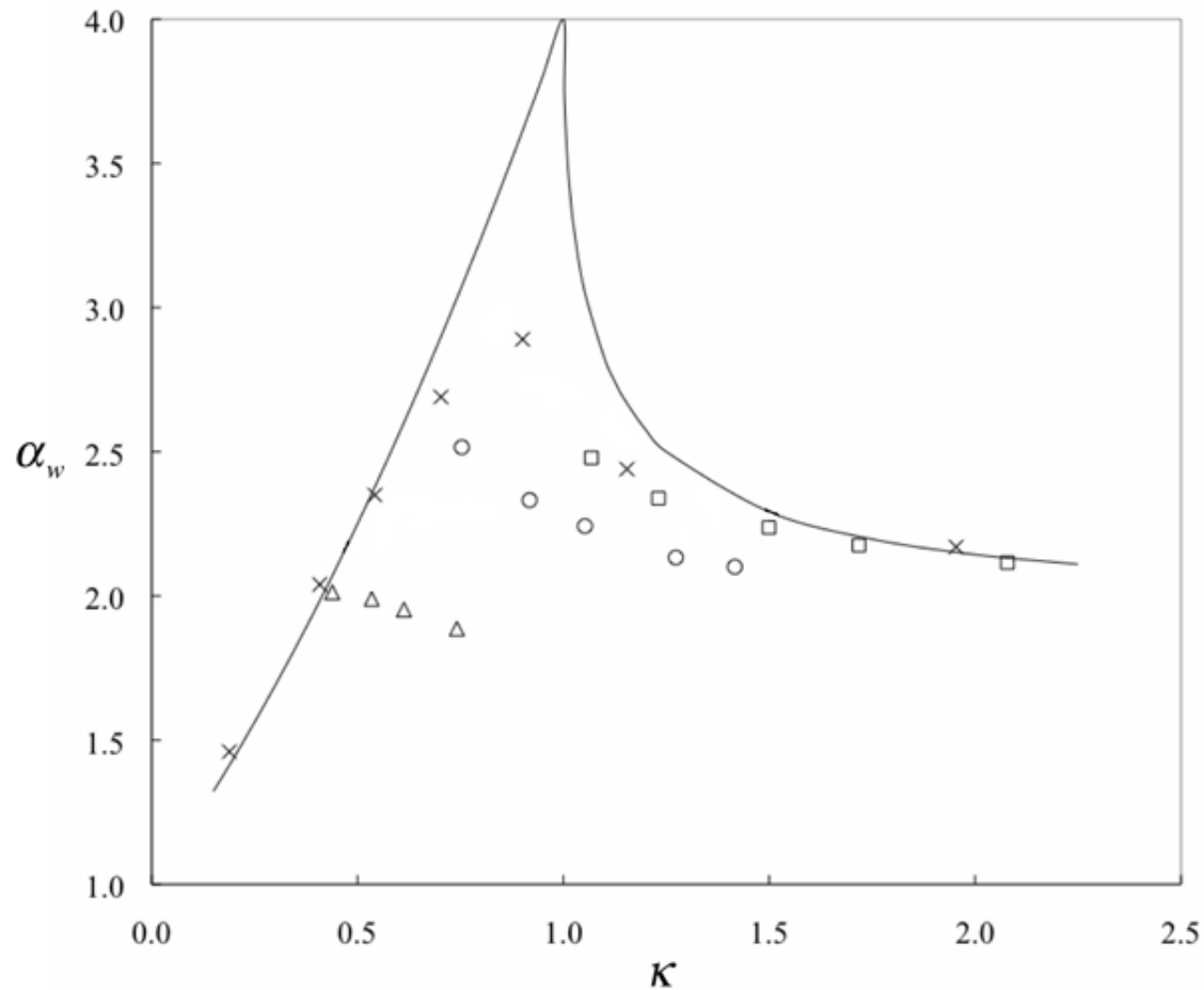
Tanaka's Numerical Data with Miles's prediction



○ plotted with the original interaction parameter $k = \frac{\psi_i}{\sqrt{3}a_i}$

● plotted with the modified parameter $\kappa = \frac{\tan \psi_i}{\cos \psi_i \sqrt{3}a_i}$

Our Laboratory Data with Miles's prediction



$$\kappa = \frac{\tan \psi_i}{\sqrt{3a_i \cos \psi_i}}$$

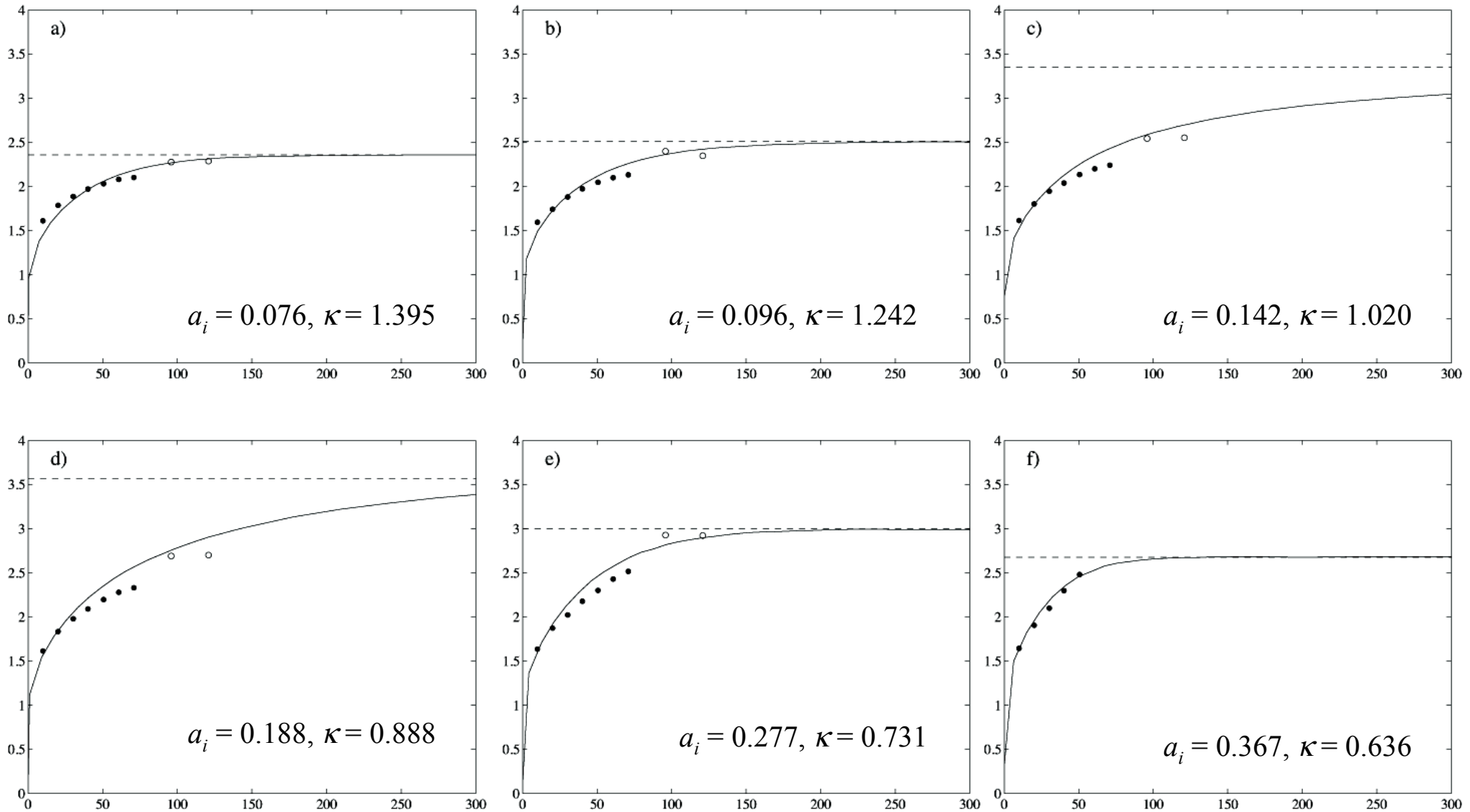
Tanaka (1993): \times

At $x = 71.1$: \square , $\psi_i = 40^\circ$; \circ , $\psi_i = 30^\circ$; \triangle , $\psi_i = 20^\circ$.

“Extended” Lab Experiments

- Large-distance measurements were made by generating the observed waveform from the parent experiment with the wavemaker and patching the data with those from the extended experiment.

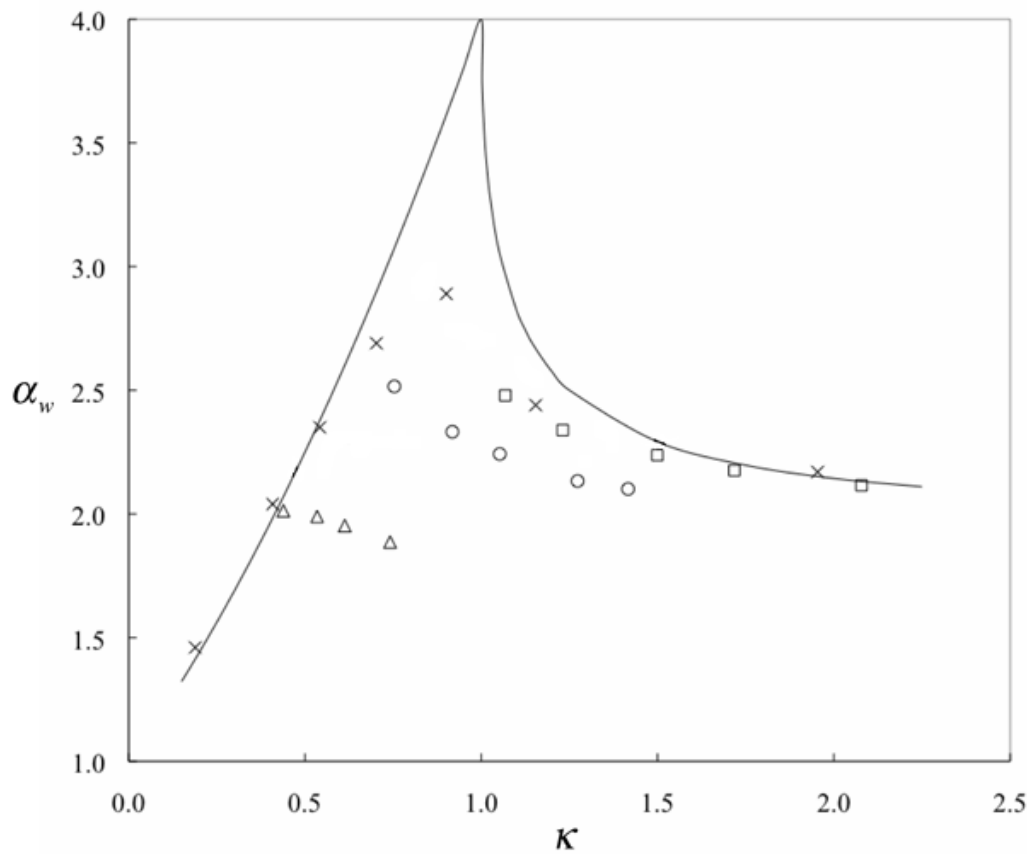
Growth of Stem-Wave Amplification with KP theory



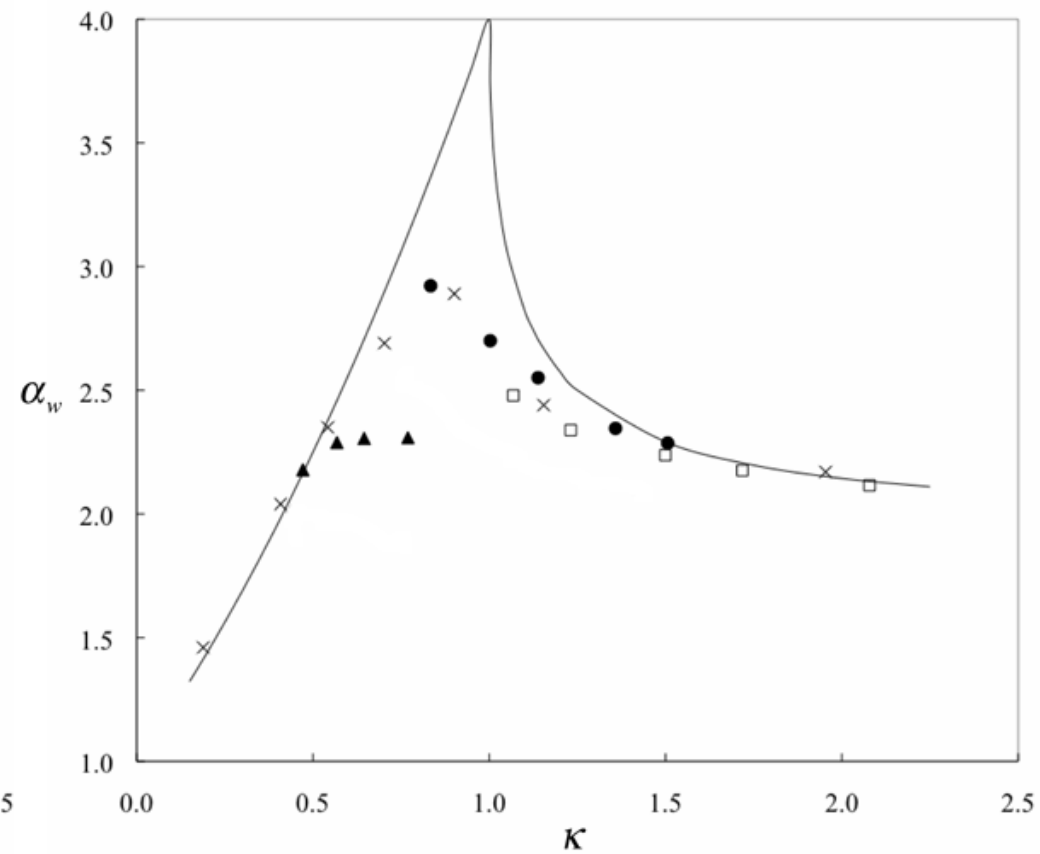
●, laboratory data; ○, extended laboratory data.

Stem Wave Amplification: Our Laboratory Data

at $x = 71$



at $x = 121.1$



$$\kappa = \frac{\tan \psi_i}{\sqrt{3a_i} \cos \psi_i}$$

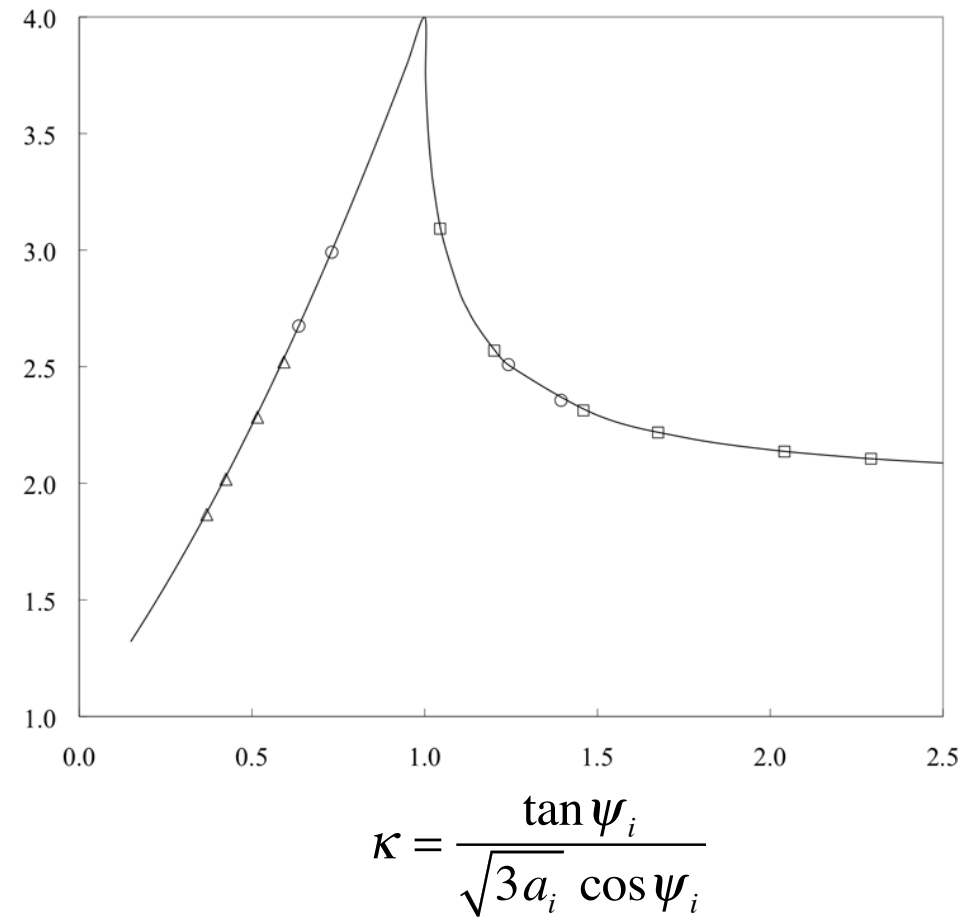
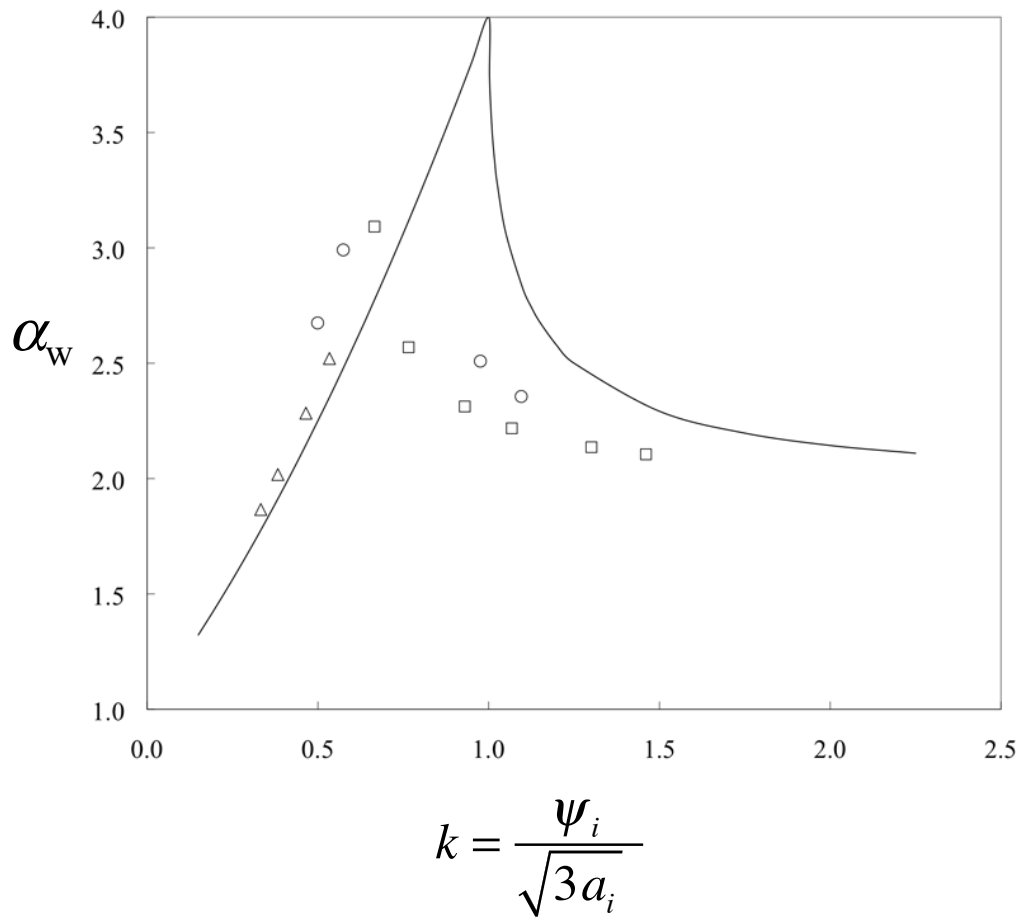
Tanaka (1993): \times

At $x = 71.1$: \square , $\psi_i = 40^\circ$; \circ , $\psi_i = 30^\circ$; \triangle , $\psi_i = 20^\circ$.

Tanaka (1993): \times

At $x = 121.1$: \bullet , $\psi_i = 30^\circ$; \blacktriangle , $\psi_i = 20^\circ$.

Stem Wave Amplification: Numerical KP Solution



\square , $\psi_i = 40^\circ$; \circ , $\psi_i = 30^\circ$; \triangle , $\psi_i = 20^\circ$.

Conclusions

- Once the revised interaction parameter κ is used for the correct interpretation of the theory, the asymptotic characteristics and behaviors are in agreement with Miles's theory except those in the neighborhood of the transition between the Mach reflection and the regular reflection (near $\kappa \approx 1.0$).
- Our laboratory observations are in excellent agreement with the numerical results of the higher-order model by Tanaka (1993) \rightarrow the maximum amplification $\alpha_w \approx 3.0$
- The present laboratory study is the first to sensibly analyze validation of the theory: note that substantial discrepancies existed from the previous (both numerical and laboratory) experimental studies for more than 30 years!

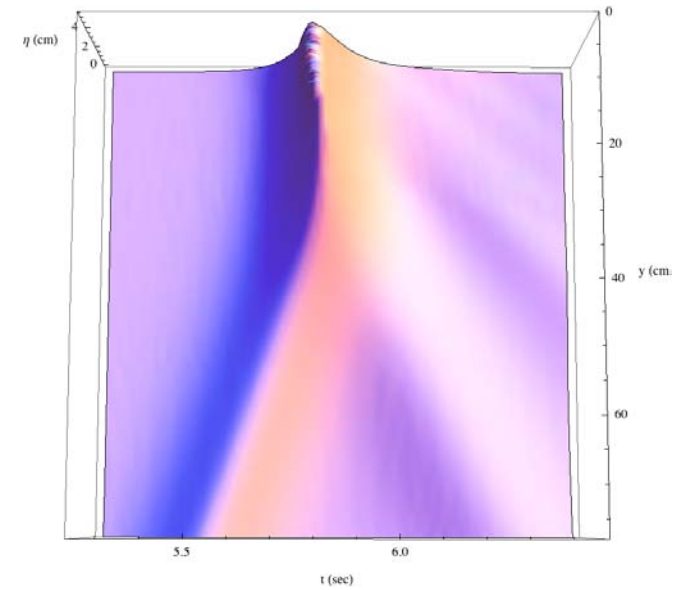
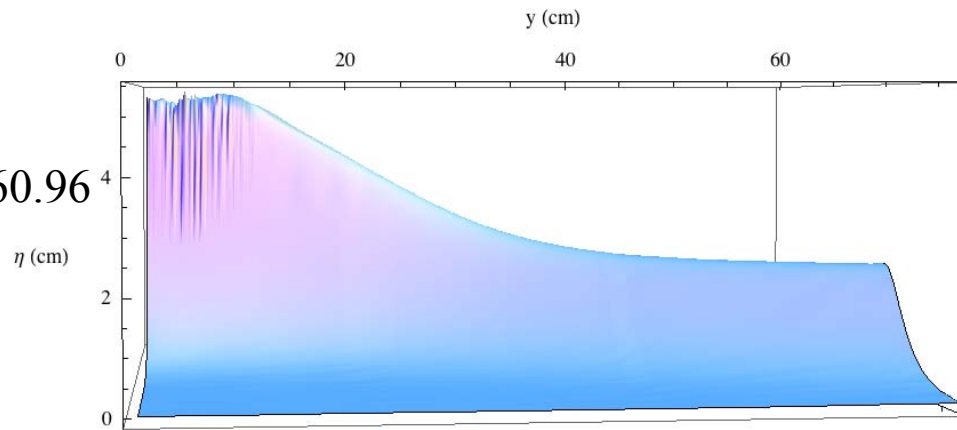
3. Some Extra Results

The 2011 East Japan Tsunamis approaching the Sendai Plain

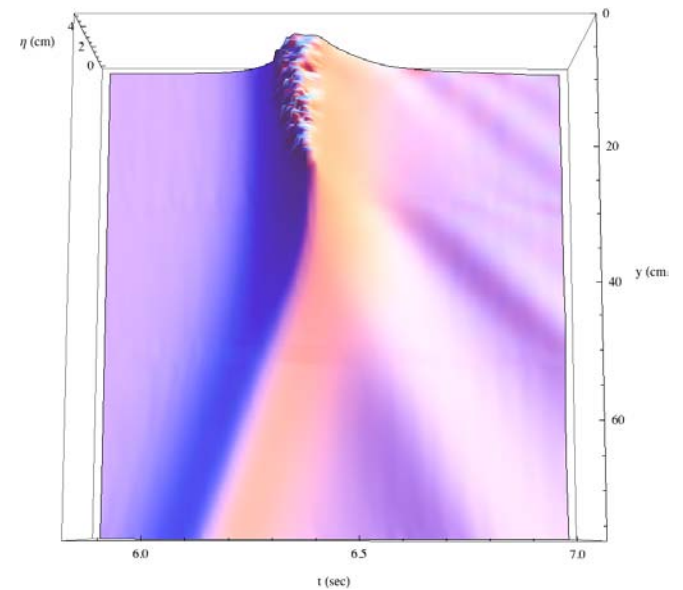
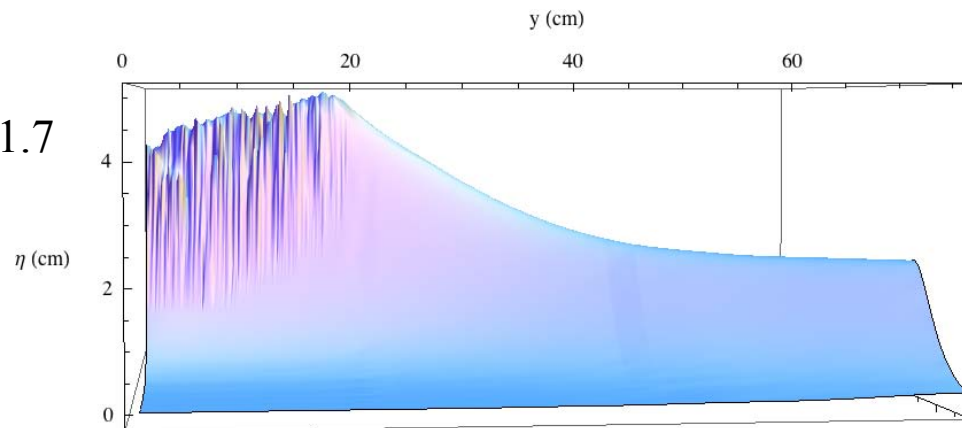


Breaking Stem Wave along the wall

at $x = 60.96$

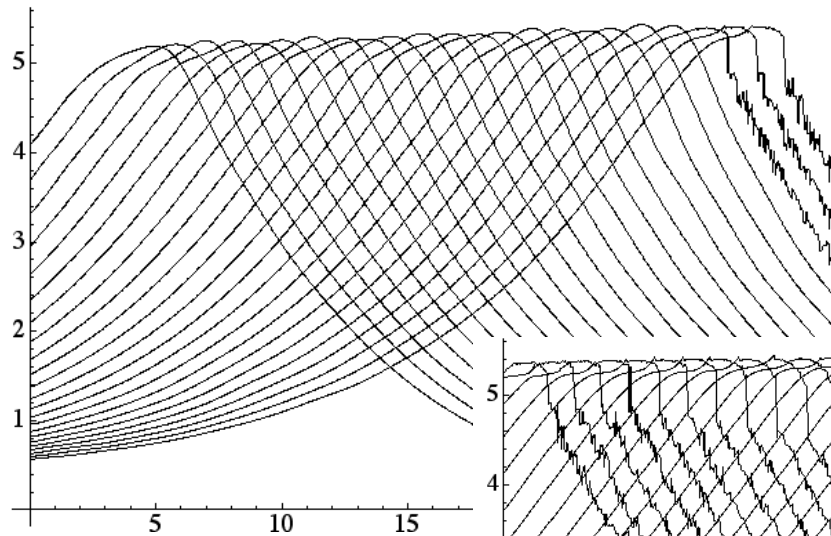


at $x = 71.7$



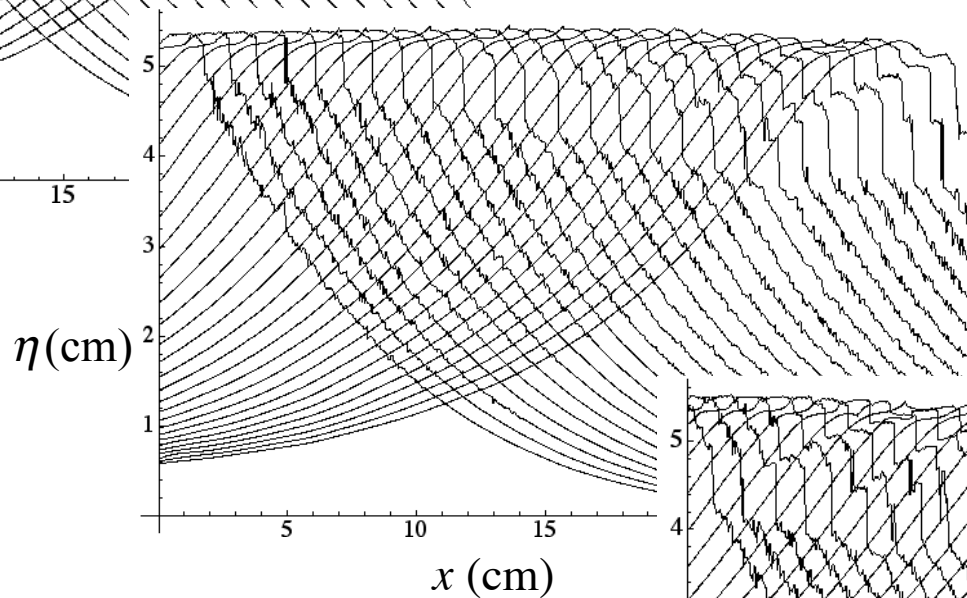
$$h_0 = 6.0 \text{ cm}; \quad \psi_i = 30^\circ; \quad a_i = 0.37$$

Breaking Stem Wave along the Wall

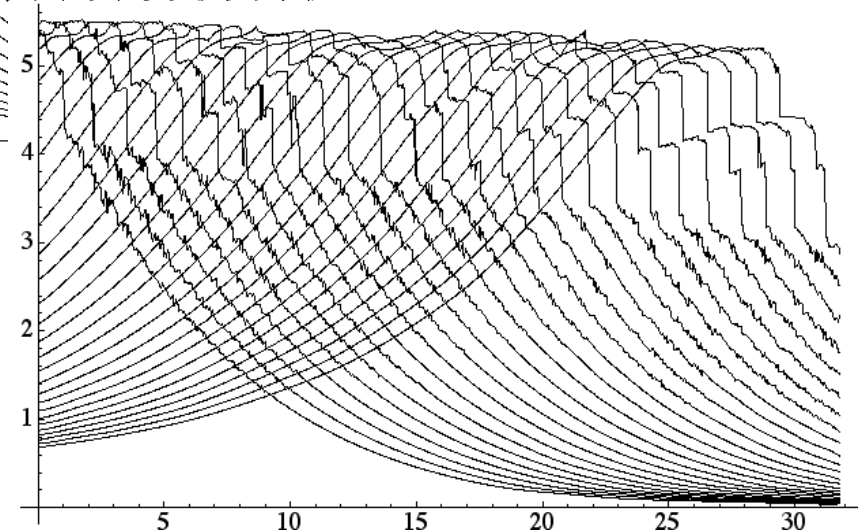


Maximum solitary wave height 0.827
(Longuet-Higgins and Fox, 1996)

Tanaka's (1993) numerical simulation:
 $a_w = 0.905$ at $x = 150$ when $a_i = 0.3$, and $\psi_i = 20^\circ$

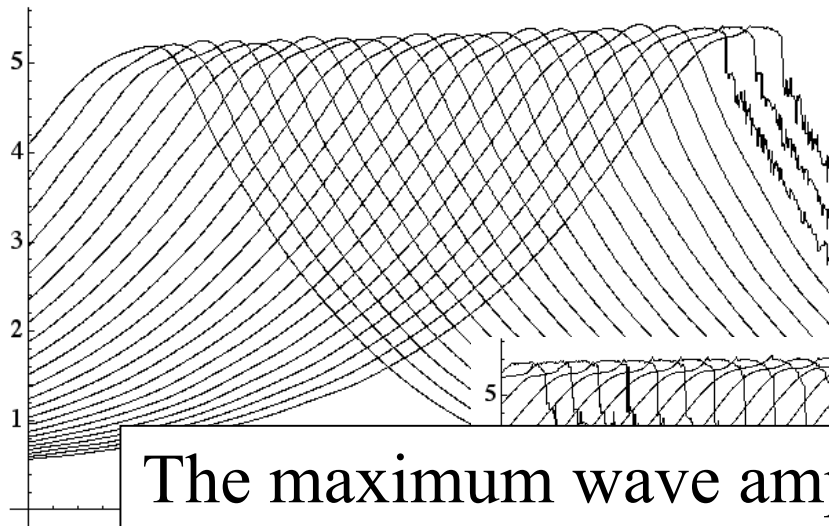


$$a_w = 0.910 \text{ (5.46 cm)}$$



$$h_0 = 6.0 \text{ cm}; \quad \psi_i = 30^\circ; \quad a_i = 0.37 \text{ at } x = 60.96$$

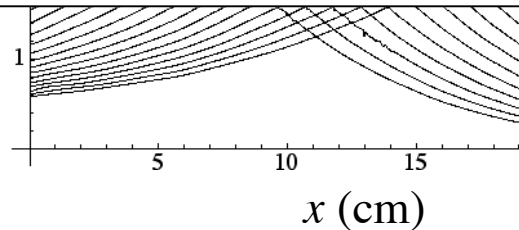
Breaking Stem Wave along the Wall



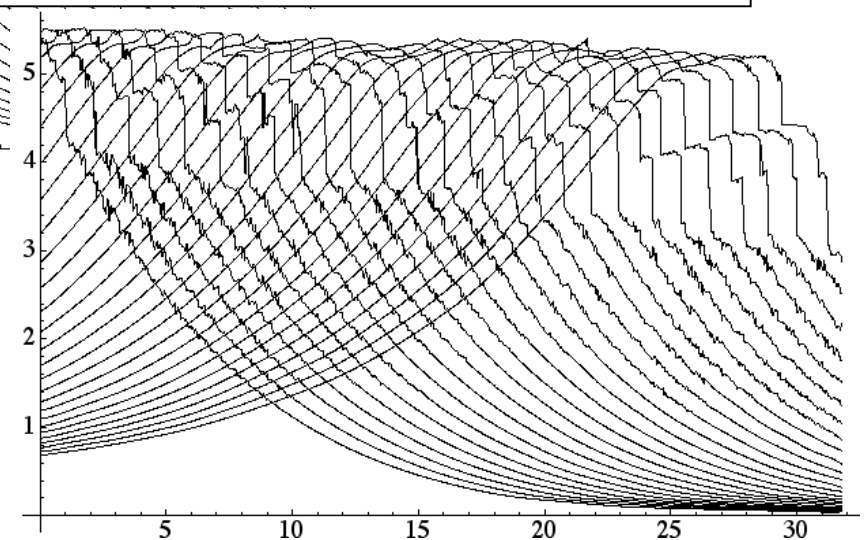
Maximum solitary wave height 0.827
(Longuet-Higgins and Fox, 1996)

Tanaka's (1993) numerical simulation:
 $a_w = 0.905$ at $x = 150$ when $a_i = 0.3$, and $\psi_i = 20^\circ$

The maximum wave amplitude prior to wave breaking was found to be $a_w = 0.910$; much higher than the highest solitary wave ($a = 0.827$).



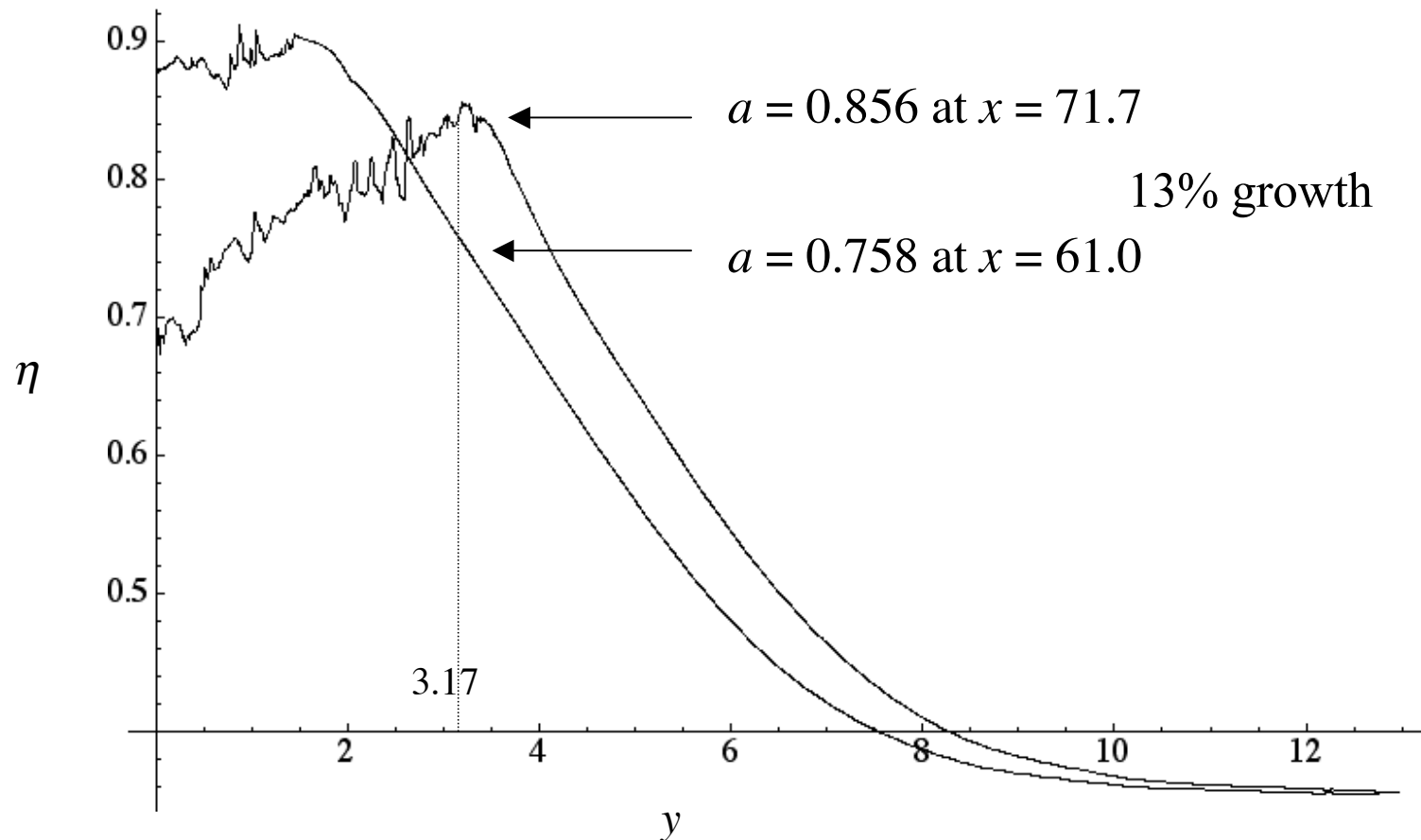
$$a_w = 0.910 \text{ (5.46 cm)}$$



$$h_0 = 6.0 \text{ cm}; \quad \psi_i = 30^\circ; \quad a_i = 0.37 \text{ at } x = 60.96$$

Cross-shore Wave Profiles

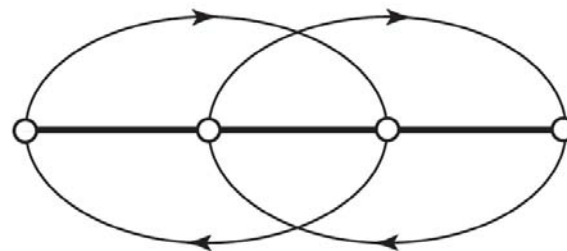
$$h_0 = 6.0 \text{ cm}; \quad \psi_i = 30^\circ; \quad a_i = 0.37$$



And, the breaking causes the wave side-slope to increase *along* the wave crest.

T-type two-solitons

$$\pi = \begin{pmatrix} 1 & 2 & 3 & 4 \\ 3 & 4 & 1 & 2 \end{pmatrix}$$



T-type

$$a_i = 0.280$$

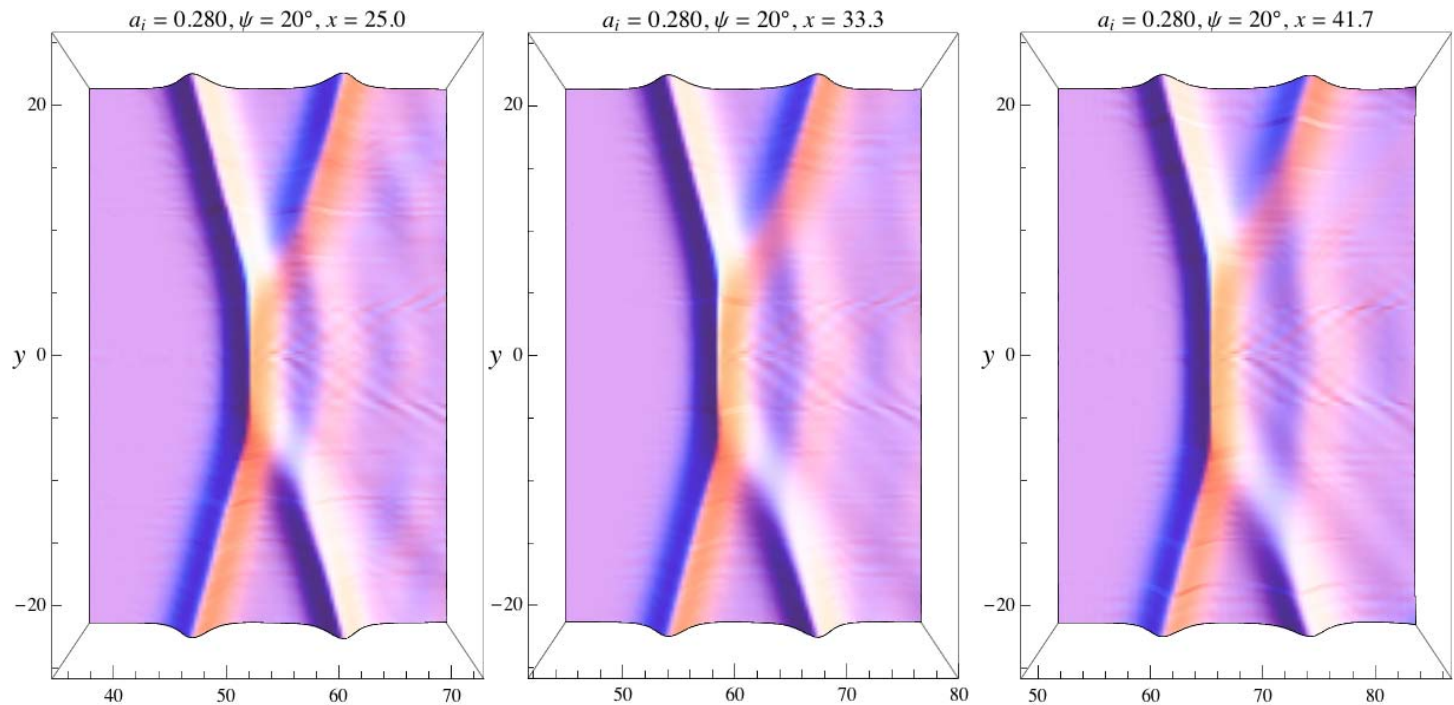
$$\psi = 20^\circ$$

Laboratory
measurements

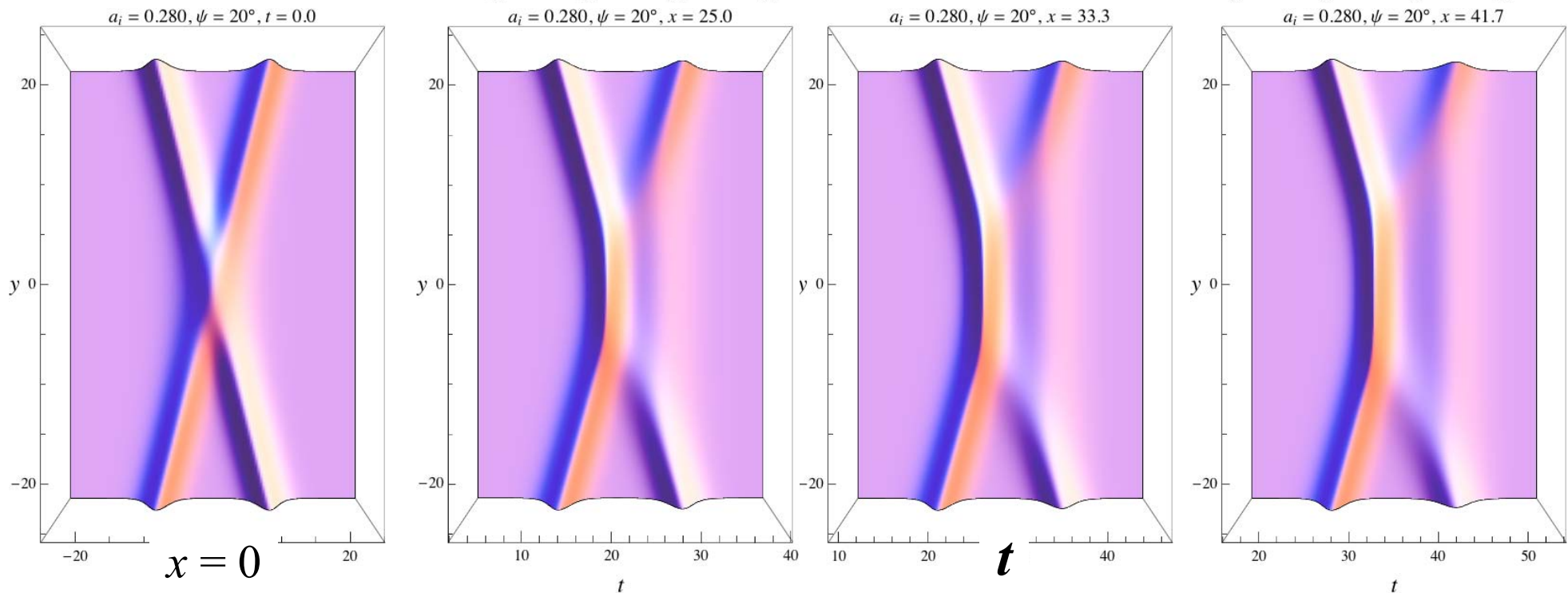
$$x = 25.0$$

$$x = 33.3$$

$$x = 41.7$$

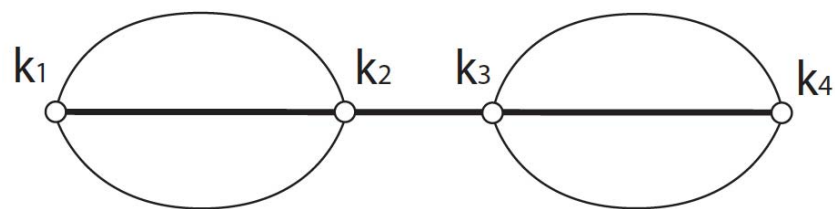


KP predictions



O-type two-solitons

$$\pi = \begin{pmatrix} 1 & 2 & 3 & 4 \\ 2 & 1 & 4 & 3 \end{pmatrix}$$



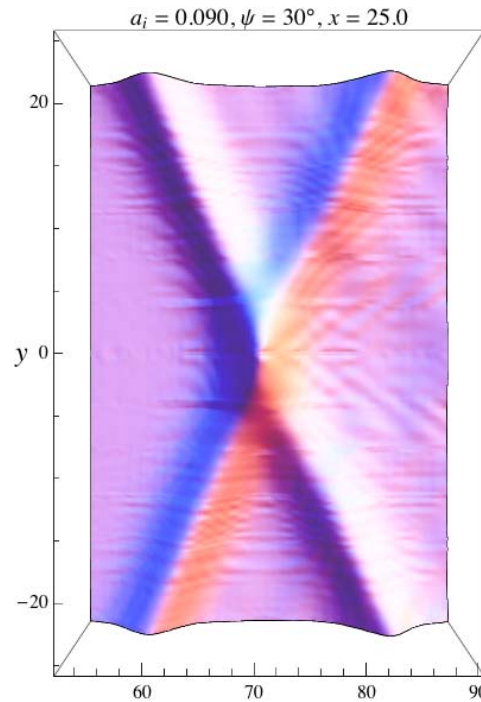
O-type

$$a_i = 0.090$$

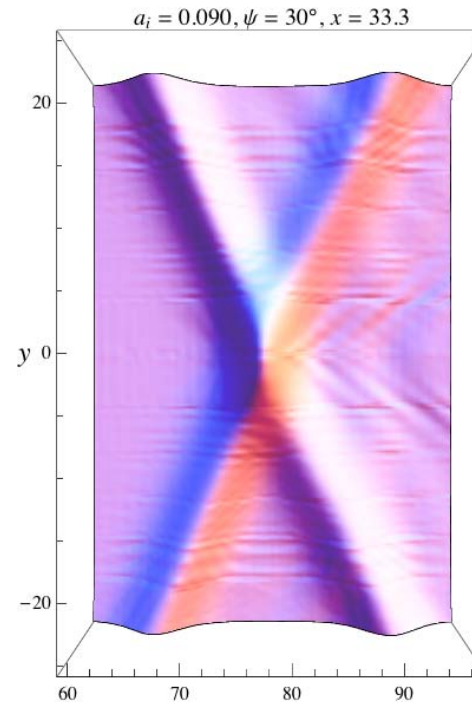
$$\psi = 30^\circ$$

Laboratory
measurements

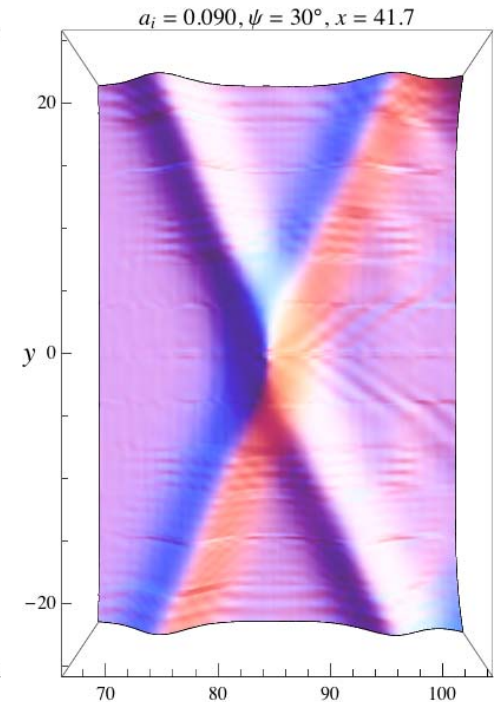
$$x = 25.0$$



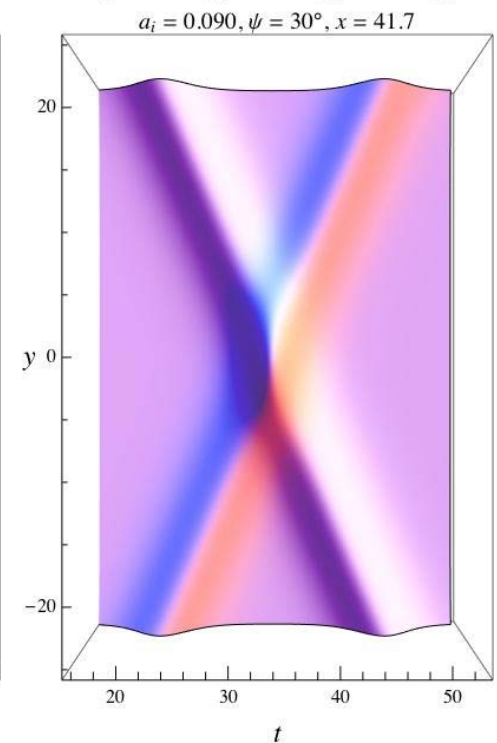
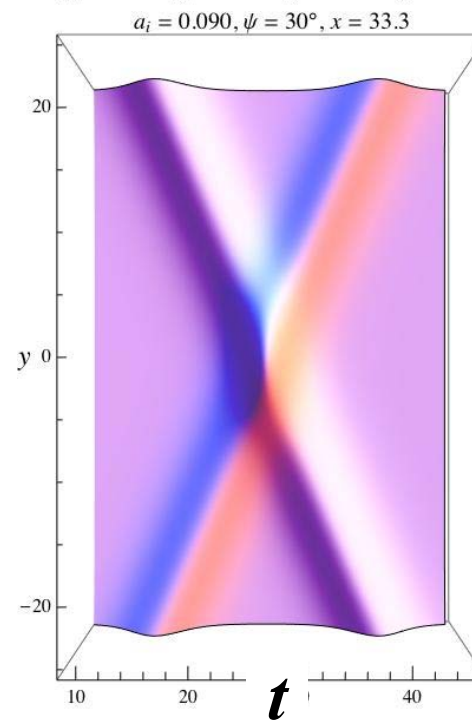
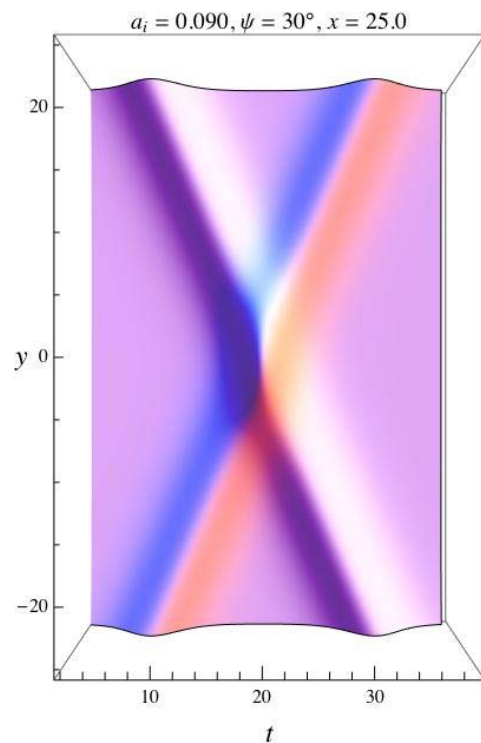
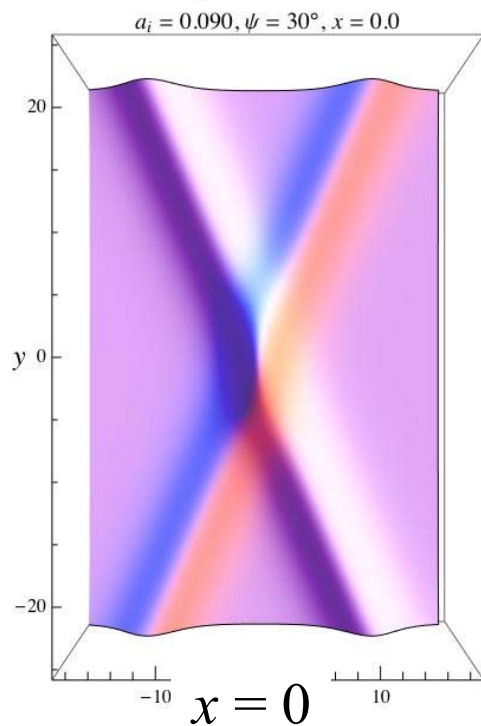
$$x = 33.3$$



$$x = 41.7$$



KP predictions



The KP theory is useful and does provide crucial interpretations and quantitative predictions for long-wave (*tsunami*) interactions and the resulting wave amplifications.